Techno-Economic Analysis of Nuclear Integrated Energy Systems for Water Desalination and Hydrogen Production

A Dissertation
Presented in Partial Fulfillment of the Requirements for the
Degree of Doctor of Philosophy
with a
Major in Nuclear Engineering
in the
College of Graduate Studies
University of Idaho
by
James Richards

Approved by:
Major Professor: Richard Christensen, Ph.D.
Committee Members: Robert Borrelli, Ph.D.; Michael McKellar, Ph.D.; Cristian Rabiti, Ph.D.; Paul Talbot, Ph.D.
Department Administrator: Indrajit Charit, Ph.D.

May 2023

Abstract

As the electricity system evolves to meet changing dynamics from new technology and environmental needs, nuclear power units have retired at an accelerated rate. Stakeholders and companies are searching for ways to improve nuclear economics while improving environmental performance across all sectors. This dissertation explores the techno-economic modeling and analysis of several Integrated Energy Systems (IES). A model of an existing nuclear plant's water system was developed to understand the economic and technical feasibility of adding a desalination unit. Several hydrogen system models were developed, including an iodine-sulfur cycle coupled with a high temperature reactor, electrolysis units coupled with existing light water reactors, and electrolysis units coupled with microreactors. Each technological analysis furthered different modeling techniques, such as the quantifying influence of synthetic input on hydrogen dispatch, limit-surface search sampling for understanding how several sensitivities affect profitability, and spatial modeling to explore the effect of centralized or co-located hydrogen production.

Acknowledgments

I would like to acknowledge and Dr. Richard Christensen, who has been an invaluable mentor and offered me the flexibility and support to pursue this line of research. From the University of Idaho, I would also like to thank Dr. Robert Borrelli and Dr. Michael McKellar who have both afforded me opportunities to grow professionally and academically.

I would also like to acknowledge the role that Idaho National Laboratory and INL played in this work. I offer a deep gratitude to the lab for bringing me on as a graduate fellow, where the majority of this research was conducted. Specifically I would like to thank Dr. Cristian Rabiti for mentoring me and helping me grow in the technical aspects of this analysis. I would also like to thank Dr. Paul Talbot for his guidance and for providing me room to contribute as a researcher.

I am also grateful to other collaborators for the roles that they played, including Dr. Aaron Epiney, Dr. Andrea Alfonsi, Lane Knighton, Dan Wendt, as well as other collaborators at Xcel Energy, Arizona Public Service, Japan Atomic Energy Agency, Argonne National Laboratory, and the National Renewable Energy Laboratory.

Dedication

Dedicated to Cori, because she's still alright.

Table of Contents

List of Tables

List of Figures

Statement of Contribution

The work comprised in Chapters 3, 4, and 5 were collaborative works with co-authors.

In chapter 3, some conceptualization, some system design work, and some interpretation of results was done by Dr. Aaron Epiney at Idaho National Laboratory. I was responsible for system design, writing the models, running and analyzing the sensitivities, developing the visualizations, developing conclusions, and writing the entire enclosed chapter. Other collaborators contributed to a larger, external technical report (see [1]), but their work is omitted from this dissertation.

In Chapter 4, Dr. Cristian Rabiti (INL) assisted with project management and some system design. Nolan Anderson (INL) also performed some project management and review comments and edits. I developed the cases, model, produced visualizations, analyzed the results, ran the sensitivities, and wrote the entirety of what is included in this dissertation.

In Chapter 5, Lane Kinghton (INL) was responsible for project management, while Amgad Elogwainy (ANL), Bethany Frew (NREL), and Daniel Wendt (INL) provided inputs that were used to develop this analysis. I was responsible for developing the model, producing results, analyzing the outputs, developing conclusions, and writing the entirety of what is included here. Other collaborators contributed to a larger, external technical report (see [2]), but their work is omitted from this dissertation.

Chapter 1: Introduction

Nuclear energy in the United States and the world at large are at a critical juncture as energy technologies and markets evolve. Nuclear plants currently provide about 19% of the electricity generation, which has been slowly declining for the last few years [3]. Despite the penetration of nuclear on the grid, nuclear plants are facing difficult economic conditions as grid operators emphasize clean and flexible technologies. The decline in renewable energy costs and natural gas prices, among other factors, have led to 4.7 GW of nuclear capacity retiring early since 2018 [3].

Studies of electricity market structure, regulatory reform, government incentives, and efforts to reduce operating costs have all provided suggestions on how to improve the economics of the existing nuclear fleet. Technical solutions such as operating in a load following configuration, switching to metal fuel or higher enriched uranium to improve fuel performance, or producing secondary commodities other than electricity have been also been investigated.

The work of this dissertation focuses on the effects that an Integrated Energy System (IES) might have on nuclear plant economics. Chapter 2 develops background on nuclear economics and IES, as well as the technical and economic challenges to IES deployment. Chapter 3 investigates the synergistic effects of a nuclear plant's existing water treatment system and a reverse osmosis desalination system. Chapter 4 discusses the technical implications of adding an iodine-sulfur cycle hydrogen production unit to Japan's High Temperature Test Reactor. The analysis also looks at the role of input data in running the economic dispatch of IES systems. Chapter 5 develops a model to understand how two existing light water reactors might benefit from flexibly operating electricity and hydrogen production, switching between the two when there is economic incentive to do so. Chapter 6 analyzes greenfield microreactor deployments and how their location, relative to hydrogen demand centers, might affect the breakeven price of hydrogen for sale.

The research in each chapter seeks improve IES modeling capability and the understanding of how IES affects the economics of nuclear plants. Each study answers unique research questions but moves the literature towards an answer to the larger research question: is it technically feasible and economically advantageous to develop IES systems at existing and/or new nuclear plants?

Chapter 2: Review of Nuclear Integrated Energy Systems

This chapter serves as a background for the theory required for techno-economic analysis of integrated energy systems. The review serves to develop an understanding of the electricity system and electricity market design, the role nuclear energy currently plays in this system, and the configurations and roles that an IES might play. An overview of the current state of nuclear fleet and their economics, an explanation of electricity markets, and a review of IES technologies is also included.

2.1 Introduction

Nuclear plants have dealt with economic uncertainty in the 21st century as the electricity system changes. Moving towards carbon free electricity resources has changed the operation of the grid such that flexibility and ability to complement to variable renewable generators (VRE) is valued [4]. The relative inflexibility of electricity generation from nuclear, coupled with cheap natural gas in North America, have led U.S. nuclear plant stakeholders to search for ways to help nuclear plants compete in today's electricity markets [5, 6].

One possibility for nuclear plants to improve their economic output is by using them in an integrated energy system (IES). An IES is comprised of a nuclear plant that can use heat, steam, and/or electricity to produce some other commodity, such as a desalination system for potable water or heat for thermal energy storage. Some IES incorporate other generators, such as wind or solar. For the purposes of this work, an IES is any system that includes a nuclear reactor and the ability to produce some commodity other than electricity.

This chapter serves as a review on the current status of IES modeling and research with a focus on the economic implications of these systems. First, there will be a review of current electricity market structures and conditions that pertain to nuclear in order to understand nuclear economic issues and how an IES might address them. Second, a review of current modeling and research efforts on the topics of IES process development and techno-economic modeling is put forth. The author then uses that review to inform discussion on gaps in understanding that should be addressed in order to understand IES value, both to the nuclear plant and electric grid at large. The final discussion proposes some solutions to address these gaps.

2.2 Background

2.2.1 United States Electric Fleet

The U.S. electricity fleet is comprised of mostly fossil fueled generators with large amounts of generation from nuclear and renewable energy. In 2020, 19.7% of electric generation came from renewable energy, including hydroelectric, and 19.7% from nuclear energy with the balance generally coming from natural gas and coal. Figure 2.1 shows the evolution of U.S. electricity generation throughout the years. Natural gas and renewables have seen their share increase, while nuclear has remained stagnant and coal has declined. Among renewable energy, wind has seen the most growth over the last 20 years, with solar

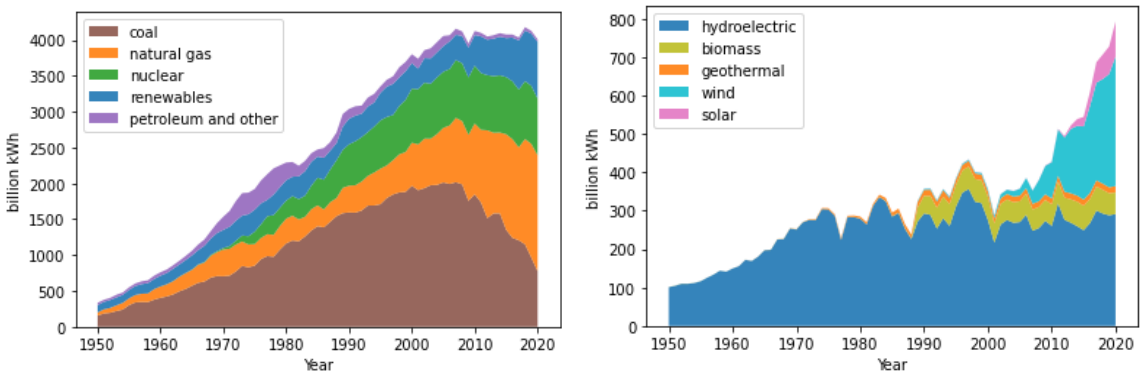

(a) (b)

Figure 2.1: U.S. electricity generation by year. (a) total electricity generation, (b) renewable electricity generation. Produced with data from [7]

increasing its market share in recent years.

The historical data from Figure 2.1 shows that the US is currently in the midst of a transitory energy period. Rapid decline and then flattening of natural gas prices, declining renewable costs, and government intervention on behalf of carbon free sources have all changed the electricity landscape. Natural gas has supplanted coal as the largest generator class in the US, and wind and solar have increased steadily throughout the last decade.

Nuclear has remained at a nearly constant percentage of total generation during these changes. This is due to many plants undertaking capacity up-rates while other plants have retired and with only one new reactor coming online between 1996 and 2022. While that trade off has kept nuclear generation essentially constant, the aging fleet is facing more rapid retirements in the next decade that would likely lead to a decline in nuclear generation share and total generation. Explanations for this uptick in nuclear retirements are explored in depth in Section 2.2.1.

The energy transition in the U.S. has changed what is valued in a generator. When the electricity system was largely fossil fuel, hydroelectric, and nuclear generation, generators would operate in either baseload or peaking/flexible generation. The baseload generators, including coal, nuclear, and some larger hydroelectric dams, would seek to operate at the highest output they could for long periods of time. The flexible generators would then adjust their output to match the rise and fall in electricity demand throughout the day. Nearly all the resources were dispatchable, meaning that the electricity output could be controlled by operators during normal conditions.

In today's system there is a greater emphasis on flexibility. Variable renewable energy provides electricity that is not dispatchable. Additionally, because of its low marginal cost and its status as a zero-carbon resource, VRE is generally treated as a must take resource. This means that despite the intermittent nature of the generator, the electricity from VREs is often prioritized for use regardless of time or current demand. Doing so creates unique challenges for the large, inflexible, baseload-style plants and encourages flexible generators.

The operators of inflexible generators, such as coal or traditional nuclear, prefer to run their generators at full power as much as possible. This makes the inflexible resources a poor compliment to intermittent, non-dispatchable generators. This is demonstrated in Figure 2.2. Three days in California Independent

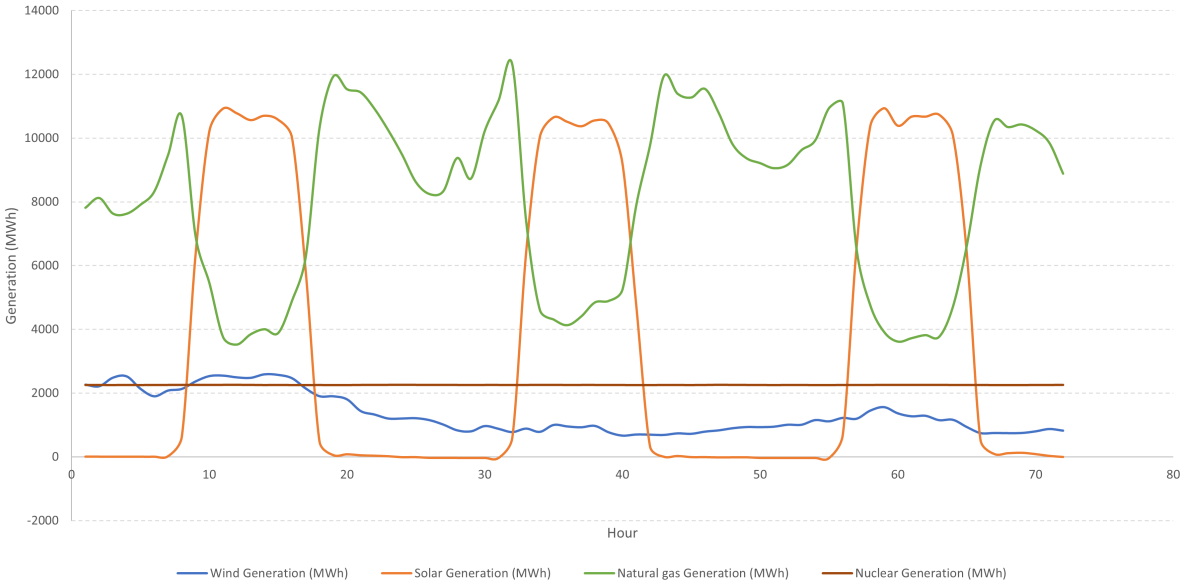

Figure 2.2: Selected CAISO generator output for a three-day window, February 1-3, 2022. Plot developed with data from [8]

System Operator (CAISO) service area are shown. Solar energy is the largest generator during the day. Fast moving natural gas plants ramp up as solar ramps down. It can also be observed that the nuclear plants have been unable or willing to operate in a flexible manner, remaining consistent despite solar drop off.

The fact that VRE generation often occurs in off-peak hours amplifies incompatibility with baseload. Peak electricity hours generally occur in the early evening, right as the sun is setting and before the high wind times at night. These daily peaks can occur at different times depending on location or seasonal differences, but in many instances the peak VRE generation does not coincide with peak electricity use. As the VRE generation declines, other generators are required to ramp back up quickly to meet demand. This is relatively simple to do with a natural gas turbine but difficult with a large baseload unit.

In addition to flexible generators augmenting renewables, large scale energy storage is being investigated and implemented. Large scale storage, in technologies such as batteries, thermal energy storage, or pumped reservoir hydroelectric, could store the electricity produced at off-peak times and shift it to peak demand during the day. For example, wind energy is most active at night when demand is very low. Storing this could reduce curtailment of VRE and other generators by storing that energy until it is needed the next day.

While storage is being deployed and costs are coming down, there are still technical questions about high penetrations of storage and renewables. Electric capacity resources are planned in order to meet load and some applied extra margin at the peak demand hour of the year. Each incremental addition of renewable capacity is less useful for meeting peak demand. Figure 2.3 shows historical wind, solar, and load data form Texas sorted by largest to smallest demand over the year. With current VRE penetrations (Figure 2.3a), all renewable generation can be used to meed demand. When VRE penetration has been increased by a factor of 5, a huge portion of generation is unusable because it is produced in the wrong time (Figure 2.3c). It is important to note that the 5x case does not meet peak demand, so this system

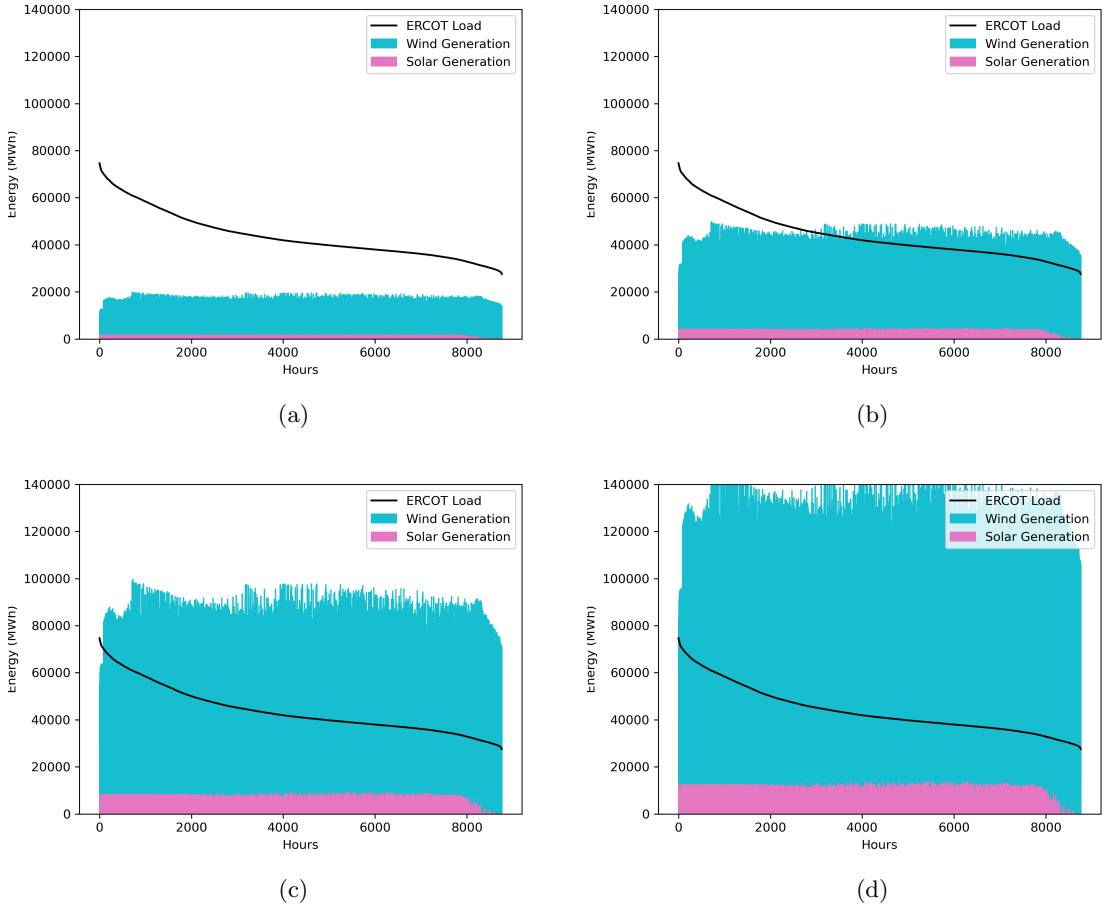

Figure 2.3: Texas load, wind, and solar generation for 2019 ordered from highest to lowest load. (a) 2019 wind and solar capacity, (b) 2.5 times 2019 wind and solar capacity, (c) 5 times 2019 wind and solar capacity and (d) 7.5 times 2019 wind and solar capacity. The plot illustrates how much VRE capacity would be needed to meet load entirely. Produced with data from [9].

would still need more renewables, storage, or a flexible generator. The 7.5x case shows that peak demand is met, but the wind and solar are over-generating in every hour of the year (Figure 2.3d).

The above example demonstrates the need for either flexible generation or long-term storage. If a storage facility could store energy in the shoulder months and sell that energy in the summer or winter peaks, the system would see much less curtailment and overbuilt capacity. This storage, generally called seasonal or long-duration storage, has gained considerable research in the last decade, but is currently expensive. A review by Yang et al. found no seasonal storage that was cost competitive with natural gas [10]. A flexible generator could also achieve this synergy by running at higher levels in the peak months. These "flexible base" options have been shown to reduce overall system costs in deep decarbonization (greater than 95% reduction) scenarios by anywhere from a 10 to 60% [11, 12]. Nuclear plants specifically have been shown to fill this role and reduce system cost if they can operate flexibly [13]. Flexible IES configurations also have the potential to supplement renewable generation. Modeling work that looks at future electricity systems usually finds that VRE generation will increase [14, 15]. In scenarios without carbon constraints, the increase in VRE is usually accompanied by natural gas

and nuclear plant retirements which can slow greenhouse gas reductions [16]. Forecasts generally show improved adoption of batteries or other clean flexible options in scenarios with a carbon price, clean electricity standards, or an emphasis on carbon reduction, but these scenarios end up being expensive when compared to using natural gas. When decarbonization is prioritize, there are few economic options for replacing gas generation. A technology that can cheaply deliver electricity around the intermittent renewable generation will an important part of a decarbonized electric grid.

2.2.2 Electricity Market Structure

To dig deeper into the value proposition of nuclear with IES, it is important to have an understanding of how electricity markets work. The US electricity grid is comprised of three individual interconnections; east, west, and the Electricity Reliability Council of Texas (ERCOT). Within each of these interconnections, load users and generators are connected via transmission lines, allowing the flow of electricity from producer to user. Interties connect the three distinct grids, but imports and exports over those interties is minimal compared to the generation within the distinct grids.

The lower 48 United States electric grid can be classified in two categories, regulated and deregulated. Regulated markets have vertically integrated utilities that operate each generator and transmission infrastructure in a service area. Regulated utilities cannot change consumer electricity rates or make certain investment decisions without the permission of a public utilities commission (PUC), usually at the state level. The utility and PUC are responsible for system reliability planning. The utility is responsible for grid operation and management.

Deregulated markets allow for different power producers to enter into the market and compete. Electricity from producers is sold to retail electricity providers who then set retail rates and sell to customers. The transmission and delivery network is operated by an Independent System Operator (ISO) or a Regional Transmission Operator (RTO). For the purposes of this paper, ISO and RTO can be thought of as interchangeable terms.

In a deregulated wholesale electricity market, different generators can bid into the day ahead market to tell an RTO how much electricity they can provide and at what cost. The RTO will project the electricity demand over next 24 hour period and allow all generators to bid in. A generator will usually bid to cover their marginal, or short run, costs. This means a generator like wind or nuclear with low- to zero-marginal costs can bid in at lower prices. Under special circumstances wind and solar generators can even bid negative because government clean energy tax credits and subsidies act as a second revenue stream. A natural gas combustion turbine plant would need to bid in at a much higher price, because it has to recover the marginal fuel costs associated with producing electricity.

The bids are ordered according to bid amount. The market is capped when enough generators have bid in to cover the expected load forecast amount. The wholesale market price is then set at the bid price of the final, most expensive electricity generator that will be needed to service the load. This price is often referred to as the market clearing price or simply the clearing price. Each generator is then paid the clearing price for the energy they allocated in their bid.

These day ahead market bids occur for each hour in a 24-hour look-ahead period. The bids are also regional, occurring in many different nodes within the RTO. The clearing price at these nodes, as well as extra costs for transmission constraints, set the locational marginal price (LMP).

In addition to the day ahead market, the real time, or spot market, provides revenue for generators.

The day ahead market bids are set on a forecast. Deviation from that forecast causes imbalance between supply and demand. The real time market fixes those imbalances by allowing other utilities and retail providers to produce electricity. Real time prices are generally more expensive than day ahead prices. Real time markets can require energy in 15-, 5-, or even 1-minute increments meaning that fast moving and dispatchable generation units are required. Existing nuclear plants generally do not extract revenue from the real time market because they do not ramp electricity production quickly enough.

Other market levels include ancillary service markets and capacity markets. Ancillary service markets are designed to compensate generators that can be used in emergency situations. These plants need to have extremely fast ramp times and some are required to have their turbines spinning to preserve system inertia. Capacity markets pay a dispatchable generator a certain amount for simply existing. A capacity market is meant to compensate generators for their contributions to system reliability. More capacity to pick up slack in event of unplanned outages or other off normal events should mean a more reliable grid. Nuclear plants often do not participate in ancillary service markets but they do receive payments in RTOs where there is a capacity market. Some deregulated systems, such as ERCOT in Texas, operate as energy only markets do not have capacity markets.

Each ISO/RTO has slightly different market design structures that impacts the economics of the current nuclear fleet and the economics of adding an IES. The implications of electricity market dynamics are explored in depth in Section 2.2.4.1.

2.2.3 Electricity Supply and Demand

Electricity demand fluctuates throughout the day, usually peaking in the late afternoon or early evening time. After peaking, the electricity demand drops through the night until it starts to increase again in the morning. Utilities or RTOs will predict the electricity demand at the peak for each day and try to have enough generators running to cover the load.

Variable renewable generators generally can only contribute to high demand hours to a point. If the peak demand time in a system is at 6pm when the sun is set, the contribution of solar to the daily peak demand is reduced to zero. Adding more solar to the system would not help meet the demand at peak time, and thus some type of storage medium or other generator would be needed.

This drop off in solar generation as electricity demand peaks is seen in the famous “duck curve” plot, shown in Figure 2.4. The plot shows net load in California, taken as total electricity demand minus the portion met by solar. As the solar starts to come offline in the evening, the net load rapidly increases. Adding more solar would not add generation to those high net load hours.

In a general sense, each incremental addition of solar is less valuable to the grid than the previous addition. The ability of the generator to assist with peak demand, termed capacity value, is reduced asymptotically to zero when adding solar alone [18]. Solar generators’ capacity value can be improved by batteries, demand response, or additional flexible generators.

The other issue that the duck curve illustrates is the need for increased flexibility when the solar drops off. As more and more solar is added into the system, the other generators need to be able to ramp up quicker to meet the peak. This means that flexible units, such as natural gas combined cycle (NGCC), natural gas combustion turbines (NGCT), or battery discharge are favored over inflexible units like coal or nuclear. The more VRE on the system, the more the system values flexible generators.

It should be noted that this duck curve affect is regional. If the peak is earlier in the day, then solar

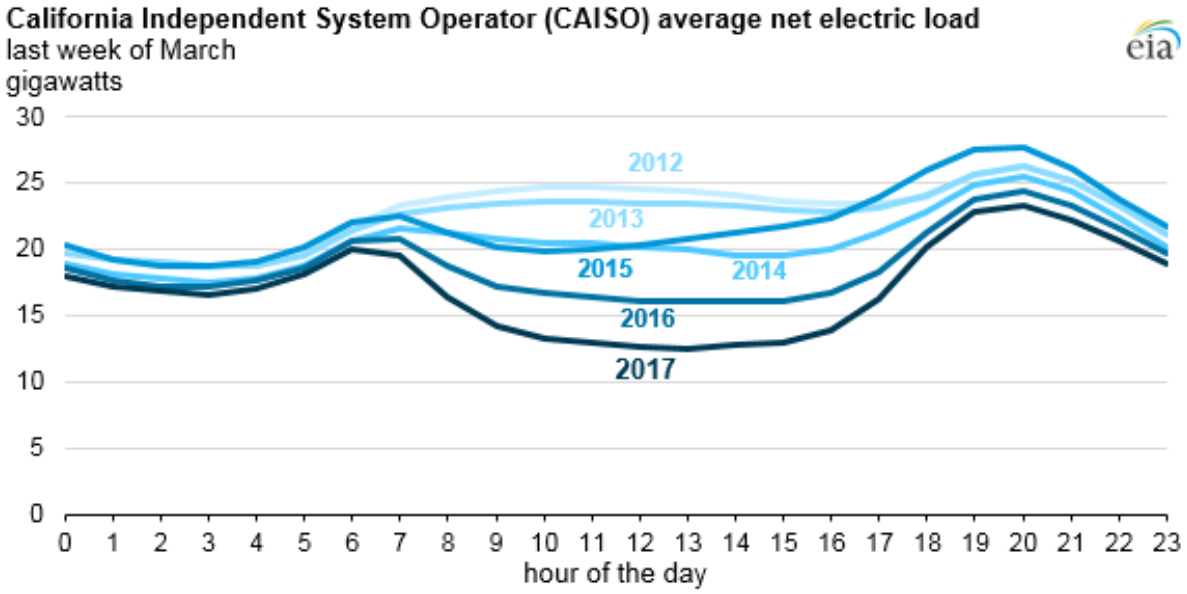

Figure 2.4: The "duck curve" plot that illustrates the quick changes when solar generation drops off and load is increasing in the evening. The plot illustrates that solar penetrations could grow to a point where they do not contribute to the peak electricity hours in a day. Plot from [17]

could be used to meet some daily peak demand. Additionally, it makes no comment on transmission or other operating generators.

The demand profile also has large seasonal effects underneath these daily fluctuations. Most areas in the United States have the peak demand in the summer as more air conditioning is used. Some milder climates, such as areas of the Pacific Northwest, or colder climates with primary electric heating will have a winter peak.

These yearly peaks will form the planning basis for utilities, RTOs, and public utility commissions. A peak is forecasted and the system operator ensures that there is enough capacity available in the year to meet that peak with an additional backup capacity margin. Because the system is designed around the yearly peak, some capacity will be used very infrequently. This is acceptable for a unit with high marginal costs and low fixed costs, such as diesel generators or NGCT. These seldom used, ultra-peaking units are almost exclusively carbon-emitting fossil resources in the U.S., with the exception of some biomass systems. Replacing these ultra-peakers will be important in a carbon constrained grid.

The comments in this section and preceding sections were not an argument for or against any particular generating technology. Rather, they are used as an illustration of the complex issues that the grid operators face as the world moves towards carbon free technologies.

2.2.4 Nuclear Economics

Nuclear economics are driven by three key features; high capital cost, high fixed operating and maintenance cost (FOM), and low variable operating and maintenance (VOM) and fuel cost.

Light water reactors (LWRs) have high fixed costs relative to their variable costs. FOM includes operating and maintenance expenditures that occur regardless of energy output. Examples include licensing fees, employee salaries, or capital improvements. VOM cost are costs that are proportional to

energy production and scale accordingly, such as parts that wear with generator usage or fuel in fossil generators. Fuel in an LWR can be thought of as a fixed cost because it is bought on a contract and changed on set cycles, regardless of energy production. When generators have a high proportion of FOM to VOM, they prefer to generate and sell as much electricity as possible, for as long as possible. When plants have higher variable costs, they expect to run only when the electricity can cover their high VOM cost.

This explains why nuclear plants try to operate with a steady output. When a deregulated market clears at a higher price than the nuclear plant's marginal cost, the excess return can cover the fixed costs. But when a nuclear plant needs to turn down in times of low demand or excess VRE generation, there is no electricity sold and thus no revenue to cover the high fixed cost. Additionally, when the clearing price is low, there is less revenue per unit of electricity sold making covering fixed costs more difficult.

In addition to fixed cost recovery, there are technical challenges with flexing nuclear plants, further hampering their economics in a system that emphasizes flexibility. Nuclear load following requires changes to the nuclear reactions and core conditions. These nuclear transients can be difficult to control, introduce excess poisons into the reactor, and induce premature wear on reactor components. These problems can be overcome, as seen in French light water reactors that load follow or U.S. reactors that participate in load shaping, but the poor economic outlook and technical hurdles have been enough to disincentivize nuclear load following. This puts current nuclear economics inherently at odds with flexibility

2.2.4.1 Effect of Market Changes on Nuclear

This section uses a hypothetical bid stack to understand the effects of cheap renewables, cheap gas, and stagnant or reduced demand on nuclear plants. Figure 2.5 shows the bid stack for this hypothetical system in the base scenario. Each generator bids according to its marginal price, with nuclear being one of the lowest. For a required load of 35 GW, the clearing price is set at \$10/MWh. This means that the nuclear plant will be able to provide electricity for \$8/MWh above its marginal cost.

With increases in renewable penetration, the entire bid stack shifts to the right. The renewables can always bid at or below zero, meaning they are the first to clear the market. This shift means that the day ahead market clears at a lower value. Illustrated in Figure 2.6, the market now clears at \$8/MWh. That means that the nuclear plant now only brings in \$6/MWh in revenue.

Decreased load also reduces nuclear plant's profit margins. Figure 2.7 shows a reduction in load from 35 GW to 30 GW. The market now clears on a natural gas plant with a lower marginal cost. The nuclear revenue decreases further as the clearing price decreases.

The last major change in the 21st century that affects the electricity markets was the depression of natural gas prices. Electricity markets that cleared on natural gas saw reduced clearing prices because the NG units could bit in lower. Figure 2.8 shows the effect of lower natural gas prices on the bid stack. Lower natural gas prices meant that short run marginal costs for gas in the U.S. started to drop below coal. The NG would either enter the market earlier and provide more electricity, or the market would clear on NG, leaving coal out entirely. Natural gas marginal costs can approach nuclear marginal costs, though some operators have started to bid nuclear plants at zero in an effort to enter the market earlier.

These three compounding trends have cut nuclear plant's revenue. In this scenario, the nuclear plant

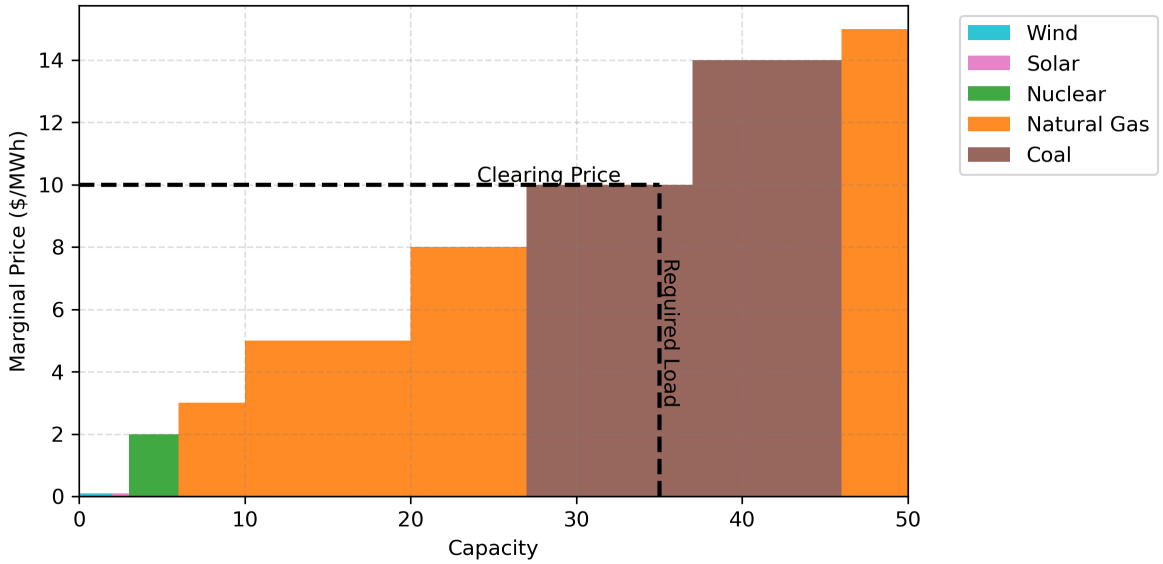

Figure 2.5: Hypothetical bidding of electricity generators into a day ahead electricity market. This plot represents the base case. The system is mostly coal and natural gas with small penetrations of nuclear and renewables.

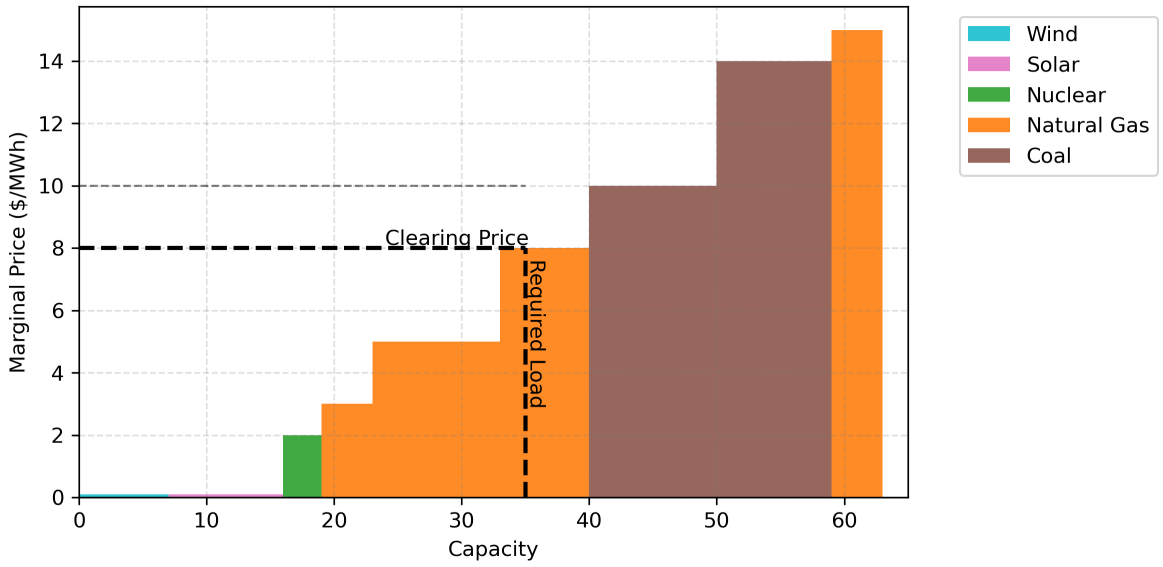

Figure 2.6: Hypothetical bidding of electricity generators into a day ahead electricity market after an increase in renewable energy penetration. The market now clears at $8/MWh rather than $10/MWh from the base case.

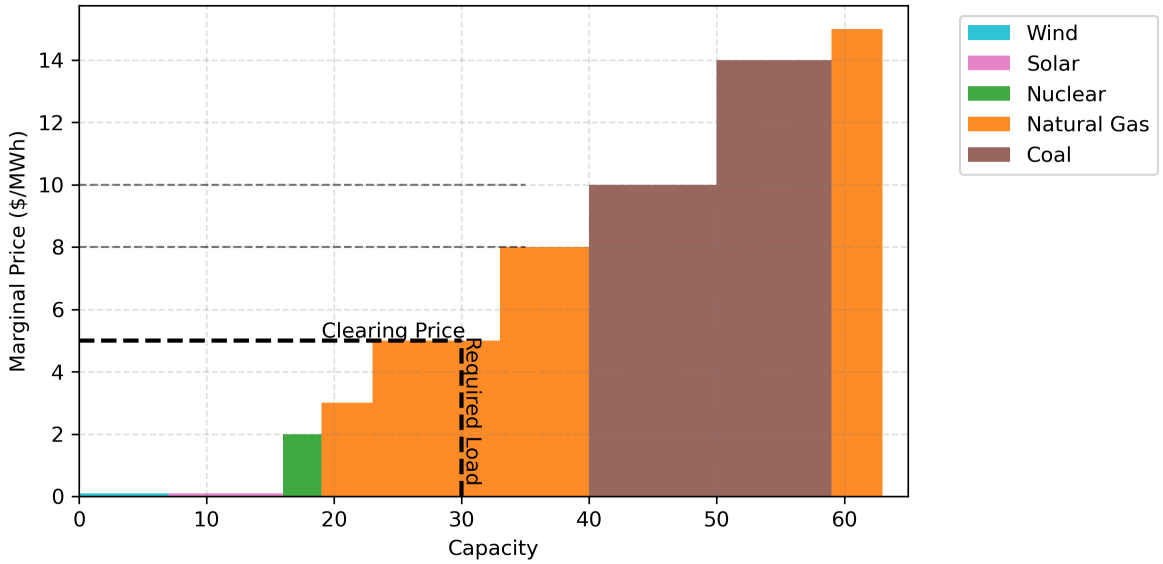

Figure 2.7: Hypothetical bidding of electricity generators into a day ahead electricity market after an increase in renewable energy penetration and a decrease in load. The lower load shifts the clearing point to the left, meaning the system now clears on a lower marginal cost generator, depressing the clearing price further.

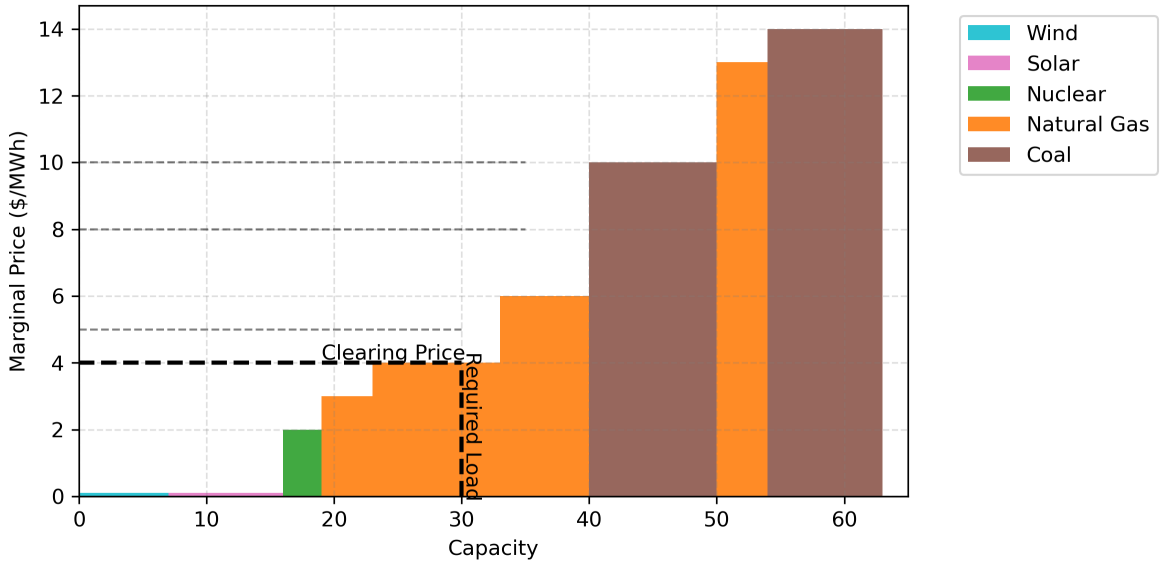

Figure 2.8: Hypothetical bidding of electricity generators into a day ahead electricity market after an increase in renewable energy penetration and a decrease in load and lower natural gas prices. Note that some of the coal would enter the market later and the revenue for nuclear is reduced.

started at $8/MWh and was reduced all the way to $2/MWh. This reduction in revenue margins is difficult for nuclear plants that are trying to recover their large fixed costs.

2.3 Integrated Energy Systems

A method for improving nuclear profitability that could 1) maintain the core at a relatively steady level, and 2) allow for the sale of some product (heat, electricity, chemicals, etc) would mitigate revenue decline from reduced wholesale electric clearing prices.

IES fit this description because the nuclear plant can use heat to produce electricity or another secondary commodity. That heat can always be used, which keeps reactor core conditions steady regardless of electricity prices.

The basic IES configuration includes a nuclear reactor, a turbine, and a secondary commodity production method. The secondary commodity can be coupled to the reactor electrically, thermally, or some hybrid of the two.

Operating IES in an arbitrage method could help nuclear plants avoid selling electricity at a loss. When electricity prices are low, the IES could maximize production of its secondary commodity and minimize electricity production. The secondary commodity sale would help the nuclear facility cover its fixed costs despite low electricity prices. Then when electricity prices are high, the IES could sell electricity and maximize revenue. In this scheme, the IES would allow the nuclear plant to use the electricity market's swings to its advantage have to simply accept the low price hours.

The price arbitrage scheme is visualized in Figure 2.9 on a price duration curve. The electricity prices for a load zone in ERCOT in 2019 are plotted. A hypothetical nuclear operating cost of $30/MWh is set. When the electricity price is above $30/MWh the nuclear plant would sell electricity. When electricity price is below the threshold, the plant can divert energy to produce and sell a secondary commodity.

The operating cost line in Figure 2.9 can be crossed multiple times over the standard daily cycle of electric load. That price fluctuation over a span of hours is why flexibility in IES is important.

While IES systems seemingly match well, several drawbacks should be addressed. The first is that there is almost always some type of consistent, parasitic load. This parasitic load, likely to be in the 10-100MW range for a gigawatt-scale nuclear plant, decreases the nuclear plant's nameplate capacity. The lower nameplate capacity reduces the amount a nuclear plant would be compensated in a capacity market. Another drawback is the significant capital investment required to build associated secondary commodity production facilities. The IES creates dispatch complexity that could preclude the nuclear plant from providing grid reliability or ancillary services. Additionally, if the IES prioritizes the secondary commodity over electricity, the nuclear plant could be squeezed into providing that commodity at inopportune times, such as when electricity is high but the IES is contractually obligated to provide a certain amount of secondary commodity. Mitigating that requires extra investment into commodity storage.

2.3.1 Hydrogen Production

One of the most commonly researched IES configurations is hydrogen production. The proposed systems, coupled thermally or in a thermal and electric hybrid manner, use energy from the nuclear plant to produce hydrogen via a chemical or electrochemical process. The hydrogen can then be sold to consumers or run through a turbine to produce electricity.

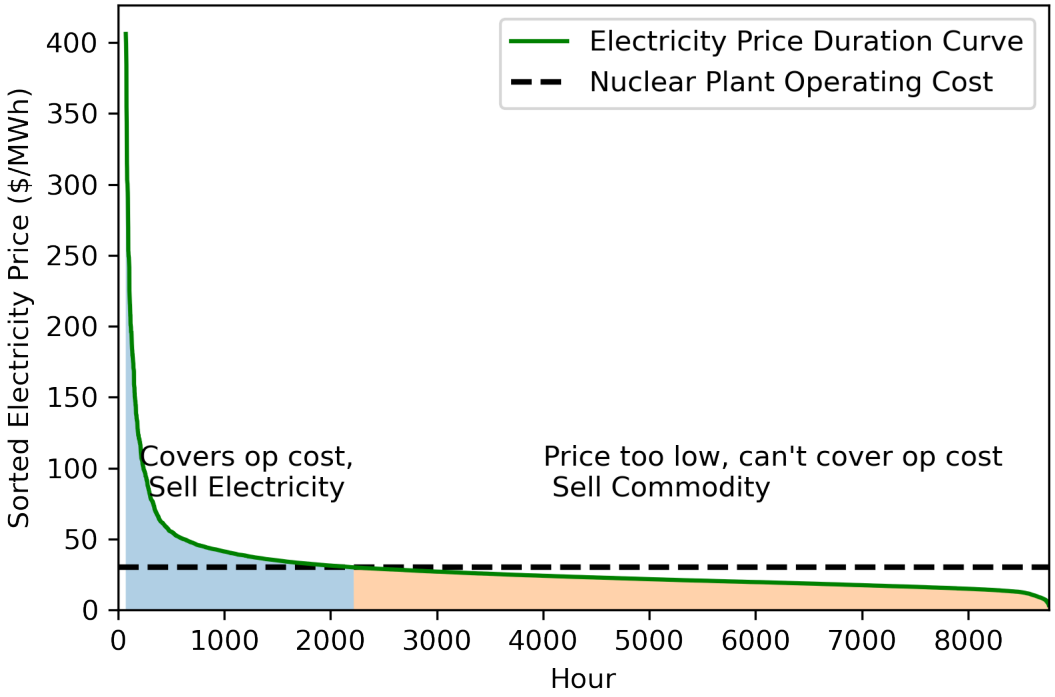

Figure 2.9: Electricity price duration curve from ERCOT 2019 historical data. The black line represents a hypothetical break-even cost that a nuclear plant must achieve when it sells electricity. If it electricity price was below that line, the nuclear plant loses money without an IES. Plotted with price data from [19].

High temperature steam electrolysis (HTSE) offers a hydrogen production method that matches well with light water reactors. The HTSE cells utilize electrochemical potential to split water into oxygen and hydrogen components. Input water can be as high as 850°C, so the HTSE will likely require hybrid coupling with direct nuclear heat and electrical resistance heat applied when coupled with an LWR [20].

Similar electrochemical hydrogen production methods include low temperature steam electrolysis or proton-exchange membrane (PEM). PEM is very similar to HTSE, but it only requires operating temperatures between 100C and 200C. Because of this low temperature requirement, a nuclear reactor could couple either electrically or thermally with a PEM unit. This is simpler than HTSE coupling, but would be less efficient. Hydrogen production via either electrolysis method does not require handling hazardous chemicals and can be operated in a fairly flexible manner [21, 22] .

Chemical processes can also be coupled with nuclear reactors to produce hydrogen. The iodine-sulfur (IS) cycle reacts water, sulfur dioxide and iodine to form HI and sulfuric acid. The HI is split to produce hydrogen and iodine. The sulfuric acid is reduced to form sulfur dioxide, water, and oxygen. This cycle requires operating temperatures of up to 830°C, making it not suitable for coupling with LWRs. Development in areas with high temperature reactors, such as Japan, is ongoing [23].

Another chemical hydrogen production method, copper-chloride (Cu-Cl) cycle works in a similar fashion. Copper and HCl are reacted to produce H_2 and $CuCl_2$. The $CuCl_2$ and water put through a series of reactions that eventually produces O_2 and Cu. The Cu-Cl cycle requires operating temperatures of 500°C, lower temperatures than the IS cycle. The cycle also produces heat via exothermic reactions that can be used to drive other reaction steps. Cu-Cl cycle research generally focuses on coupling with pressurized heavy water reactors (PHWR) [24].

Despite the large research efforts in nuclear hydrogen production, there are drawbacks such as hydrogen market conditions, transportation, and cheap competitors. Hydrogen markets are still relatively small, with the majority of demand coming from oil refining processes that produce and consume their hydrogen on site via steam methane reforming. Steam methane reforming produces hydrogen cheaply, but does produce carbon emissions, so a carbon tax or production tax credit could improve the economics of IES produced hydrogen. If an IES is further away from hydrogen demand, transportation costs could be prohibitive over large distances. The transportation costs could influence citing smaller SMRs or microreactors around hydrogen consumers to mitigate hydrogen transport costs.

2.3.2 Water Purification and Desalination

Another mature IES configuration is to use heat or electricity to purify and desalinate water.

The simplest method is to electrically couple a reverse osmosis (RO) plant to a reactor. RO operates at high pressures and pushes water through successive membranes, leaving behind the salts. The main energy requirement comes from pressurizing and pumping the water. Some configurations proposing using the nuclear plant's secondary loop or reject heat to preheat water.

Multi-stage flash distillation is another RO technology that has been proposed for use in IES [25]. Salt water is heated and pressurized as it enters the multistage flash desalination plant. The salt water pressure is quickly reduced, vaporizing the water and leaving being a brine stream. This process is repeated until desired salinity conditions are achieved. The heat from the nuclear plant could drive the vaporization through each successive stage. This desalination method is a good candidate for advanced reactors rather than LWRs because it requires higher temperatures than the LWR could provide [26].

Desalination is generally one of the simplest IES systems because water is an easy commodity to handle. There is also operational experience from nuclear plants in Japan, Kazahstan, India, California, and elsewhere [27]. Transportation and storage costs are relatively low compared to hydrogen. Coupling can be done entirely electrically, avoiding complex engineering problems.

2.3.3 Process or District Heat

Rather than producing a commodity, an IES could simply sell heat. Buyers could include industrial processes or district heating applications. Industrial heating generally requires higher quality heat than an LWR can provide, so industrial heat IES proposals traditionally focus on advanced reactors. District heating has been proposed in locations with steam district heating infrastructure. LWRs match well with district heating because it requires lower temperature heat [28, 29].

2.3.4 Other IES

Another popular IES configuration is to simply store heat and shift electricity production hours. Molten salt storage has been applied to nuclear with several companies developing designs to allow for load following [30, 31]. These systems use a hot tank that accepts heat from the reactor. The high sensible heat of molten salts means that the heat can be stored for approximately a week. The heat can be extracted from the salt and used in a steam generator to produce steam for electricity production or industrial use. This process is commercially deployed by concentrating solar plants.

Forsberg et al. [32] proposed using ceramic firebricks to store heat from high temperature gas reactors. The system stores heat at temperatures greater than 1000°C, making it a good candidate for high heat industrial processes.

Garcia et al. demonstrate an IES for producing synfuels and coupling directly with renewables. In this system the heat from a nuclear plant is used in production of synfuels from natural gas feedstocks [33].

Figure 2.10 shows the approximate operating temperatures of the processes reviewed and the associated outlet temperatures of three types of nuclear reactors. Many of the IES processes require higher heat than LWRs can provide. This is why many IES studies focus on a select few technologies, such as reverse osmosis or hydrogen production via electrolysis.

2.4 Review of IES Techno-Economic Analysis and Dispatch Modeling

Integrated energy system modeling can be divided into three categories: process modeling, fixed plant techno-economic analysis (TEA), and dynamic TEA. Process modeling refers to plant level models that quantify physical parameters in the system. Process modeling is useful for detailed engineering work and understanding efficiencies, energy flows, etc. Static TEA analyses extend process models to understand the economics behind the system. This type of modeling effort generally uses static electricity or secondary commodity prices and does not include interaction with the system. A dynamic TEA differs because models will seek to understand the IES interactions with outside markets, energy suppliers, or service companies. For example, a static TEA analysis might assume an electricity price to find its economic figures of merit. An interactive TEA model tries to capture the interaction between fluctuating

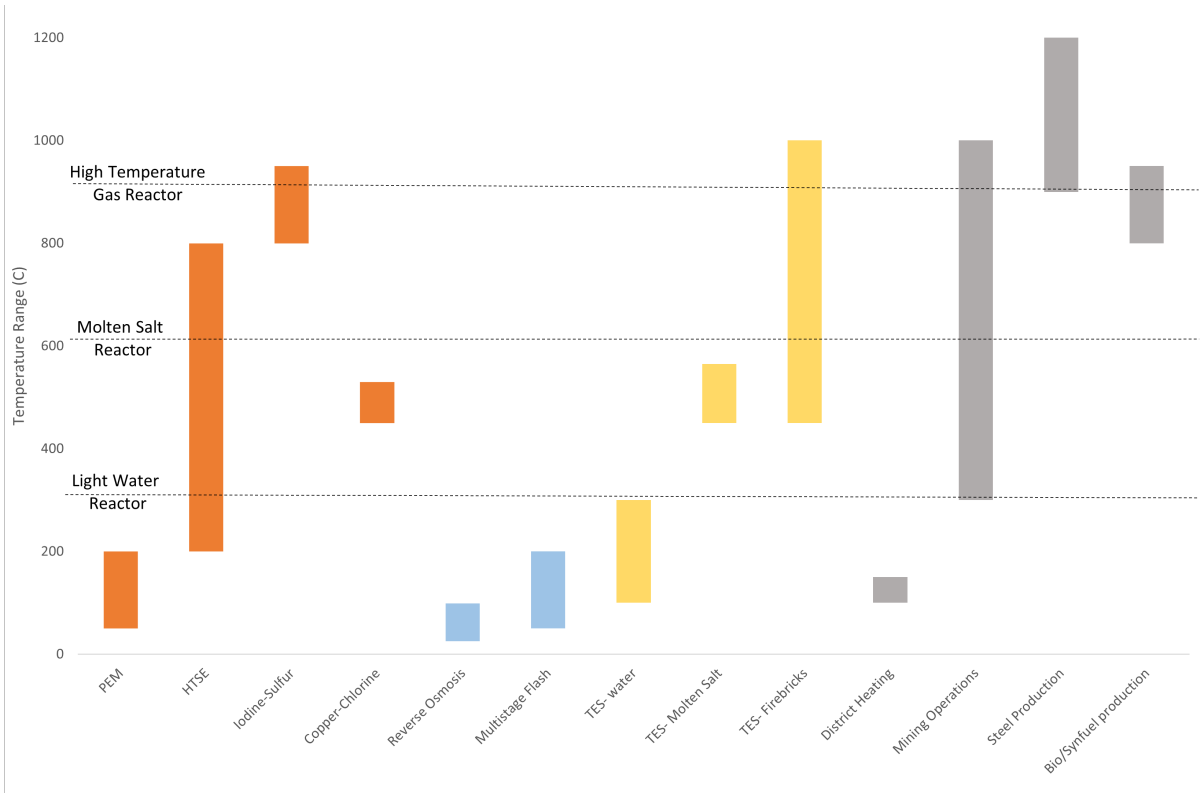

Figure 2.10: Operating temperatures of systems with potential to be coupled to nuclear, compared against the outlet temperatures of three different types of nuclear reactors. Orange are hydrogen production systems, blue are desalination, yellow are thermal energy storage and gray are other systems.

electricity prices and maximize the profits from those fluctuations. This can inform profitability at a deeper level than static models by developing understanding of how different operation modes might affect profitability, how the IES might affect the secondary market prices, or how the IES would fit into specific locations or existing plants.

2.4.1 IES Process Modeling

The literature on process modeling of IES is the largest of the three simulation categories. The main goal of these studies it to understand the engineering implications and the feasibility of adding another commodity to a nuclear plant. Most studies include a first principles approach or use a specific thermal and/or chemical simulation tool such as Aspen Hysys, Modelica, DWsim, or Aspen Plus. These studies have been done on a wide breadth of IES configurations and styles.

One such study by Yan et al. [34] develops a plant layout for using an iodine-sulfur (IS) cycle with a high temperature reactor to produce hydrogen. Detailed designs for individual equipment, such as compressor sizes, heat exchanger operating parameters, etc were investigated. Operating modes for this system were developed based on physical parameters. Similar process modeling work on high temperature reactors has also been done in [23, 35, 36, 37, 38]. Even more detailed studies, such as study by Kim et al., use nuclear IES models for the development of specific components such as the intermediate heat exchangers for an IS cycle [39]. Sabharwall developed a thermosiphon loop to improve heat transfer between a nuclear heat source and a hydrogen process [40]. These detailed studies help develop sizes and material requirements that inform TEA work.

Process modeling work to integrate steam electrolysis with nuclear follows a similar pattern. Zhang et al. evaluate the efficiencies of HTSE based IES and conclude that nuclear produced hydrogen could be competitive when compared to other hydrogen producers [41]. Kim et al. develops a control scheme within a process model to show an HTSE's ability to run in modes such as load-following or constant output [21]. The authors show that a nuclear plant with HTSE can effectively match fluctuations in electricity demand throughout the day but makes no comment on the economic implications that load following would have on the IES or the electricity system at large.

Process evaluations of nuclear with desalination are robust and focus on reverse osmosis and multistage flash. Khalid et al. perform an exergy analysis on a reverse osmosis desalination plant coupled with different types of nuclear reactors [42]. They conclude that higher temperatures from a sodium fast reactor would result in higher exergetic efficiencies then a heavy water reactor. They find that preheating water in preparation for RO would increase exergy efficiency. In an investigation of desalination plants' ability to help smooth net load fluctuations, Hills et al. [43] develop a Modelica model to handle the IES control throughout a 24-hr period. They find that the parasitic load of the RO plant would reduce the nuclear plant's capacity enough for the potential to miss electric load that the wind-nuclear-RO system is expected to meet. This is because the RO plant was also expected to provide water and could not build up enough water in storage to meet both electricity and water demand. They also find that freeze desalination would be flexible enough to always meet demand. Similarly, Kim et al. develop a control algorithm for a wind-nuclear-RO IES [44]. Their study finds that the nuclear and RO plant is physically able to load follow with the fluctuations in demand and wind generation. This study prioritizes meeting electric load over water delivery.

The studies in this section either do not discuss or only briefly touch on the economics of nuclear

IES system. Their purpose to interrogate technical feasibility of such systems is achieved, but more should done to understand the economic feasibility and implications of IES. Integrated techno-economic analyses are required to provide a broader comment on system feasibility and applicability to real world scenarios.

2.4.2 Static Techno-Economic Analysis

The large body of process modeling work summarized in the previous section has informed TEA work. Static TEAs have been able to take the outputs from those process models and apply capital costs, O&M costs, and commodity sale prices to comment on economics and profitability.

Hydrogen production has been a large focus of static TEA work. O'brien et al. developed a detailed process model for an HTSE with an HTGR. That process model informed a techno-economic analysis that showed hydrogen could be produced for $3.23/kg [20]. This analysis assumed a static electricity price and a new-build HTGR to provide heat.

Several direct process heat applications of IES can be found in literature as well. Germeshuizen and Blom studied the integration of a high temperature nuclear reactor with steel production [45]. While they found the nuclear + steel IES to reduce emissions, the steel produced was 12.3% higher than current steel production costs. The TEA assumes a static hydrogen price of $3.00/kg.

Khan uses a custom model and the International Atomic Energy Agency's (IAEA) Hydrogen Economic Evaluation Program (HEEP) to look at coupling hydrogen with different types of reactors [46]. The model varied the hydrogen market size, but assumed that the nuclear with hydrogen systems could only sell hydrogen. The author finds that plants that support thermal coupling will be able to provide economic hydrogen. The study assumes a greenfield, or new build, system.

2.4.3 Interactive Techno-Economic Analysis

The static TEA work is important for informing capital cost or basic break-even hydrogen prices, but it lacks nuance. There is potential value in arbitraging the daily or seasonal swings in electricity markets. Prioritizing electricity or prioritizing the secondary commodity have different value propositions. These different economic realities can also inform operation modes that are likely more complex than simply running the system at a certain capacity.

Locatelli et al. performed a dispatch optimization and let an IES produce hydrogen or electricity. The authors used hourly electricity price data to find an NPV for a nuclear plant with HTSE and various hydrogen sale prices [47]. The electricity is sold in either the Short Term Operating Reserve or Fast Reserve markets; United Kingdom equivalents to the U.S. real time and reserve markets. They found that the most profitable configuration would produce hydrogen most hours of the year and electricity would be sold across the two markets in 443 hours per year. The IES was profitable under certain high price and low HTSE capital cost conditions. The authors recommended running a Monte Carlo or more stochastic simulation to better understand investment risks.

A hydrogen dispatch problem was performed on a Midwest U.S. system by Frick et al. [48, 49]. Hydrogen market supply curves were developed using Hydrogen Delivery and System Analysis Model (HDSAM) and coupled with electricity market data from PJM. A hydrogen storage system was also implemented to allow for consistent hydrogen delivery. Three price thresholds were used to dictate whether the system was producing and selling electricity, producing and selling hydrogen, or producing,

selling and storing excess hydrogen. This is an example of how the dynamic TEA can inform operation modes of IES.

Zhang studied the effects of a wind, nuclear, and hydrogen IES on grid system cost [50]. The author developed a model called the Hybrid-Nuclear-Renewable Tool (HyNuRT) that tracks the cash flows of each physical component and dispatches the electricity in an optimal manner. The model uses load and wind data from representative months and extrapolates the value to the IES over the modeling lifetime. The author found that the addition of hydrogen storage could increase the IES internal rate of return (IRR) by at least 2%, dependant on sensitivity scenario. This conclusion has uncertainties that propagate from the model's coarse temporal resolution where they have static values of wind and load in representative months rather than more granular hourly or sub-hourly time scales. The HyNuRT model, as constituted in this study did not have inherent stochastic capabilities, though the author plans implementation in the future.

Epiney et al. developed a stochastic model for a hydrogen-wind-nuclear IES that found the equivalent LCOE for various penetrations of wind and various hydrogen prices [51]. The authors found that the optimal LCOE system was the lowest marginal cost system in a system with no intertia. In a system with inertia, modeled in Modelica, raising wind penetration on the system generally increased LCOE. This highlights the need for coupling physical models with economic models rather than relying solely on the marginal costs to understand dispatch or system sizing. They also found that using representative days instead of the yearly profile underestimates the LCOE.

Forsberg et al. explored the implications of a nuclear plant with thermal energy storage system [52]. They model the thermal storage IES in the Tokyo electricity market, using an hourly demand profile to dispatch units accordingly. They conclude that adding the thermal energy storage system to the nuclear plant increases revenue for both wind and solar as the solar penetration increases.

The previously reviewed models all have varying temporal resolutions, but they do not include any spatial component to their analysis. Ruth et al. studied the economics of several IES configurations in several different locations [53]. Their IES included nuclear, hydrogen, thermal energy storage, and synthetic fuel options. The main findings were that if a system is profitable on its own, it was built into the IES complex. For example, synthetic fuels were prioritized in Texas where feed stocks were plentiful and desalination was prioritized in Arizona where water is expensive. The spatial component to the model was to study a few locations and pick a priori what the products would be in the location.

Table 2.1 is a summary of each of the dynamic TEA studies reviewed in this section.

2.5 Review Analysis And Recommendation

Much work has been done to assess the technical and economic feasibility of integrated energy systems. Process modeling work has been done extensively in various nuclear-hydrogen systems, especially electrolysis. Desalination process modeling is also well developed in literature. Static techno-economic analysis of IES is also well developed, but has shortcomings. Static electricity prices do not capture the value of price arbitrage or participation in different electricity markets.

Dynamic TEA in for various IES configurations is being developed in literature, but there are gaps and unique challenges. Much of the work has low temporal resolution, using representative days rather than hour or sub-hour timesteps over a year that are required to understand an IES participation in

Table 2.1: Dynamic TEA Literature Summary

Study	Reactor Type	Commodities	Electricity Market Representation	Stochastic or Deterministic	Temporal Resolution	Spatial Resolution	Sensitivities	Economic Metrics
Locatelli et al.	LWR (SMR)	Hydrogen	Real time and reserve	Deterministic	Hourly, representative days	General location	CAPEX, OPEX, H_2 cost	NPV, IRR
Frick et al.	LWR	Hydrogen	Day ahead market	Deterministic	Hourly over a year	Midwest U.S. (MISO)	H_2 market size, storage size, HTSE capacity,	NPV
Zhang	LWR (SMR)	Hydrogen (and wind)	Day ahead market	Deterministic	Hourly for four representative months	United Kingdom	Meeting load vs balancing economics	LCOE, IRR
Epiney et al.	LWR	Hydrogen (and wind)	Day ahead market	Stochastic	Hourly over a year	General Location	H_2 price, wind capacity, industrial process capacity	LCOE
Forsberg et al.	HTGR	Thermal energy storage (and solar)	Day ahead market	Deterministic	Hourly over a year	Tokyo	TES vs no TES, solar penetration	Generator revenue

diverse energy markets. Others exclude certain electricity market dynamics or commodity markets. Rarely are both markets included. The feedback of the IES on those markets is also rarely discussed.

In order to further the body of dynamic TEA work, four suggestions are given.

First, studies should focus on specific locations and conditions rather than use general assumptions. As seen in the literature review, a wide body of work has provided context for general IES. It is now important to understand the specific effects of regional electricity prices and markets, specific plant dynamics, and local laws.

Second, stochastic and off normal situations should be studied further. Electricity systems are designed to meet peak demand in each year and contend with a host of different events that may upset the standard diurnal or seasonal electricity demand curve. This could be done by using more stochastic model inputs or by understanding how an IES would behave in more extreme conditions. Either method would reduce uncertainty in IES economics and give insight into how different conditions would affect profitability or reliability.

Third, models should be run with several sensitivities to understand interplay between economic inputs. There are a host of cost drivers in these systems, including, but not limited to; nuclear cost, electricity price, commodity price, capital cost incurred when adding the commodity, amount of commodity that can be produced, or the amount of commodity that can be stored. Understanding the important cost drivers in context of one another is difficult and modeling efforts should aim to inform readers, stakeholders, etc as to how they might make informed economic decisions.

Lastly, dynamic TEAs should seek to quantify the effects of different operational modes. This could include when an IES expects to dispatch electricity versus dispatching its commodity and what the added value of that operation method would be. An example of operational methodology would be quantifying how a system might fill and discharge its storage units. This generally requires high temporal fidelity.

As always with electricity modeling, IES techno-economic models should be interpreted as a possible outcomes under the given assumptions rather than an exact prediction of future outcomes. As such is important to convey the assumptions and limitations of each case.

Chapter 3: Techno-Economic Analysis of Integrating Palo Verde Nuclear Generating Station with a Regional Desalination Plant

3.1 Introduction

One IES configuration pairs a nuclear plant with water desalination systems. These desalination plants can remove dissolved salts from sea or brackish water. The IES could then use the water for plant thermal cooling systems or sell potable water to industrial users or residential consumers.

Waste treatment is a large expense that affects the economic feasibility of new desalination systems. During regular operation, desalination plants create a highly concentrated saline waste stream. Most operating plants simply discharge this concentrate into the ocean, though there is significant environmental push back to the practice. A more ecologically friendly approach is to dispose of the concentrate in isolated evaporation ponds or inject it into very deep aquifers. Both of these solutions require significant capital investments [54]. Management of the concentrate is also important for inland desalination plants so that ground water sources are not contaminated. If some value can be found in the concentrate, or an outside process has significantly large water disposal and treatment capabilities, they could partner with desalination plants to take the waste.

This research proposes using an LWR nuclear plant as a partner to take desalination concentrate. If the nuclear plant can accept the waste stream from the desalination process, the system would not need to invest as much back end saline waste management. The nuclear plant would be able to receive the concentrate as "free" water or even charge a fee for taking the waste. The plant could then discharge salt concentrate via its own evaporation pond systems. Thus, both entities could potentially benefit from the relationship.

This type of system would be possible in nuclear plants with water purification and containment systems for wastewater after plant cooling activities. The Palo Verde Generating Station (PVGS) in Tonopah, Arizona is an example of a nuclear plant that already has the requisite water treatment and disposal capabilities. The plant is currently cooled by effluent wastewater from the Phoenix area. Water is initially treated at the Wastewater Treatment Plant (WWTP) on the outskirts of Phoenix and then sent to the PVGS site. Onsite, the Water Reclamation Facility (WRF) reduces total dissolved solids (TDS) to appropriate levels for use in the plant's forced draft cooling towers. The cooling tower blowdown, or liquid water left after the evaporative cooling process is complete, is sent to evaporation ponds. This water treatment and cooling system at PVGS is referred to as the tertiary loop.

In addition to the water treatment infrastructure, PVGS might also make a good candidate for coupling because water is expensive in Arizona. Any water that can be had for low cost could be of value to PVGS, even if it is concentrated. This creates potential economic incentive for PVGS to accept concentrate from a regional water desalination system.

The purpose of this work is to explore the value of a nuclear-desalination IES relative to standard nuclear operation. Traditionally, IES systems use energy provided by a nuclear plant to drive a process.

The modeling work provided in this chapter explores a novel configuration that use the nuclear plant's water system to manage the waste an reverse osmosis (RO) desalination plant would produce.

The study focuses on the PVGS nuclear plant, but other plants with wastewater treatment facilities or plants that are water investigating treatment additions can benefit from this work.

3.2 Case Description

This analysis investigates a dual RO water treatment system that is fully integrated with nuclear cooling loops. One smaller RO is co-located at PVGS, referred to as RO1. RO2 is a regional RO plant that produces potable water for sale to consumers or municipalities.

RO2 is located outside PVGS fence in the Phoenix area for the purposes of this analysis. Locating RO2 at PVGS is not ideal because both the west valley brackish water source and potable water consumers are located miles from the plant. An RO2 closer to population centers would reduce water transmission and pumping costs. The RO2 concentrate can be sent to the PVGS tertiary water system for management and disposal.

RO1, however, is located inside the fence at PVGS. RO1 is only used internally to purify the water in the PVGS tertiary water system. Co-locating RO1 at PVGS would also minimize pumping and treatment cost because the input comes from the WRF at PVGS and the desalinated water goes to the cooling towers. Co-location also allows RO1 to utilize PVGS's evaporation ponds for disposal.

The ROs in this analysis are assumed to be loosely electrically coupled with PVGS. RO2 would likely use grid electricity and RO1 could buy from the grid or use behind the fence electricity from PVGS. For the purpose of this analysis, assumed wholesale electricity prices are used. In the future, an onsite RO could benefit from thermal coupling to preheat inlet water.

To understand system economics, two cases were investigated.

3.2.1 Case 0

Case 0 represents the most economic configuration of Palo Verde's water system without any desalination, as found in [55]. Effluent water, or waste water, that is bought from area municipalities is sent from the WWTP to the WRF. The effluent water is then mixed with brackish water, which reduces overall cost by reducing the required amount of the expensive effluent water. Water is treated in the WRF to reduce concentrations of dissolved sulfates, calcium, and magnesium. The treated water moves to reservoir ponds where it is held for use in the PVGS cooling towers.

Mechanical draft cooling towers cool PVGS. The secondary loop heat is exchanged with the tertiary water loop in a condenser. The tertiary loop is connected to the cooling towers which cools the hot water via evaporative cooling. This in turn cools the reactor.

The discharge from a cooling tower is a concentrated liquid that must be managed. The amount of total dissolved solids (TDS) in the water source and the cycles of concentration dictate the TDS level of the blowdown, or discharge. PVGS is unique because it is designed to handle higher TDS and chloride levels than other cooling towers. In practice, this means the towers require more of cycles of concentration before discharging the concentrated blowdown.

The blowdown cannot simply be discharged to the environment like it could at other locations because of the higher initial TDS and higher outlet concentration. Instead, the water is sent to large, isolated evaporation ponds where it is contained.

The relation between mass of evaporated water, blowdown, and cycles of concentration is given in Equation 3.1. The blowdown mass flow rate, m_{BD}, is proportional to the mass flow rate of evaporated water, m_E, and cycles of concentration, *coc*. The salinity or TDS in the water and the cooling tower design limit set the cycles of concentration. A cooling tower that is more tolerant of salinity or TDS will run with a lower blowdown, effectively using less water.

$$m_{BD} = m_E/(COC - 1) \tag{3.1}$$

Figure 3.1 displays the flows and equipment for Case 0.

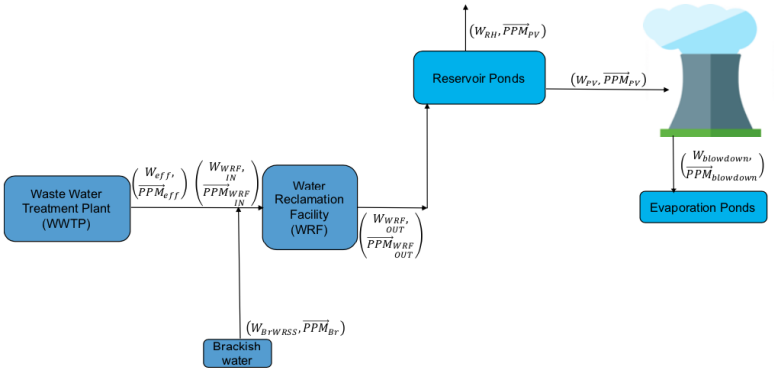

Figure 3.1: PVGS cooling water system for most economic configuration without any desalination. Note that the WWTP is located miles from the PVGS.

Case 0 is only used as a baseline by which capital and operating and maintenance costs can be compared to case 1.

3.2.2 Case 1

Case 1 takes the case 0 configuration and adds two RO plants.

RO2, the regional RO, draws brackish water from the a local aquifer and provides desalinated potable water to local municipalities. The concentrate, or waste stream, from RO2 is mixed with the effluent water and sent to PVGS. Case 1 also has an option to input brackish water from the brackish aquifer directly to the PVGS water system further reducing water costs. The WRSS water is treated in the WRF in the same manner as Case 0.

After the WRF, a certain slipstream is treated by RO1. This helps reduce the salinity of the water, which is especially important if PVGS accepts the concentrate from RO2 or receives brackish water directly. The slipstream percent, α, is designated as the percent of WRF outlet flow that is treated in RO1 and is the main driver for RO1 sizing. The RO1 waste stream is discharged to the evaporation ponds and the clean water is sent to the reservoir ponds. Water from the WRF that bypasses RO1 enters the reservoir ponds directly.

After the water enters the reservoir ponds, the water is sent to the cooling tower where it is used to cool the reactor. Water is evaporated and the remaining blowdown is sent to the evaporation ponds. Figure 3.2 shows the whole water system schematic for Case 1.

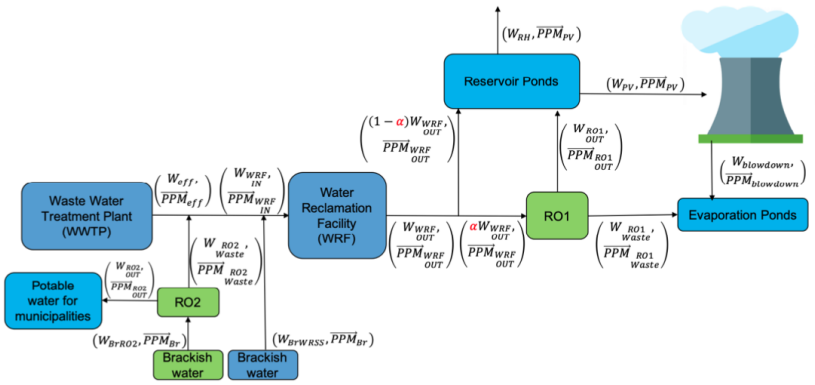

Figure 3.2: PVGS cooling water system with two ROs included; RO1 to control the tertiary water system chloride concentration and RO2 to produce potable water

3.2.3 Model Framework and Overview

Both the technical feasibility and economic competitiveness of the previously described IES desalination system are evaluated.

A model of PVGS and corresponding RO plants was developed using the Risk Assessment Virtual Environment (RAVEN) framework. RAVEN is a modeling tool that allows users to perform data analysis, advanced statistical regression, and optimization [56].

The RAVEN model manipulates inputs in order to run extensive sensitivity studies on physical and economic parameters. RAVEN takes a range of inputs for each studied variable and then samples the associated grid space. RAVEN manages each iteration and returns data for every point sampled, meaning that sensitivity studies can be run quickly.

With the inputs and sample space defined, RAVEN runs a physical model to determine PVGS circulating water system parameters. The water chemistry and flow at inlets and outlets of significant equipment and evaporation ponds are calculated. The model outputs determine the boundaries of feasibility.

The physical model outputs are sent to the Tool for Economic Analysis (TEAL) RAVEN plugin for tracking the system economics. Cash flow drivers are sent to TEAL where economic parameters including levelized cost of concentrate treatment and levelized cost of potable water. The economic information from TEAL is sent back to the RAVEN sampler, where RAVEN compiles each sensitivity run and outputs the calculated data.

3.2.4 Water System Model

The model used for this system tracks the inlet and outlet flows and concentrations at each piece of equipment or split-stream. At points of mixing, such as the addition of brackish water to the WRSS, weighted averages are used for calculating concentrations.

The WRF is modeled via a transfer function that scales cost with chemical usage. As dissolved solids in the inlet water increase, lime and soda ash dosage increase, increasing the variable costs. Shown in Equation 3.2, the variable cost of the WRF, V_{WRF} is a function of water concentrate and flow rate.

$$CV_j^0 = \sum_{i=1}^{12} V_{WRF}(W_{i,WRF_{in}}, PPM_{i,WRF_{in}}) \tag{3.2}$$

The RO plants were modeled using a low-fidelity surrogate model from the process described in [1] The RO operates in two stages and incorporates pumping and pre- and post-treatment requirements. A diagram of the RO system is given in Figure 3.3. Both RO1 and RO2 use this model.

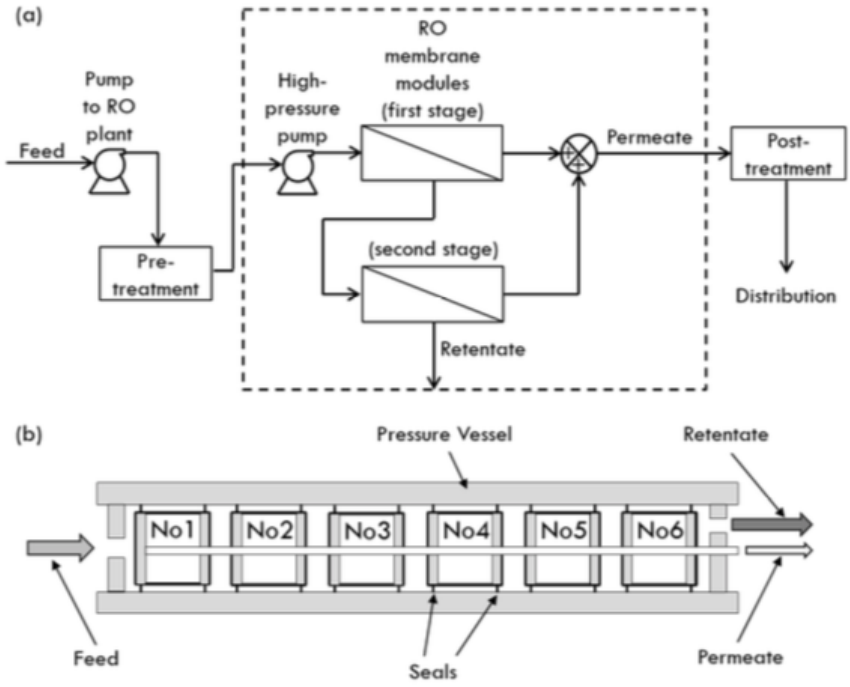

Figure 3.3: RO Desalination plant schematic. (a) Process flow diagram of RO system and (b) schematic of the RO vessel [44]

The low-fidelity surrogate is used in place of a complete process model so that the larger IES model can run quickly over many different sensitivities. Epiney et al. found that the surrogate model applied captured the RO power consumption with an R^2 of 1, which is sufficient for this modeling effort [1]. Equation 3.3 shows the RO power consumption (P_{RO}) as a linear function of flow rate (m_f). Table 3.1 shows the regressed parameters from the high fidelity models for fitting Equation 3.3. This model is valid for brackish ROs with salinity of 900 ppm or less. Pump power can be divided by 0.904 to find total RO power consumption because pumping accounts for 90.4% of an RO plant's power consumption.

$$P_{ro} = (k_1 * m_f + k_o) \tag{3.3}$$

Table 3.1: RO Model Constants

Parameter	Value	Unit
k_o	0.2886	W_e
k_1	1.5e3	$W_e * s/kg$

The cooling tower is assumed to operate at 25 cycles of concentration under normal operation. This equates to 4% of the water input to the cooling tower being sent to the evaporation ponds by volume. The cooling tower water requirement then scales linearly with chloride concentrations in excess of 450 ppm. The absolute operational limit of these cooling towers exceeds 12,000 ppm Cl^-.

3.2.5 Economic Model Inputs

The economic inputs are given in Table 3.2. A tax depreciation of 15 years for RO plants and 7 years for pumps was included. It is assumed that newly built equipment will retire at the same time as PVGS. The discount rate assumed is a real discount rate.

Table 3.2: Scalar Model Inputs

Parameter	Value	Unit
Number of Years	27	Years
Wholesale Electricity Price	35	$\$/MWh$
Retail Electricity Price	25	$\$/MWh$
Brackish Water Price	0.02	$\$/m^3$
RO Plant CAPEX	6.48e7	$\$/(m^3/s)$
Pump CAPEX	2.1e6	$\$/(m^3/s)$
Discount Rate	10%	-
Inflation Rate	3%	-
Tax Rate	21%	-
Cooling Tower Cycles of Concentration	25	-

The price of effluent water is represented as a multi-tiered structure that increases by water consumption and year. There is also a penalty that PVGS incurs for acquiring less than 9.87e7 m^3 effluent water per year. The penalty can be reduced by the amount of brackish water pumped directly into the WRSS. This means that if the PVGS tertiary water system takes in brackish water instead of effluent, it will not be penalized for reducing the effluent water below the contractual threshold.

Note that the WRF O&M cost, WRSS pumping cost, and cost of brackish water sent directly to WRSS are traditionally spread across a multi-party ownership group. This analysis only looks at the system from a single owner perspective, in this case APS. Those costs are multiplied by the APS ownership stake (29%) to represent the cost incurred by APS exclusively. The costs are handled in this manner so that the capital expenditures and revenues from building ROs can be realized by a single owner, simplifying the cash flow analysis.

The time dependent physical model inputs from PVGS operators are given in Table 3.3. The given values are historical averages for cooling needs and concentrations. Note that more cooling water is needed in summer months. Chloride concentration in the effluent water also increase during the summer. These numbers are directly input into the TEA model, so that salinity, cooling needs, and other dissolved solids' effect on costs are quantified.

Table 3.3 also lists the Redhawk Plant cooling water consumption. Redhawk is a natural gas plant that draws its cooling water from the PVGS reservoir ponds. This simply acts as a static water demand in the TEA models.

Table 3.3: Monthly Inputs to PVGS Water System Model

Month	Jan	Feb	Mar	Apr	May	Jun	Jul	Aug	Sep	Oct	Nov	Dec	Unit
PVGS Cooling	6.71e6	6.20e6	7.10e6	5.00e6	8.17e6	8.46e6	8.73e6	8.65e6	7.99e6	5.07e6	7.02e6	6.86e6	m^3
Redhawk Cooling	1.23e5	1.53e5	2.34e5	1.01e5	6.60e5	5.22e5	6.11e5	5.19e5	4.70e5	1.74e5	6.38e5	2.77e5	m^3
Effluent Calcium Concn	194.0	222.0	175.3	193.3	181.2	165.5	187.0	157.8	198.8	190.7	188.5	196.8	ppm
Effluent Magnesium Concn	140.0	154.0	139.5	135.7	132.4	139.3	150.8	141.8	143.0	139.3	146.0	142.8	ppm
Effluent Sodium Concentration	264.0	250.0	215.0	250.0	297.0	293.5	383.7	258.0	284.5	229.3	182.3	244.5	ppm
Effluent Alkaline Conc	163.0	175.0	169.3	160.0	154.4	164.0	161.0	151.4	153.5	159.7	169.5	166.5	ppm
Effluent Sulfur Conc	215.0	248.0	186.5	186.5	167.0	191.5	185.8	195.0	177.8	164.0	159.0	183.5	ppm
Effluent chloride Conc	301.0	345.0	292.5	292.5	359.0	445.5	477.0	448.8	471.0	353.7	168.0	286.0	ppm

3.2.6 Constraints and Sensitivities

This proposed IES has a highly interconnected water system that has several constraints that need to be adhered to.

First, the dissolved chloride concentration needs to be below 450 parts per million (ppm) concentration inside the cooling tower. Higher concentrations degrade components and concrete faster. This constraint is important because chloride concentration increases as more concentrate is sent from RO2 to the PVGS tertiary loop and/or as more direct brackish water is used. RO1 capacity has an inverse affect on chloride concentration, where a larger RO will be able to treat a greater percentage of the water going to the reservoir ponds and cooling towers. The concentration from the standard Phoenix effluent water also fluctuates throughout the year, which is accounted.

The second constraint, cooling tower blowdown flow rate, is set by the PVGS evaporating pond capacity. The blowdown is a function of the inlet salinity, with more water required if there are more dissolved chlorides in the inlet fluid. Blowdown limits are set by the operator at 4.38e6 m^3 (3550 Acre-Feet) or less per year.

Prior to the larger IES analysis, a case 0 sensitivity on direct brackish water input was run to understand the effect on dissolved chloride concentration and blowdown. Figure 3.4 shows the concentration in the reservoir pond (and into the cooling tower) as a function of direct brackish water injection. The system can take up to 1.9e7 m^3/yr of brackish water before the 450 ppm constraint is violated.

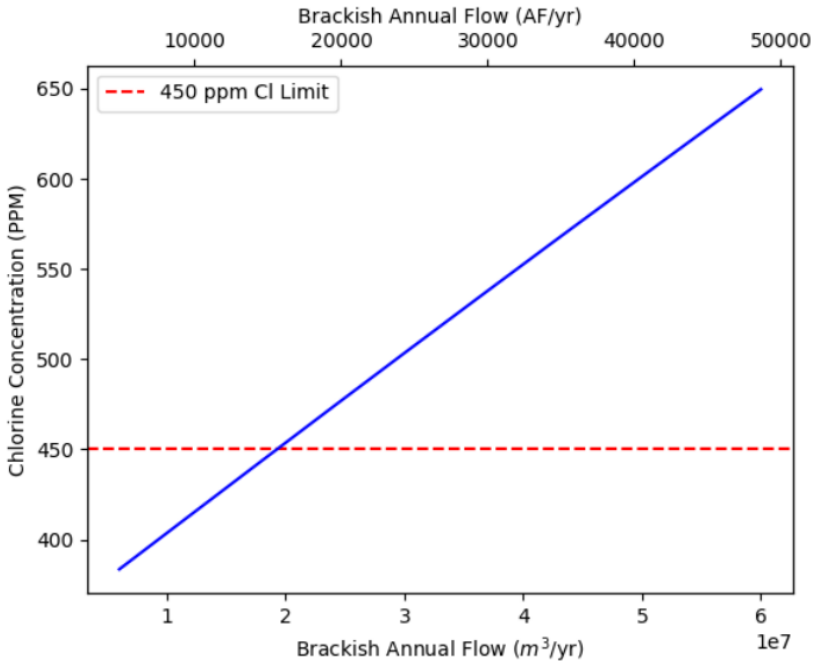

Figure 3.4: Reservoir pond as a function of direct brackish water input. The red line represented the upper bound of brackish water use based on the chloride concentration constraint.

The second constraint, the total blowdown, is shown in Figure 3.5 as a function of direct brackish water input. The red line is the brackish water input at which the chloride constraint is violated and the green line is limit of the blowdown constraint. The chloride concentration is the limiting constraint

in case 0. This analysis shows that at most, 1.9e7 m^3/yr of brackish water can be introduced into the cooling system. The optimal configuration of case 0 uses the maximum brackish water allowable in order to reduce effluent water acquisition cost.

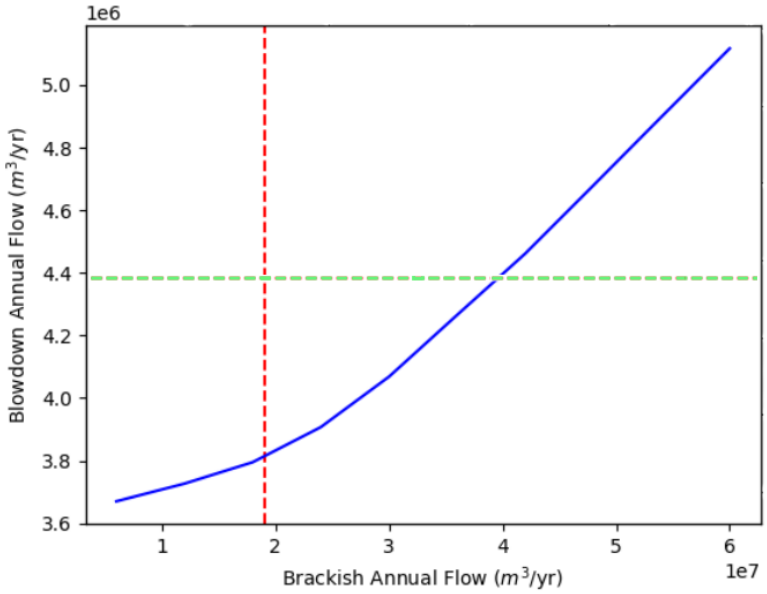

Figure 3.5: Blowdown flow rate as a function of brackish water input. The red line represents where the reservoir dissolved chloride constraint is binding. The green line represents the conditions where the blowdown flow rate exceeds allowable limits. Note that the system would violate the chloride constraint first, so the brackish water cannot exced 1.9e7 m^3/yr.

The preliminary case 0 tests informed the upper bound of direct brackish water injected into the system.

Table 3.4 shows the sensitivity limits that were run in the Case 1 model. The regional RO (i.e. RO2) capacity is driven by the amount of brackish water that is withdrawn. The upper brackish inlet limit in case 1 is set by the case 0 bounds.

Table 3.4: Case 1 Sensitivity Parameters

Parameter	Minimum	Maximum
Regional RO (RO2) Size, as inlet flow into RO	1.2e6 m^3/yr	3.6e7m^3/yr
PVGS RO (RO1) Size, as percent of reservoir pond stream treated (α)	0%	5%
Direct Brackish Water Input	0	1.9e7m^3/yr

3.3 Results

The results explore the RO capacities that adhere to physical constraints. Those capacities are then used as bounds to understand under what conditions the most economic configuration occurs.

3.3.1 Case 1 Physical Results

Case 1 required an understanding of the blowdown and salinity constraints. There are three variables that affect salinity; RO1 size, RO2 size, and direct brackish water input.

3.3.1.1 Waste Disposal Limits

Case 1 is bounded by the same blowdown limits as Case 0, but RO1 now contributes wastewater to the evaporation ponds. Blowdown in this section refers to all the wastewater sent to the evaporation ponds, including the RO1 waste and the cooling tower blowdown. The size of the regional RO and the input of brackish water to the WRSS were varied to find the largest RO2 that can be built. Blowdown as a function of RO1 and RO2 is shown in Figure 3.6. Larger RO1 facilities produce more waste than the evaporation ponds can handle when 3% of more of the water going to the cooling towers is treated.

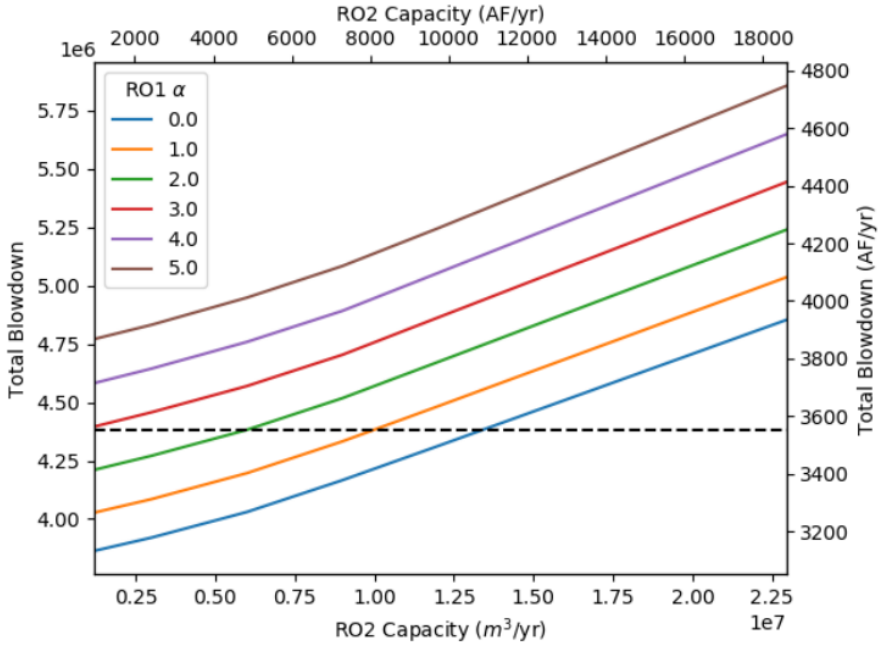

Figure 3.6: Total blowdown vs RO2 and RO1 size. Black line indicates the maximum amount the evaporation ponds can handle.

Figure 3.7 shows the same sensitivities with no RO1 and an RO1 added that treats 5% of the WRF output. Figure 3.7b shows that there is no configuration, regardless of brackish water injection, that satisfies blowdown constraint. This suggests that, on a purely physical basis, the RO1 is not necessarily required and, in some cases, can actually violate the blowdown constraint, thus inhibiting the use of brackish water as a supplementary feed to the nuclear cooling system.

3.3.1.2 Water Chemistry

Next, sensitivities were run to investigate water chemistry and find the optimal configuration based on chloride concentration. The regional RO concentrate and the brackish groundwater are consistent

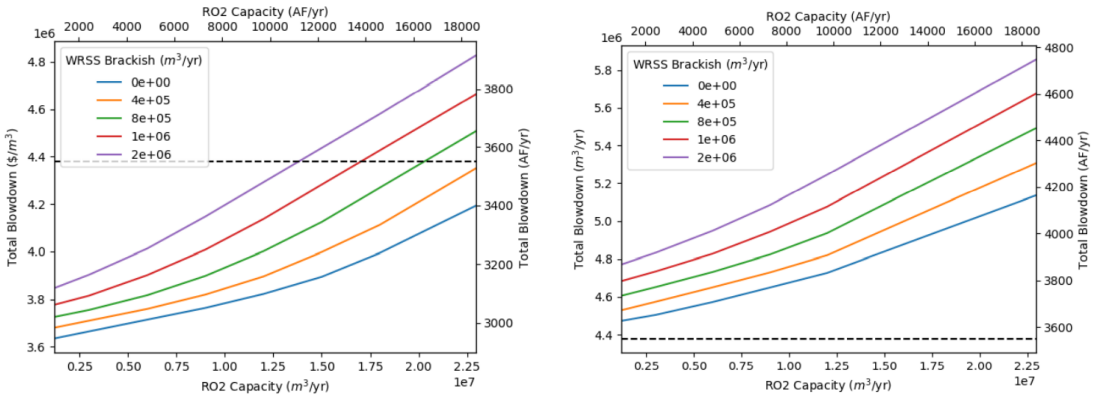

(a) (b)

Figure 3.7: Blowdown flows vs brackish water inputs for a) no RO1, and b) an RO1 that treats 5% of the cooling water.

throughout the year, but the effluent water fluctuates between 168 ppm Cl^- in the winter and 477 ppm Cl^- in the summer. Figure 3.8 shows the results varying RO1 and RO2 sizes with a fixed brackish input of 1.9e7 m^3/yr. Chloride concentration in the WRSS is a function of the RO2 capacity because the regional RO injects its waste concentrate into the WRSS. RO1 size has a very small affect on salinity because the purification reduces the blowdown and water requirement slightly.

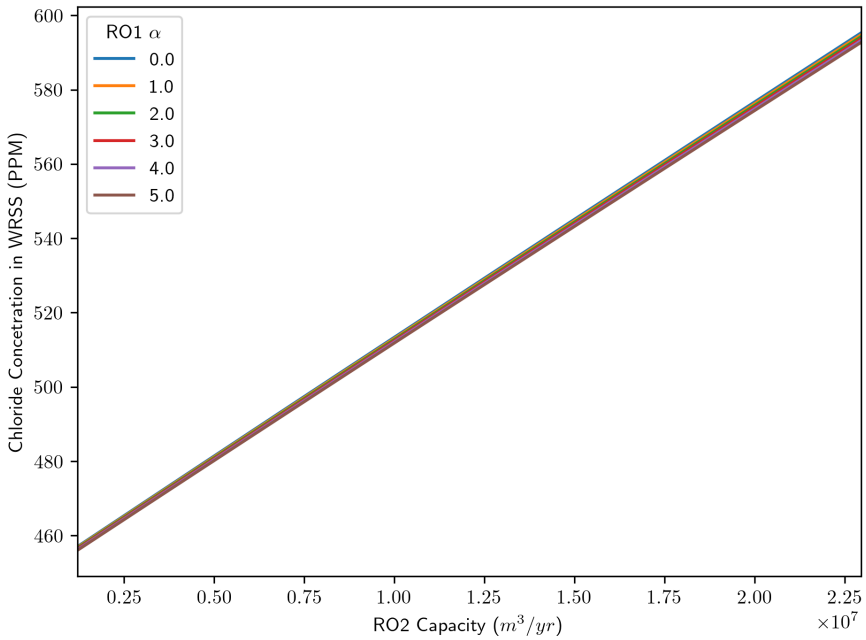

Figure 3.8: Chloride concentration in the WRSS as a function of RO1 alpha and RO2 size at 1.9e7 m^3/yr direct brackish input.

Figures 3.9 and Figure 3.10 show the average monthly constituents for WRF inlet and outlet, respectively. The shaded band represent the range of concentrations for the different RO1 and RO2 size

combinations that do not violate the blowdown constraint. The WRF has the ability to treat sulfur, calcium, and magnesium, as shown in the reduction from Figure 3.9 to Figure 3.10.

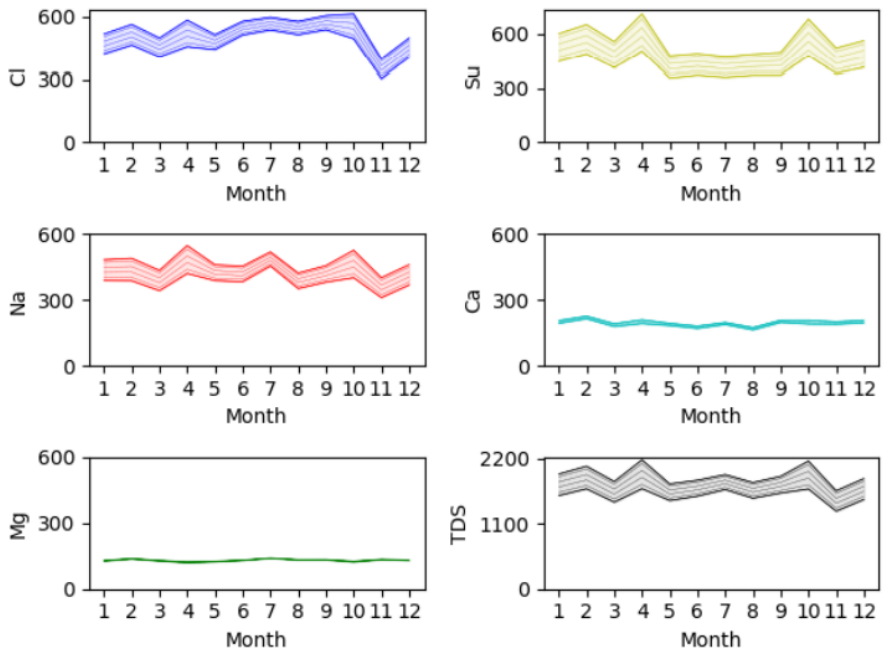

Figure 3.9: PVGS Water Reclamation Facility inlet. The shaded bands represent the physical limits at which blowdown limit is respected. Direct brackish water injection is at 1.9e7 m^3/yr.

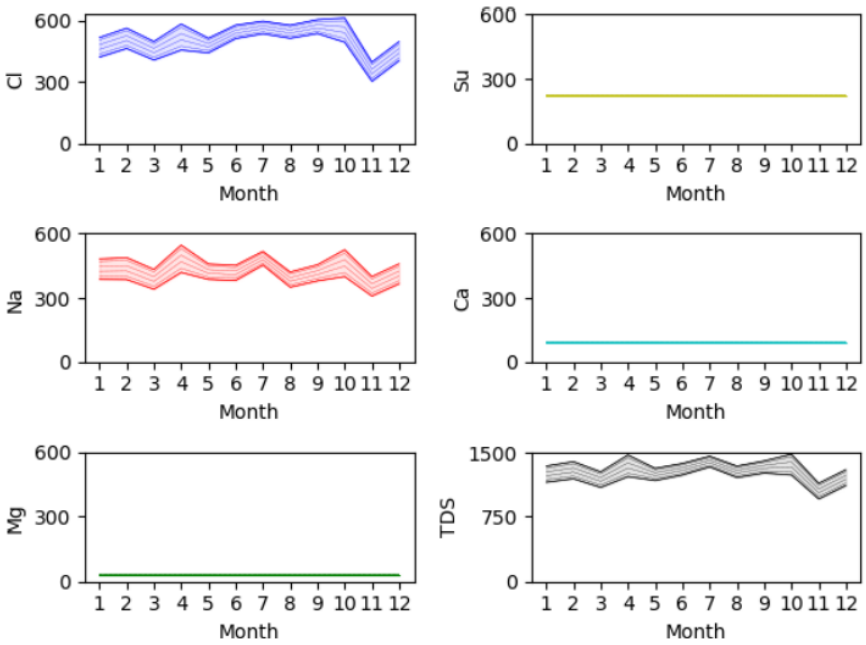

Figure 3.10: PVGS Water Reclamation Facility outlet. The shaded bands represent the physical limits at which blowdown limit is respected. Direct brackish water injection is at 1.9e7 m^3/yr.

After the water leaves the WRF, some split stream is treated in RO1 to reduce the salinity and the rest is sent directly to the reservoir. Figure 3.11 shows the average chloride concentration in the reservoir for various regional RO sizes. RO1 size (α) is also varied. The brackish input into the WRSS is set at 0. The reservoir chloride concentration surpasses 450 PPM at approximately 1.5e7 m^3/yr.

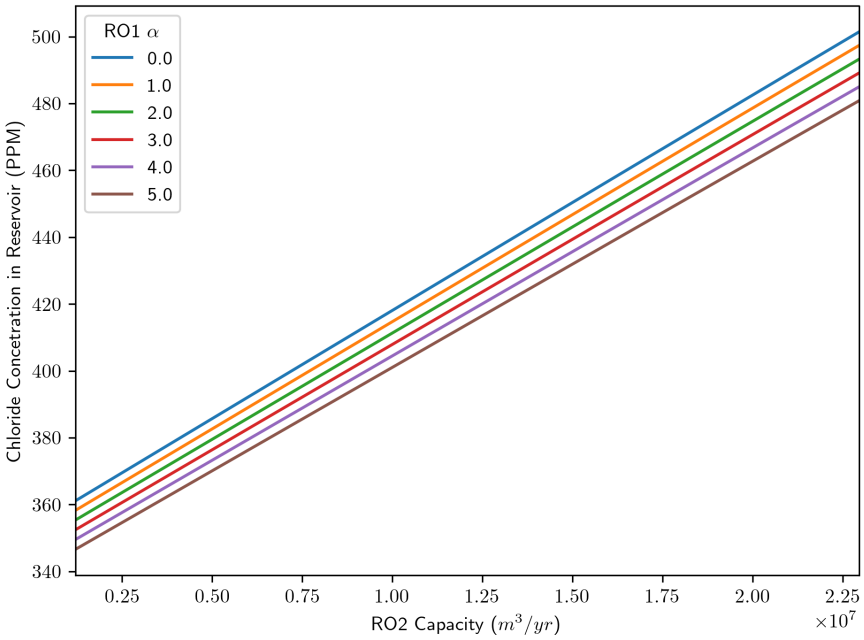

Figure 3.11: Chloride concentration in the reservoir as a function of RO1 alpha and RO2 size at 0 m^3/yr direct brackish input.

In Figure 3.12, which is reservoir chloride concentration as a function of RO2 capacity with a brackish WRSS input of 1.9e7 m^3/yr, the reservoir surpasses 450 PPM with either no RO1 and any size RO2, or the largest RO1 and a very small RO2.

The tertiary water system chloride margins are very small making it infeasible to take large amounts of brackish water and regional RO concentrate into the PVGS water system at the same time. A large RO1 would be needed for PVGS to take brackish water into the tertiary system with the RO2 concentrate. With the blowdown constraint analysis from the previous section, the only physically feasible system would be a regional RO with little to no brackish uptake into the WRSS and either a small RO1 or none at all.

To determine which configuration is recommended, the system economics were incorporated into the water system analysis.

3.3.2 Economic Results

Each cost in the overall IES system was set up to compare Case 0 to Case 1 for different sensitivities, including brackish water input and RO sizes.

Figure 3.13 shows the IES costs incurred within the PVGS fence in case 0 and case 1, as well as the change between the two. The WRF cost and water acquisition cost dominate the inside the fence costs, regardless of RO1 addition. Note that effluent water acquisition cost is lower in case 1 for smaller RO1

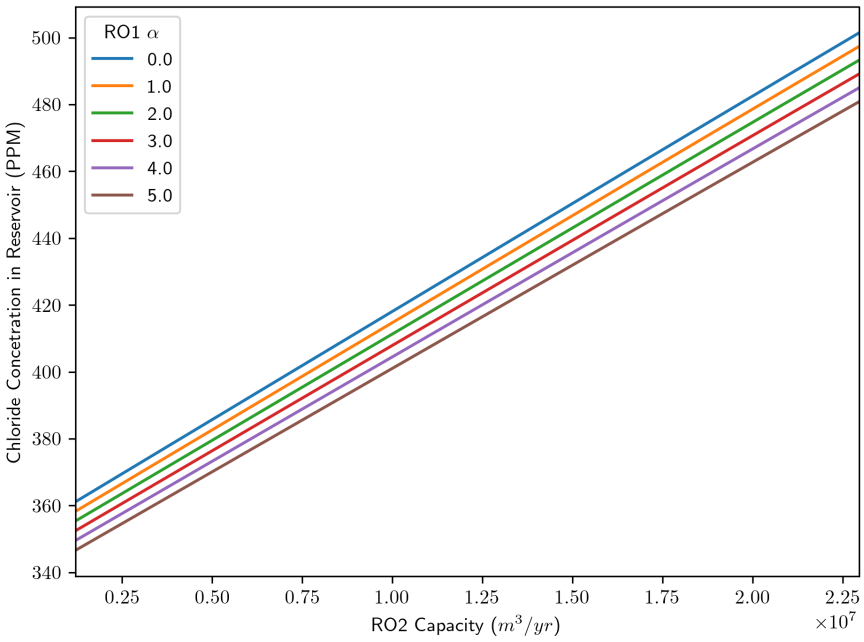

Figure 3.12: Chloride concentration in the reservoir as a function of RO1 alpha and RO2 size at 1.9e7 m^3/yr direct brackish input.

capacities. As RO1 increases size, more water is consumed in the system, so more effluent is acquired. The increase in inflows of water also increases the WRF O&M.

The outside the PVGS fence cash flows are shown in Figure 3.14. The plot only represents case 1 because there are no differing case 0 cash flows from outside the fence. Similar to RO1, RO2 CAPEX increases linearly with capacity. Pump CAPEX and O&M are quantified and also increase linearly with RO2 size because the there will be more concentrate that needs to be moved to the PVGS water system.

With each cash flow quantified, two metrics were developed to evaluate the overall economic fitness of this system: levelized cost of potable water (LCOPW) and levelized cost of concentrate treatment (LCOCT).

LCOPW is used when the entire system is under one economic umbrella. It represents the price that potable water from RO2 could be sold at to break even on the added capital and O&M associated with this entire IES system. This includes all water treatment facilities and both ROs. The LCOCT is used when the IES only encompasses the water treatment facilities and RO1 at PVGS. In this instance the regional RO would pay PVGS for the treatment of its RO concentrate. The LCOCT is the cost that the PVGS system would need to charge to break even on capital investments and O&M costs associated with accepting the RO2 waste. Charging for concentrate treatment would leverage PVGS tertiary water system without requiring a regulated utility to actually sell potable water. The cash flows involved in calculating LCOCT and LCOPW are shown in Table 3.5.

Because the system could be either a single IES economic entity or two distinct economic entities, both metrics are used.

Both the LCOPW and LCOCT represent break even points where the Δ NPV is zero. This means that the NPV from case 0, where there is no RO, is equal to the NPV from case 1 and both configurations'

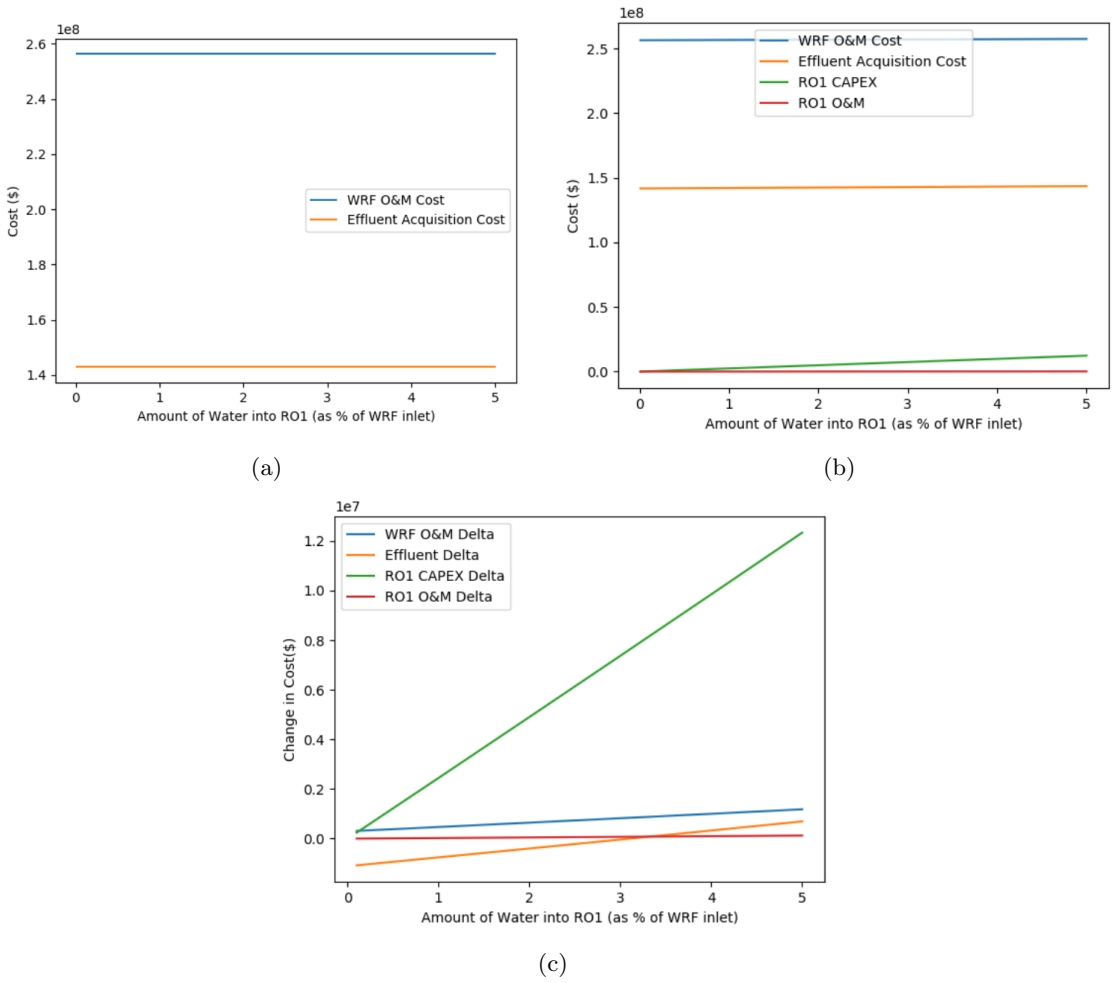

Figure 3.13: O&M and acquisition costs for the IES in both cases. a) Case 0 acquisition cost, b) case 2 acquisition cost, and c) the difference between the two cases. In (c), negative values mean that the cost in case 0 is greater than case 1.

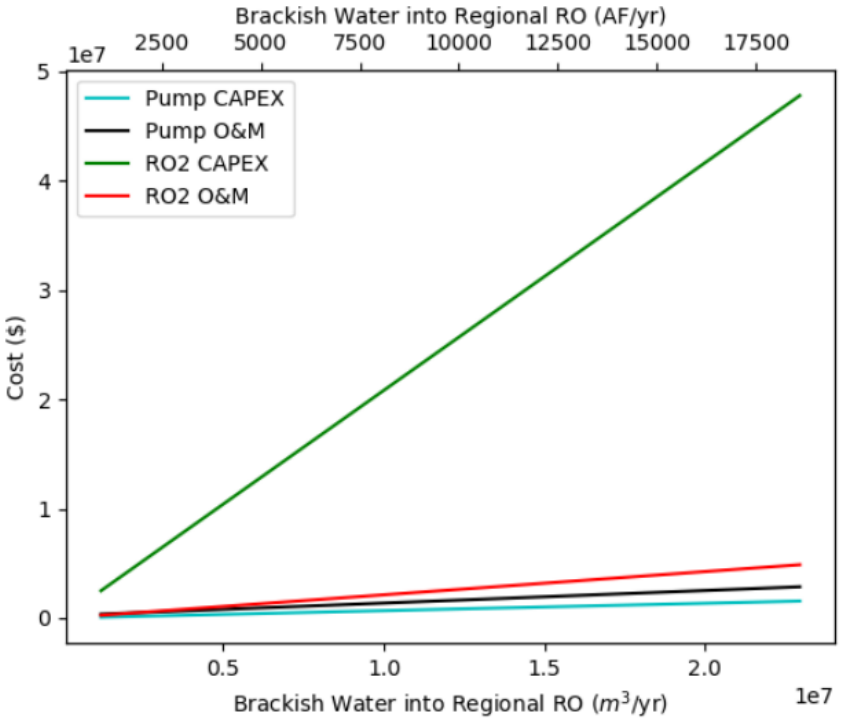

Figure 3.14: Case 1, outside the fence costs varied by RO2 capacity.

Table 3.5: Cash Flows included in LCOCT and LCOPW calculations

Parameter Name	Levelized Cost of Concentrate Treatment	Levelized Cost of Potable Water
RO1 CAPEX	X	X
RO1 O&M	X	X
Effluent Water Acquisition Cost	X	X
Brackish Water Pump	X	X
Brackish Water Pump O&M	X	X
WRF O&M	X	X
RO2 CAPEX	-	X
RO2 O&M	-	X
RO2 Concentrate Pump CAPEX	-	X
RO2 Concentrate Pump O&M	-	X

profitability is equal.

LCOCT is plotted in Figure 3.15 as a function of RO1 and RO2 size. Larger RO1 sizes result in higher LCOCT because more water is being consumed. Additionally, smaller RO2 capacities result in higher LCOCT. Larger RO2 plants require less effluent water is acquired and there is more concentrate to charge for on a per m^3 basis.

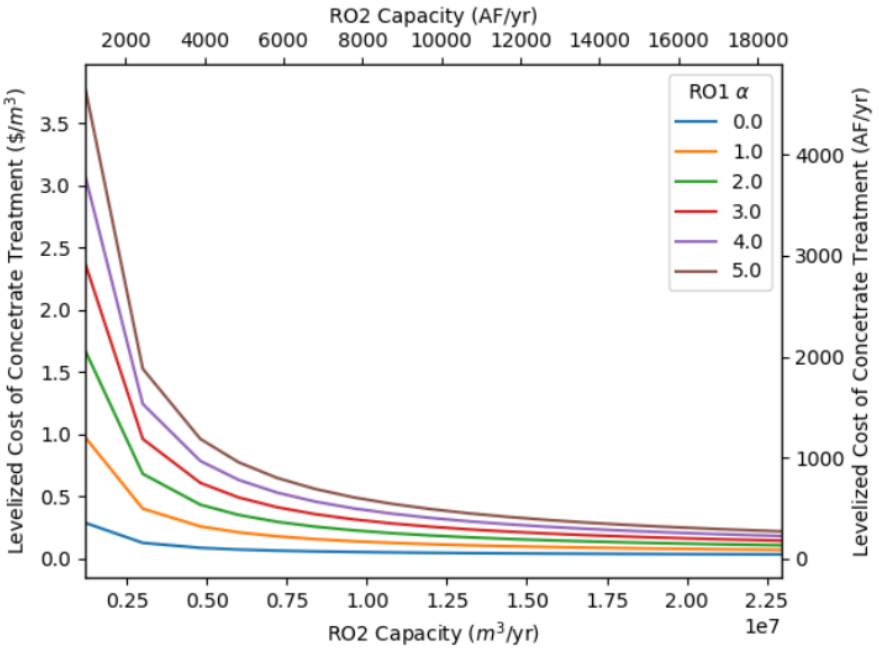

Figure 3.15: LCOCT as a function of RO1 and RO2 size.

Figure 3.16 shows the LCOCT as a function of direct brackish water input. The LCOCT is inversely proportional to the direct input of brackish water. This is the is the same, regardless of RO1 size. Adding more brackish water has the same effect as increasing RO2 size; more water is acquired by sources other than the effluent water.

The effects of brackish water uptake and RO size show the same trends as LCOCT. Figure 3.17 shows LCOPW as a function of the RO sizes. Figure 3.18 shows the effects of brackish water input on LCOPW.

The LCOPW and LCOCT reduction demonstrates that any ability to reduce effluent water can improve profitability at PVGS.

3.3.3 RO Efficiency Sensitivity

The effect of regional RO efficiency on LCOCT and LCOPW was studied. The default RO efficiency for RO2 treating the brackish input water was 60%. A model sensitivity was run to vary the RO efficiency between 60% and 90%. RO technology has been shown to reach near 90% efficiency in certain conditions.

Figure 3.19 shows the potable water flow based on RO2 size and efficiency.

The levelized costs as a function of RO2 size and efficiency are plotted in Figure 3.20. The plotted scenarios do not include direct brackish input or an RO1. The LCOCT increased as the regional RO

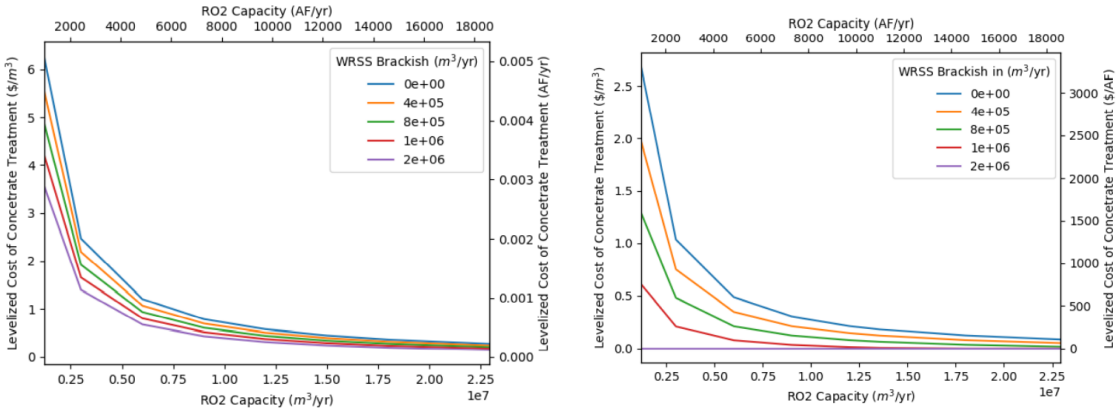

(a) (b)

Figure 3.16: LCOCT as a function of RO2 size and brackish water input. a) has an RO1 that treats 5% of the WRF outlet stream and b) has no RO1.

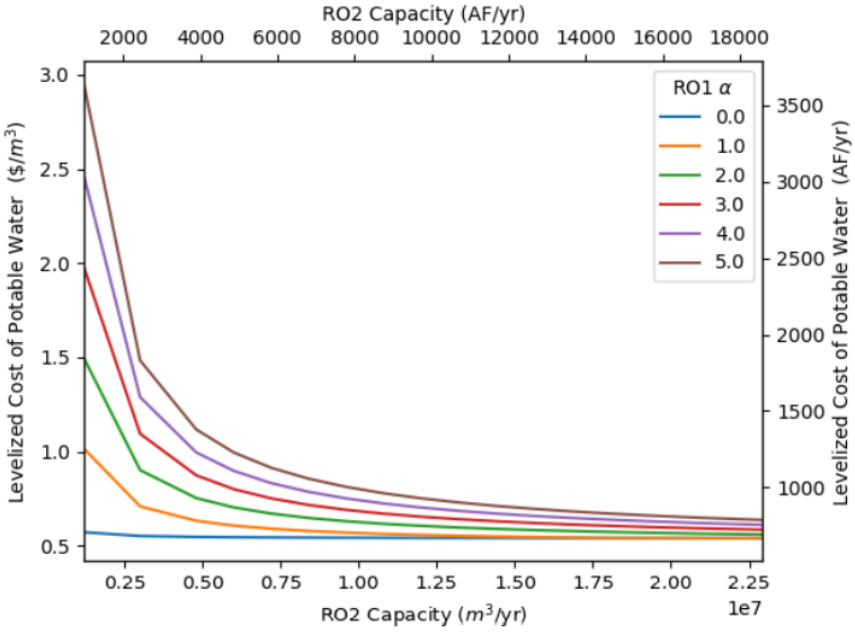

Figure 3.17: LCOPW as a function of RO1 and RO2 size.

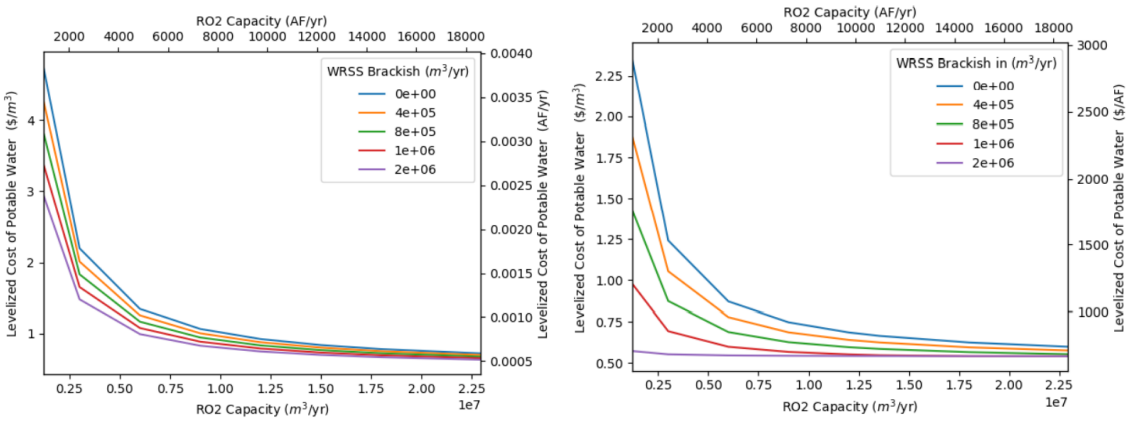

(a) (b)

Figure 3.18: LCOPW as a function of RO2 size and brackish water input. a) has an RO1 that treats 5% of the WRF outlet stream and b) has no RO1.

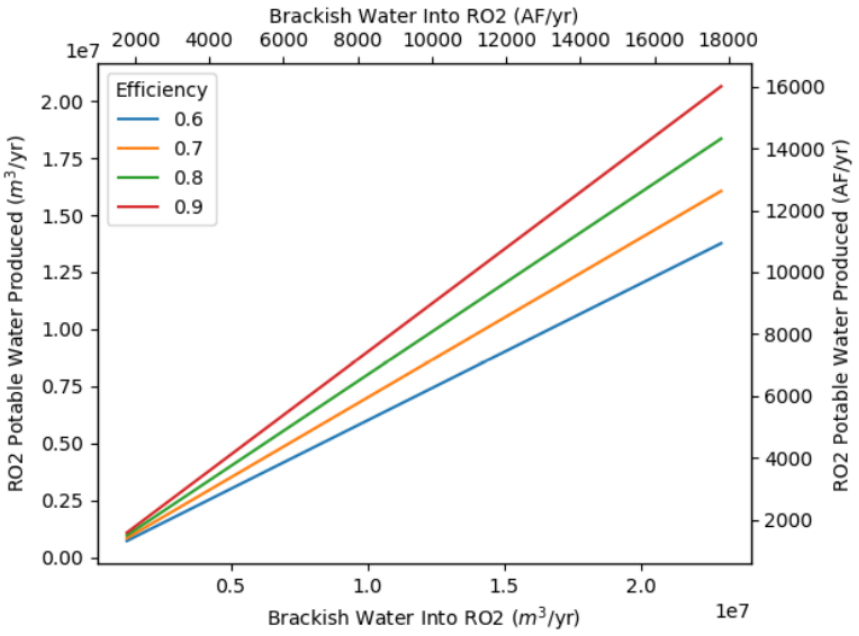

Figure 3.19: Effect of RO efficiency on potable water production.

became more efficient. This is because a lower volume of water comes to PVGS at a higher concentration. There is less water offset and more treatment required. On a per m^3 basis, PVGS would have to charge more for higher efficiencies.

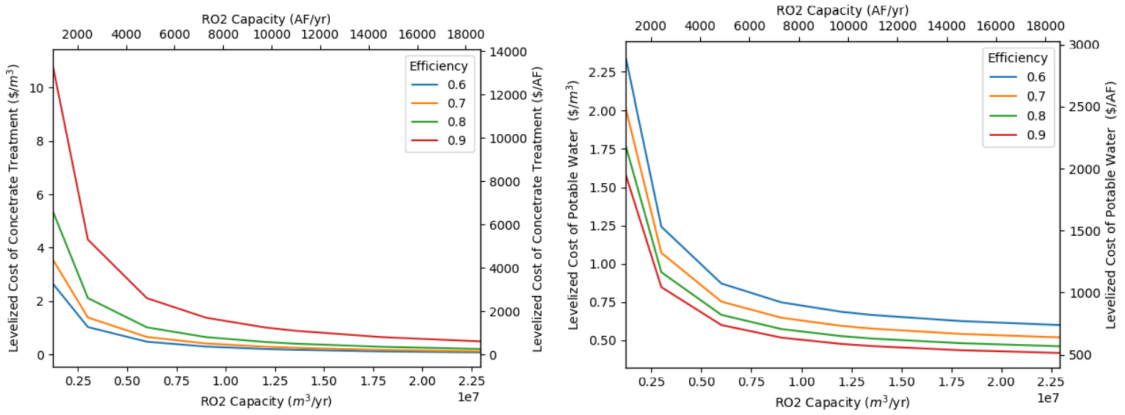

(a) (b)

Figure 3.20: LCOPW as a function of RO2 size and brackish water input. a) has an RO1 that treats 5% of the WRF outlet stream and b) has no RO1.

Efficiency has the opposite affect of LCOPW. The cost of potable water is brought down as efficiency increases because increased amount of water RO2 produces offsets the increased treatment costs that PVGS might incur. This illustrates that if the RO and PVGS water system are one entity, a more efficient system is advantageous. If they are not one system, PVGS would need to charge more to take the concentrate.

3.3.4 Financial Sensitivities

Two financial sensitivities were also looked at; PVGS lifetime and discount rate.

Each reactor at Palo Verde has received a license extension to run until 2046 or 2047. The base cases run the financial analysis until 2046. A second case was run to simulate PVGS receiving a second license renewal and running until 2066. The results are shown in Table 3.6.

Table 3.6: Effect of PVGS Lifetime on Levelized Costs

Parameter	Single License Renewal (27 years)	Second License Renewal (47 years)
LCOCT ($/m^3)	3.56	3.33
LCOPW ($/m^3)	2.95	2.76

The longer life is slightly more advantageous in both LCOPW and LCOCT. Discounting of the money reduces the effect that the later years will have, but longer lifetime is still a net positive. The longer lifetime would effectively smear the capital costs over a longer period.

3.3.5 Economically and Physically Feasible Configurations

With the data from previous sections outlining where the evaporation pond discharge constraint is satisfied, where the salinity is under the operational guideline, and where the system is economically feasible, a region of operation can be found. The region of operation, where both constraints are

satisfied and the system is economically the same as case 0, can be seen in the contour plots given in Figure 3.21, for both LCOCT and LCOPW. The region within the black box represents conditions where evaporation pond discharge constraint is satisfied. The region within the red box represents where the chloride concentration limit is satisfied. The region outlined in yellow designates where the system is within both physical limits. From this analysis, the lowest LCOCT and LCOPW can be found with a medium sized RO2 and a small RO1 (2-3% of water treated). For context, the regional RO at the optimal configuration of 16 million m^3 per year could provide water for 65,000 average Arizona households.

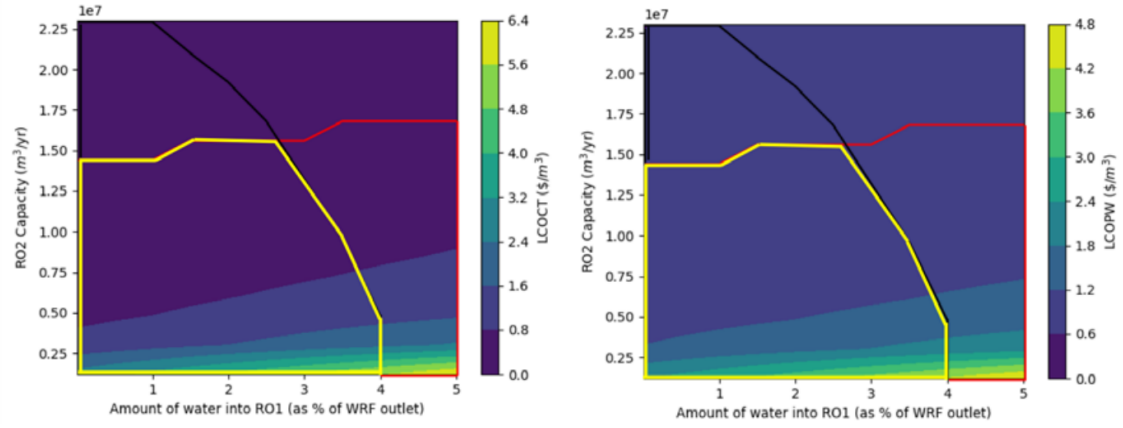

(a) (b)

Figure 3.21: Levelized cost of (a) concentrate treatment and (b) potable water for the PVGS water treatment system with a direct brackish water injection of 1.9e7 m^3/yr (15500 AF/yr). The black line show the limit of the blowdown constraint and the area under the red line shows where the chloride constraint is satisfied. The yellow box outlines the region where both constraints are satisfied.

The blowdown and salinity limits compete with each other. If the inlet water to the PVGS tertiary loop has too many dissolved chlorides, then an onsite RO1 is needed. In turn, that RO1 produces a large amount of liquid waste to be sent to the evaporation ponds. This can be seen in 3.21 where a larger RO1 can support a larger RO2 from a salinity perspective, but the evaporation pond discharge is generally only satisfied with smaller a RO1 (less than 4%). From an economic standpoint, maximizing the regional RO size reduces LCOCT or LCOPW.

The scenarios without direct brackish water injection are also plotted to investigate where the system would be technically and economically feasible. Figure 3.22 shows the bounds of technical feasibility overlaid the LCOCT and LCOPW for various RO sizes. Note that the red box, regions where the salinity constraint is met, and the black box, regions where the blow down constraint is met, never overlap. There is no technically feasible solution for this water system when brackish water is input directly into the WRSS.

When viewed against each other, the plots in Figures 3.21 and 3.22 show that brackish water should not be directly injected into the PVGS water system when ROs are present. This report did not explore intermediate brackish flow amounts, so there may be a smaller flow rate of brackish water that satisfies all conditions and is economically advantageous. The effect of brackish water on overall LCOCT or LCOPW was small when large RO2s were present. Future work could explore the direct brackish water injection effects in greater detail.

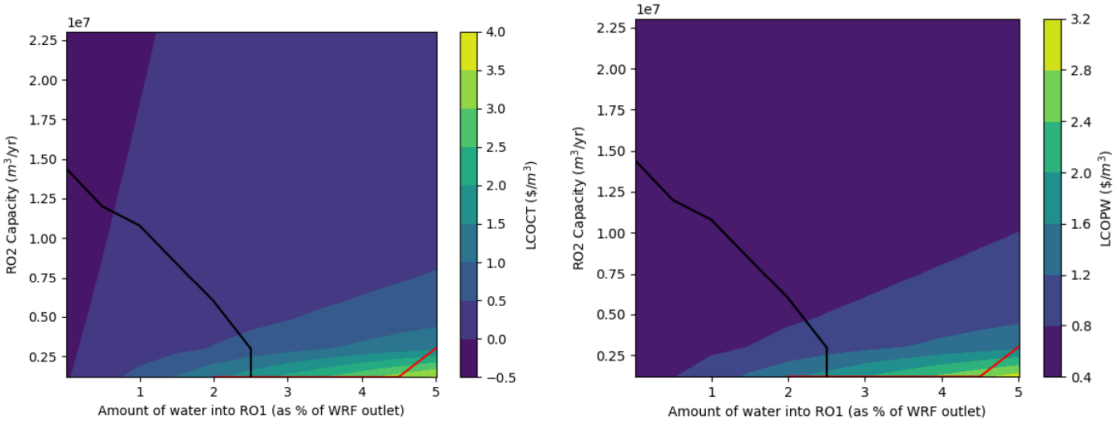

(a) (b)

Figure 3.22: Levelized cost of (a) concentrate treatment and (b) potable water for the PVGS water treatment system with a direct brackish water injection of 1.9e7 m^3/yr (15500 AF/yr). The black line show the limit of the blowdown constraint and the area under the red line shows where the chloride constraint is satisfied. There is no overlap of the two, so there is no case where both constraints are satisfied.

3.4 Conclusions

This research proposes a method for coupling reverse osmosis desalination with an existing nuclear plant. The Palo Verde Generating Station was researched because of its unique water system and proximity to brackish water. The system provides a way that potable water could be produced and RO waste be disposed of.

It was found that the PVGS tertiary water system could handle concentrate up to 14 million m^3 simply by increasing the cycling in the cooling towers and disposing of the blowdown water in evaporation ponds. Larger regional RO plants would require an onsite RO system to reduce salinity. Economically, the ideal case would be to size the regional RO to avoid the onsite RO.

PVGS taking the RO2 concentrate treatment without the need for a second RO demonstrates good synergy for this integrated energy system as a whole. The RO plant can produce water for sale in the developed areas and the PVGS facility can take the concentrate water, reducing its overall water consumption.

In the future, this work could be extended to other nuclear plants, especially those with onsite water treatment facilities or cooling towers. This research is not meant to make recommendations on water rights and permitting, but rather to demonstrate the ability of a nuclear plant to economically facilitate water production and treatment.

3.5 Acknowledgements

The research work in this chapter was performed by a contractor of the US Government for the U.S. Department of Energy, Office of Nuclear Energy (DOE-NE), under DOE-NE Idaho Operations Office contract DEAC0705ID14517.

Chapter 4: Economic Dispatch Model of Nuclear High-Temperature Reactor with Hydrogen Cogeneration in Electricity Market

Richards, J.; Rabiti, C.; Sato, H.; Yan, X.L.; Anderson, N. "Economic Dispatch Model of Nuclear High-Temperature Reactor with Hydrogen Cogeneration in Electricity Market." *Energies*, vol. 14, 2021, https://doi.org/10.3390/en14248289

4.1 Introduction

In recent years, research on hydrogen use, production methods, and economics has increased as countries began attempting to reduce their carbon footprints. As a power source, hydrogen offers flexible electricity generation, with the potential to serve as load following or peaking power units. Hydrogen could also be used to shift electricity demand to off-peak hours, acting as a large-scale demand response or energy storage medium. Producing hydrogen via nuclear power and using it as a flexible load resource is being investigated by numerous organizations [57, 58, 59] . Several of these nuclear hydrogen configurations are also currently in development.

These nuclear integrated energy systems (IES) could provide economic benefits to nuclear power plants (NPPs). Competing with cheap fossil resources and declining renewable energy costs has left NPPs at an economic disadvantage [60]. Hydrogen production allows NPPs to diversify their revenue streams, and has potential to increase NPP profitability [49].

In Japan, fossil fuel import requirements have led to high electricity prices and investigation into methods of producing electricity cheaply and locally [61]. Nuclear power could be advantageous to fossil fuels, since uranium is much more energy dense, requires less frequent imports, and can be stored onsite for future use. Furthermore, following their initial installation, sources of renewable energy do not require any additional imports. Combining these technologies in a way that also reduces carbon emissions while maintaining low electricity prices is important for the future of Japan's electricity system. An IES that enables NPPs to sell a secondary commodity instead of losing money on electricity sales could help boost overall system profitability.

Besides addressing cost and security concerns, hydrogen produced via nuclear energy could help in meeting the greenhouse gas reduction goals set by Japan's Ministry of Economy, Trade, and Industry (METI). METI has also set cost-reduction goals for hydrogen produced via low- or zero-emission sources [62]. With sufficient infrastructure, this clean hydrogen could be used to aid in decarbonizing Japan's industry or transport sections. Currently in Japan, hydrogen is sold at a wholesale price of 100 JPY/Nm^3. METI's goal is to reduce this price to 30 JPY/Nm^3 by 2030, and to 20 JPY/Nm^3 by approximately 2050 [62].

Government and research entities in Japan have also achieved expertise in nuclear high-temperature gas-cooled reactors (HTGRs) and the applications thereof. The operating High-Temperature Engineering Test Reactor (HTTR) has aided in acquiring HTGR experimental and operational experience. The HTTR is a 30-MW_{th}, helium-cooled reactor that uses graphite moderated prismatic fuel assemblies.

The outlet temperature is 950°C—high enough to integrate different process applications (e.g., hydrogen production) for testing purposes [63].

The iodine-sulfur (IS) cycle for hydrogen production appears a strong candidate for pairing with an HTGR [23]. The IS cycle utilizes a Bunsen reaction to convert water, I_2, and SO_2 into HI and H_2SO_4. The HI is then split up into its hydrogen and iodine components. A side reaction converts the H_2SO_4 into SO_2, water, and oxygen, thus completing the cycle. The reactions are listed in Table 4.1.

Table 4.1: IS Cycle Reactions

Stafe	Reaction
Bunsen Reaction	$I_2 + SO_2 + 2H_2O \rightarrow 2HI + H_2SO_4$
H_2SO_4 Decomposition	$H_2SO_4 \rightarrow 2SO_2 + 2H_2O + O_2$
HI Decomposition	$2HI \rightarrow I_2 + H_2$
Net Inputs/Outputs	$2H_2O \rightarrow 2H_2 + O_2$

Several difficulties have inhibited the deployment of IS cycles, such as heat input and material requirements. This cycle requires high quality heat at upwards of 800°C for the H2SO4 decomposition reaction, meaning that coupling with the current fleet of light-water reactors is difficult because they output steam at approximately 300°C [64]. Additionally, material challenges associated with catalyst, reactant and container interactions or highly corrosive environments require special materials, such as Hastelloy C-276 [65], zirconium alloys [66], or special design features that isolate highly acidic environments from metals to avoid acidic oxidation.

Because of the unique positioning with an operating high temperature reactor, the Japan Atomic Energy Agency (JAEA) has emphasized the development of the IS cycle for hydrogen production [65], going so far as to design an HTTR and IS cycle co-generation facility known as the HTTR-GT/H_2. The HTTR-GT/H_2 is a design for coupling the HTTR with an IS cycle in order to demonstrate hydrogen–HTGR coupling capabilities. The process diagrammed in [66] adds an intermediate heat exchange system to the HTTR in order to send heat to the nuclear-IS. A turbine for generating electricity is also planned. Thus, the demonstration could entail the choice of whether to dispatch and sell hydrogen or electricity, depending on regional electricity prices, hydrogen agreements, or other economic incentives.

While the technical development of the HTTR-GT/H_2 has been detailed in previous studies, this report focuses on developing a techno-economic model to flexibly dispatch the HTTR-GT/H_2 for electricity and/or hydrogen co-generation. The goal is to investigate the potential impacts of different input assumptions or real-world conditions on the profitability of such a system. This work seeks to improve our understanding of the assumptions necessary for eventually making investment decisions pertaining to commercial hydrogen systems.

The HTTR-GT/H_2 system was chosen for this economic model, due to its simple design and the availability of process modeling data. Compared to commercial-scale systems, the HTTR-GT/H_2 is relatively small, both in terms of nuclear plant size and hydrogen production. The small size means that electricity price feedback to the operation changes of the HTTR-GT/H_2 would be minimal. The HTTR-GT/H_2 has undergone detailed process modeling and has developed operation modes. Knowing the operating conditions for both the electricity sale and hydrogen sale modes makes the economic dispatch easier to model, and the smaller nature of this system helps further simplify the problem, since the system would participate in fewer electricity markets and have a lessened impact on the electricity

and hydrogen markets at large. This makes the impact of certain inputted data (e.g., electricity price data) more readily apparent. These effects and assumptions should be known prior to expanding this modeling methodology to larger, commercial systems as part of a broader study.

The HTTR-GT/H_2 dispatch model acts as a price-taker model. Electricity is sold when regional electricity prices exceed the HTTR's operating costs, and hydrogen is produced when the electricity price falls below HTTR-GT/H_2 electricity production costs. The hydrogen is produced via the co-located IS cycle, as detailed in [34]. The price-taker assumption means that the model does not have any feedback between the changing load from the nuclear-IS cycle and grid electricity prices. This assumption is generally made for small generators and loads, such as the HTTR-GT/H_2.

The goal of the dispatch model is to determine the price at which the system can sell hydrogen while breaking even economically. This price, also known as the levelized cost of hydrogen (LCOH), is the point at which sufficient money is made to justify building the hydrogen facility and dispatching energy to hydrogen production instead of selling only electricity.

The dispatch model was developed using the Risk Analysis Virtual Environment (RAVEN) model, developed at Idaho National Laboratory [56]. Two RAVEN plugins, the Holistic Energy Resource Optimization Network (HERON) and the Tool for Economic Analysis (TEAL)—also developed at Idaho National Laboratory—were used for creating the dispatch algorithm and tracking the economic parameters within the model [67].

4.2 HTTR-GT/H_2 Dispatch Model Methodology

The HTTR-GT/H_2 dispatch model was developed to generate insights into the optimal dispatch of nuclear IES and how different factors can affect that dispatch. As such, this model demonstrates how the HTTR-GT/H_2 might best be dispatched in response to fluctuating hourly electricity prices throughout the year. The model also allows for investigation of different input assumptions and their effect on the stochastic optimization of decision to dispatch hydrogen or electricity.

4.2.1 Modeling Framework

The RAVEN framework is a multi-purpose optimization, data analysis, and uncertainty quantification code. It can be used in conjunction with the HERON plugin to develop economic dispatch models.

HERON creates a two-loop dispatch algorithm that incorporates RAVEN's optimization and synthetic time history generation abilities. The general structure of the stochastic dispatch model is given in Figure 4.1. The outer loop optimizes some grid parameter(s) (e.g., generator capacity), while the inner loop samples synthetic time histories, performs the economic dispatch, and tracks discounted cash flows via the TEAL plugin.

The HERON plugin was used to build the HTTR-GT/H_2 dispatch model in RAVEN. HERON simplified the creation of this model, which might otherwise prove complicated for typical RAVEN users. HERON enables users to quickly develop inputs based on technology prices, commodities such as electricity or hydrogen, and the hydrogen and electricity markets. HERON then translates these user-friendly inputs into RAVEN scripts that utilize RAVEN's sampling, data transfer, and stochastic optimization capabilities to perform the dispatch.

Figure 4.2 shows the decision process for the HTTR-GT/H_2 dispatch model. This specific dispatch model utilizes an inner loop to perform the hydrogen/electricity (e- in Figure 4.2) dispatch, and an outer

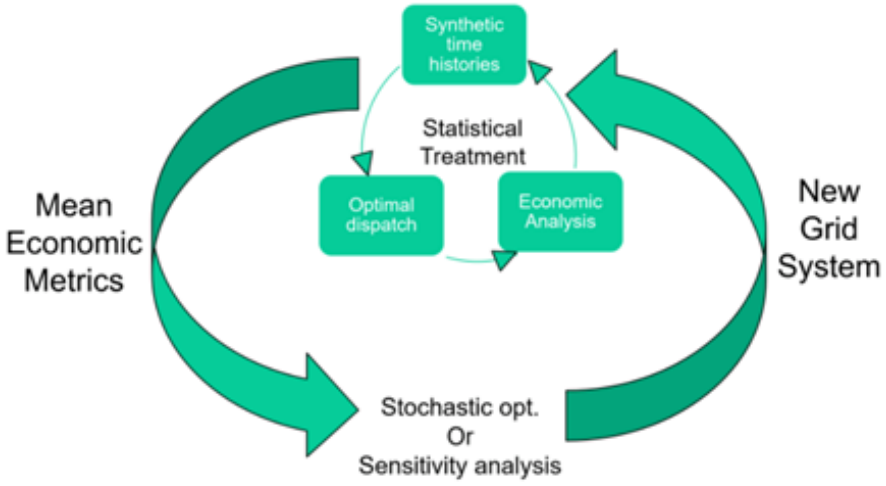

Figure 4.1: General schematic of the HERON dispatch model workflow [67].

loop to track hydrogen prices.

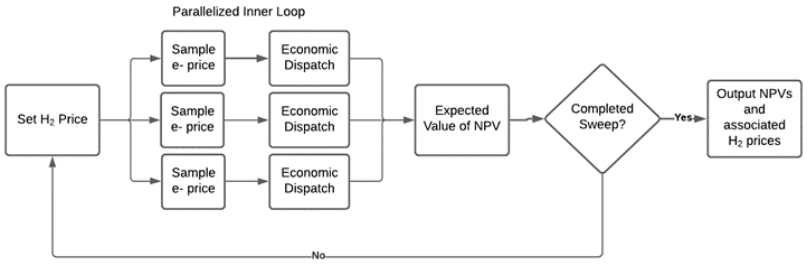

Figure 4.2: Algorithm used in the HTTR-GT/H_2 price-taker dispatch model. The model can run a different inner loop for each stochastic time history in order to generate an expected net present value.

4.2.2 Synthetic Time History Production

For the dispatch model to perform the stochastic optimization, a method of producing synthetic data was required. An autoregressive moving average (ARMA) model coupled with a Fourier series detrending model, known as a FARMA model, was trained and used to produce synthetic electricity-price time histories. RAVEN's capabilities allow users to train a FARMA on historical, time-dependent datasets, then sample that model to create synthetic time histories. The FARMA model takes a time history as input and uses a Fourier fast transform to extract the signals that occur on different time scales. The Fourier detrending equation is given in Equation 4.1, as taken from [68]:

$$x_t = y_t - \sum_{i=1}^{p} [a_m sin(2\pi f_m t) + b_m cost(2\pi f_m t)] \tag{4.1}$$

After the Fourier detrending, the ARMA statistically quantifies the noise and allows for stochastic reproduction in future samples. The Fourier detrend pulls out all the strong, time-dependent trends in the dataset, leaving the noise. An ARMA algorithm can be used to model that noise. Equation 4.2

describes the ARMA process:

$$x_t = \sum_{i=1}^{p} \Phi_i x_{t-1} + \alpha_t + \sum_{j=1}^{q} \Theta_j \alpha_{t-1} \tag{4.2}$$

where x is the output vector for a given dimension n. The input vectors, θ and ϕ, are n by n matrices, and α is the error term. The variables p and q are the autoregressive and moving average terms, respectively. When parameter p is zero, only the moving average is used. When q is zero, the process is exclusively autoregressive.

The dispatch model can then sample the FARMA model and produce large numbers of synthetic time histories for stochastic optimization purposes. As a price-taker model, its dispatch is based on economic decisions dependent on the electricity prices from trained FARMA.

Historical electricity prices for the HTTR operating region (i.e., the Tokyo region of Japan's electricity system) were used for training the FARMA model. The HTTR-GT/H_2 was assumed ineligible for the non-fossil or baseload markets, due to its status as a small-scale test reactor. Larger commercial reactors could likely participate in the spot and intraday markets, in addition to the baseload and non-fossil markets. The input data were separated into 30-minute increments covering a 1-year period. Prices reflect 2018 historical prices.

RAVEN's advanced clustering methods were leveraged to improve the accuracy of the synthetic price data [68]. While the Fourier detrending is useful for capturing seasonal effects, the clustering takes it a step further by isolating those segments with major differences.

RAVEN clustered the data set into representative 4-day periods. Each representative 4-day period is known as a cluster, and each cluster was trained as an individual FARMA. By training these individual 4-day clusters—as opposed to a single FARMA—over the year, RAVEN can achieve improved accuracy by further isolating the effects of long-term seasonal trends. Each specific 4-day window, or segment, is then assigned to the cluster that best represents it. The clustering algorithm offers improved accuracy compared to over-training the FARMA over the entire year.

Figure 4.3 shows each cluster and the time at which it occurred in the year. Each panel shows the 4-day periods that are similar to each other and are thus representable by a single FARMA model. Note that the 4-day periods in the shoulder months (usually in the spring and fall) tend to be similar. Additionally, the summer or winter peaks may have only a few 4-day segments in their cluster. This is a feature of the clustering algorithm: by training a different FARMA for each representative window, the peak price events will not impact the production of synthetic data for the more typical shoulder months.

In Figure 4.4, a complete synthetic time history is plotted against the original data. This synthetic history reflects a possible time history of electricity prices that is statistically similar to the original input data. The FARMA can be sampled many times over to produce a broad range of synthetic time histories statistically similar to the input price profile.

For each model run, the FARMA was sampled 100 times to reduce the modeling uncertainties in the input electricity prices. The price duration curve (PDC) is shown in Figure 4.5.

The historical PDC is largely identical to the average synthetic PDC, except when comparing the 100 or so highest electricity price hours.

This dispatch model will be used to investigate the impact of the PDC discrepancy found in the 100

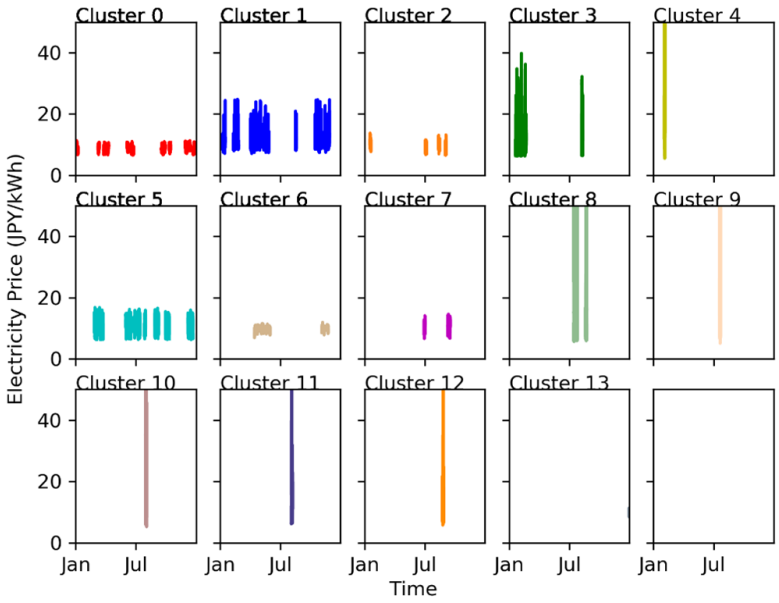

Figure 4.3: Four-day segments plotted by cluster, as produced by RAVEN when training the FARMA.

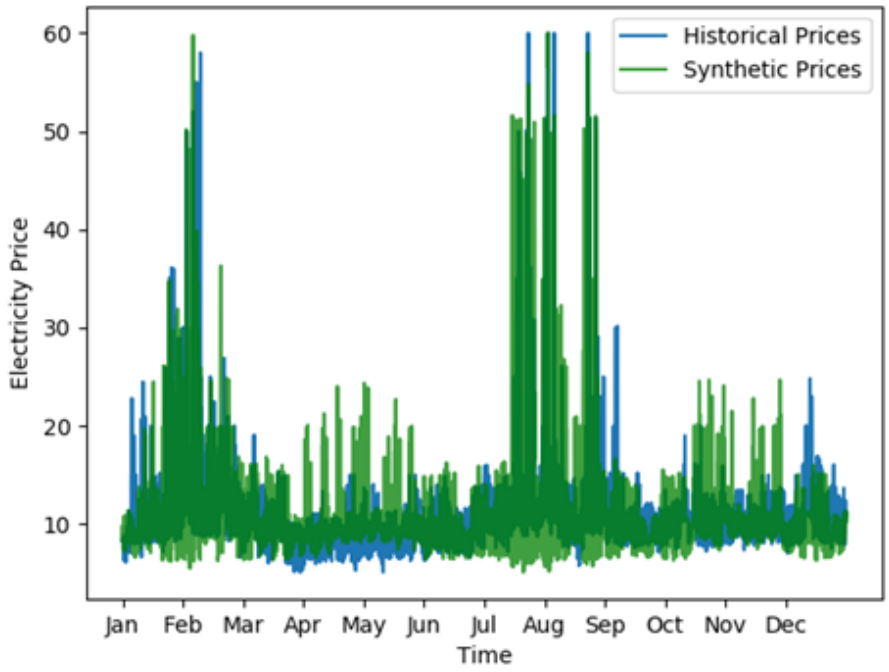

Figure 4.4: Historical 2018 Tokyo region electricity prices plotted against the synthetic time history produced by sampling the RAVEN FARMA.

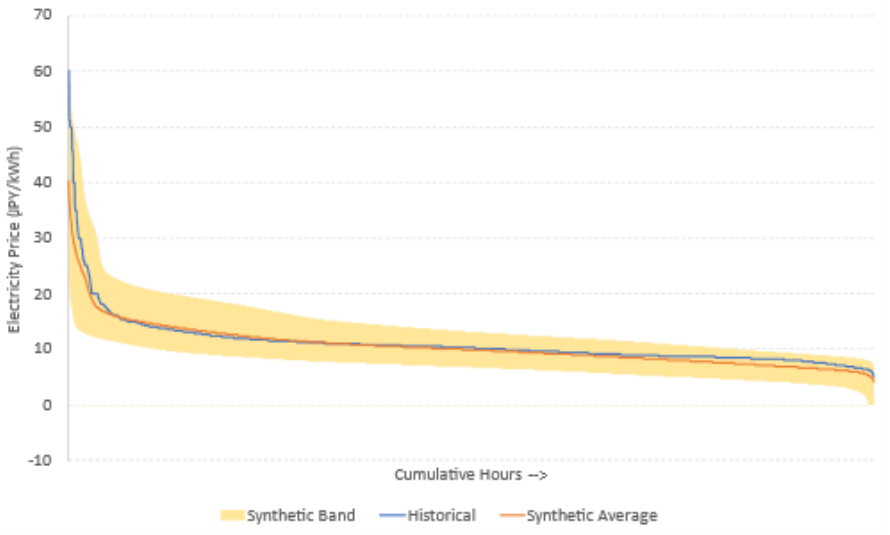

Figure 4.5: PDC comparison between the synthetic and historical data.

or so highest electricity price hours. Therefore, the model was run in two modes: one using 100 synthetic price histories and returning the expected break-even sale price of hydrogen, and the other using the historical PDC to determine the expected break-even sale price of hydrogen.

4.2.3 HTTR-GT/H_2 Dispatch Dynamics

After sampling the FARMA to produce a synthetic data set, the model dispatches either electricity or hydrogen, depending on the electricity price at each time step. When the electricity price exceeds the cost of producing electricity, electricity is produced and sold. When the electricity price falls below the cost of producing electricity, hydrogen is produced and sold. In this manner, the model chooses the most economically advantageous commodity to produce and sell during each hour.

The dispatch algorithm assumes that the HTTR-GT/H_2 operates in one of two modes, as put forth by Yan et al. [34]. These modes are given as (a) and (b) in Table 4.2. The dispatch algorithm decides between dispatching electricity in accordance with operation mode (a), or dispatching hydrogen in accordance with mode (b). The system is assumed flexible enough to switch back and forth between modes within the 30-minute time steps allotted. Note that these configurations are based on proposed test designs for the HTTR-GT/H_2, which may not necessarily utilize the HTTR's entire 30-MW_{th} heat for hydrogen/electricity production.

Table 4.2: HTTR-GT/H_2 Operational Modes (Data Reproduced from [34])

Parameters	Electricity Mode	Hydrogen Mode
Reactor outlet temp, °C	850	950
Reactor power, MW_{th}	30	30
Power generation, MW_e	0.6	0.4
Hydrogen production, Nm^3/h	0	29.5

The IS cycle design developed by JAEA is sized to provide 29.5 Nm^3/ hr of hydrogen, as per the design in [34].

The amount of hydrogen delivered during each hour (m_{H_2}) is represented in Equation 4.3. When the price of electricity (P_{elec}) falls below the electricity production cost (C_{elec}), the system dispatches hydrogen in accordance with the previously defined operation modes. When electricity price is higher than the cost of producing electricity, hydrogen is not produced; instead, the power is used to make electricity.

$$\dot{m}_{h_2} = \begin{cases} 29.5\frac{Nm^3}{h}, & P_{elec} < C_{elec} \\ 0\frac{Nm^3}{h}, & P_{elec} \geq C_{elec} \end{cases} \tag{4.3a}$$

$$e = \begin{cases} 0.3MW & P_{elec} < C_{elec} \\ 0.6MW & P_{elec} \geq C_{elec} \end{cases} \tag{4.3b}$$

4.2.4 Cash Flow Analysis

Once the dispatch is complete, the model collects economic data to produce a system net present value (NPV). These cash flows include the capital cost, operating and maintenance costs of the IS cycle, and an assumed hydrogen storage cost. Revenue comes from the sale of hydrogen and electricity.

The NPVs in this report represent a differential NPV, shown in Equation 4.4. NPV_{ref} is the NPV of the HTTR-GT/H_2 when only electricity is sold and no hydrogen process has been built. NPV_{ref} serves as a baseline against which $\text{NPV}_{\text{cogen}}$ is compared. When ΔNPV is positive, the co-generation system is more profitable than only selling electricity. When ΔNPV is negative, the system would be more profitable focusing on electricity and not building the IS unit. Thus, when ΔNPV is 0, the profitability of the co-generation system equals that of only generating electricity. This is the break even point, at which the hydrogen price represents the LCOH for this system.

$$\Delta NPV = NPV_{cogen} - NPV_{ref} \tag{4.4}$$

Using ΔNPV means that only cash flows that differ between reference and cogeneration cases need to be tracked. Expenditures such as fixed HTTR costs and capital investments associated with the nuclear reactor can be disregarded, as they are equivalent in both the reference case and cogeneration cases. The limitation of this method is that ΔNPV only reflects the nuclear-IS profitability relative to the reference case, rather than deter-mining its absolute profitability. More information on the economics of the HTTR-GT/H_2 are required before an analysis of total system profitability can be conducted.

Equation 4.5 gives the mathematical basis for disregarding equivalent cash flows that appear in both the reference and cogeneration NPVs.

$$NPV_{ref} = CF_{e-sales} - CF_{nuc,FOM} - CF_{nuc,marginal} - CF_{nuc,CAPEX} \tag{4.5a}$$

$$\begin{aligned} NPV_{cogen} =& CF_{H_2,sales} + CF_{e-sales,cogen} - CF_{nuc,FOM} - CF_{nuc,marginal} - CF_{nuc,CAPEX} \\ & - CF_{IS,FOM} - CF_{IS,marginal} - CF_{IS,CAPEX} \end{aligned} \tag{4.5b}$$

$$\begin{aligned}\Delta NPV =&(CF_{H_2,sales} + CF_{e-sales,cogen} - CF_{IS,FOM} - CF_{IS,marginal} \\ &- CF_{IS,CAPEX}) - CF_{e-sales}\end{aligned} \tag{4.5c}$$

The NPVs are calculated by summing the discounted cash flows associated with each case. Equation 6 details the NPV calculation. For this analysis, the discount rate, r, is 8%

$$NPV = \sum_{yr=0}^{lifetime} \frac{CF_{total,t}}{(1+r)^t} \tag{4.6}$$

The cash flows accounted for in the co-generation case are (1) cost of electricity generation from HTTR-GT/H_2, (2) IS capital and operating cost, (3) hydrogen storage, (4) revenue from electricity sale, and (5) revenue from hydrogen sale. Only the cost of electricity generation and revenue from electricity sale are tabulated in the reference case. The simulation is run for 1 year and used for every year of the project's 30-year lifetime.

The output for this model is the break even cost of hydrogen. Hydrogen prices exceeding the LCOH would make building the nuclear-IS system and strategically dis-patching hydrogen more profitable than just selling electricity. Prices below the LCOH mean that the system would lose money relative to only selling electricity. The model allows for investigating the uncertainty that certain model inputs (e.g., electricity price data) impose on the LCOH.

To find the LCOH, the hydrogen price was varied, and the point at which ΔNPV equaled zero was found. This can either be achieved via optimization or by sweeping the solution space on a grid and locating the zero point. For this analysis, the grid sweep was used, since the only variable being perturbed was the hydrogen price.

4.2.5 Economic Parameters

The cost of hydrogen production from the nuclear-IS system is given in Figure 4.6, as estimated by JAEA in [35]. The capital cost is driven by the capacity of the IS cycle. For example, the provided capital cost of 3.4 JPY/m^3 was multiplied by the IS cycle capacity of 29.5 m^3/hr and the 8,760 hours in the year. The loss of chemicals during operation of the IS was treated as a variable operating cost.

The dispatch model also assumes a hydrogen storage cost for a tank sized to hold 4 hours of production from the IS cycle. Storage flexing and hydrogen overproduction is not included in this analysis. The storage acts as a simple addition to the capital cost. A price of $600/kg was used [49], equivalent to 5326.5 JPY/Nm^3 at an exchange rate of 106 JPY = 1 USD.

4.3 Results

Two scenarios were run: dispatch using synthetic price histories and dispatch using the historical PDC. For the synthetic case, each dispatch instance was run with 100 synthetically generated electricity price time histories to produce a more stochastic optimization. The historical case used the 2018 historical electricity prices as input. The outer loop varied hydrogen prices from 0 to 120 JPY/Nm^3. A sample 8-hour dispatch window is shown in Figure 4.7. The amount of revenue that the system would generate during each hour is calculated for hydrogen and electricity sale while operating in hydrogen production mode and electricity production mode, respectively, as shown in Figure 4.7a. Hydrogen or electricity is

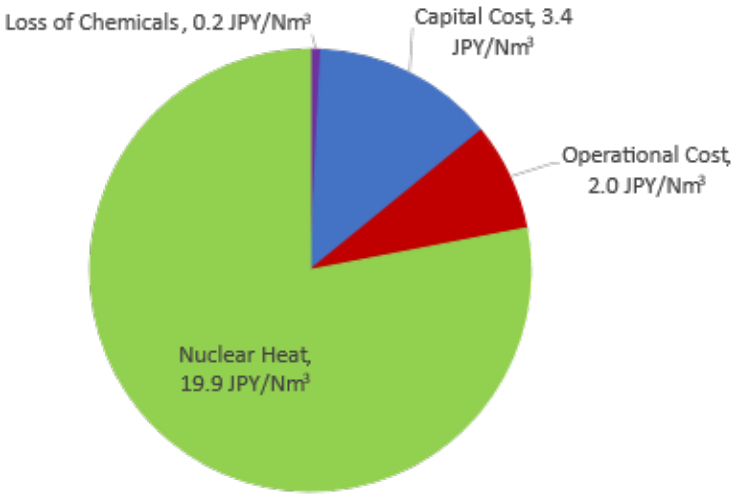

Figure 4.6: Cost breakdown of hydrogen production by nuclear-IS system. Note that, for this analysis, the capital cost is taken on a capacity basis (i.e., Nm^3 of capacity). The figure is reproduced with data from [35].

then produced, depending on which opportunity cost is greater (see Figure 4.7b).

4.3.1 Stochastic Optimization of LCOH

The stochastic optimization case performed economic dispatch on 100 different synthetic price time histories generated by sampling the trained electricity-price FARMA. The individual economic parameters were gathered for each of these runs, and the model re-turned the expected ΔNPV.

Figure 4.8 shows the relationship between hydrogen price and ΔNPV. Breakeven LCOH occurs at 67.5 JPY/m^3, when the ΔNPV is zero. Hydrogen prices were evaluated in increments of 10 JPY/m^3 (from 20 to 120 JPY/m^3), with higher resolution around the break even price of hydrogen.

Hydrogen prices above and below the LCOH offer insight into the system dynamics. With the IS cycle dispatched while hydrogen prices are less than the LCOH, too few hydrogen-producing hours exist to recover the capital expenditures incurred by building the IS unit. With hydrogen prices greater than LCOH, hydrogen sale becomes economically advantageous in ample time, ultimately recovering—even exceeding—the capital cost.

Figure 4.9 shows the number of hours per year during which the IS cycle dispatches hydrogen. At 40 JPY/m^3 or less, the hydrogen price is so low that the IS unit is never economically advantageous to dispatch. An LCOH of 67.5 JPY/m^3 equates to 431 expected hours of hydrogen production per year. Price increases result in boosting the number of hours in which hydrogen production is economically advantageous. At a high enough hydrogen price, the system would choose to dispatch hydrogen exclusively.

Table 4.3 summarizes the expected parameters for dispatch at the LCOH.

4.3.2 LCOH with Historical Price Duration Curve

Comparing the stochastically optimized LCOH to one optimized using historical PDC data is useful for understanding the implications of the distribution tails on cost. The stochastic optimization case

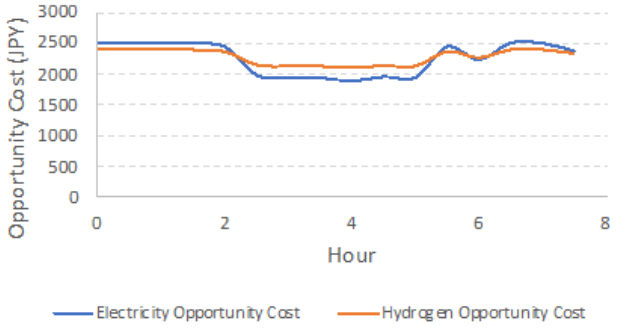

(a)

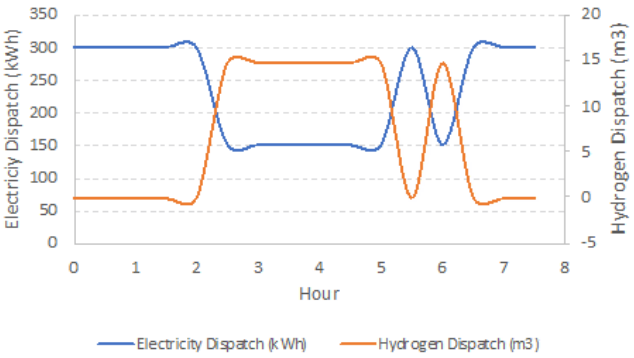

(b)

Figure 4.7: Example of dispatch logic over an 8-hour period. (a) The opportunity cost for producing hydrogen or electricity. (b) Hydrogen or electricity modes dispatched in accordance with higher opportunity cost. This strategy ensures that electricity is sold only when profitable.

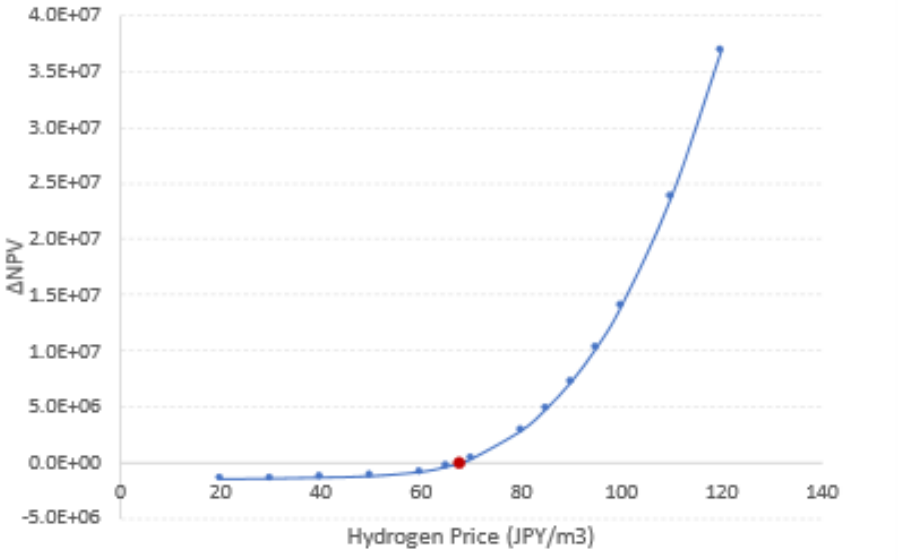

Figure 4.8: ΔNPV for various hydrogen prices, using the synthetic PDC as input. The red dot represents the break even LCOH.

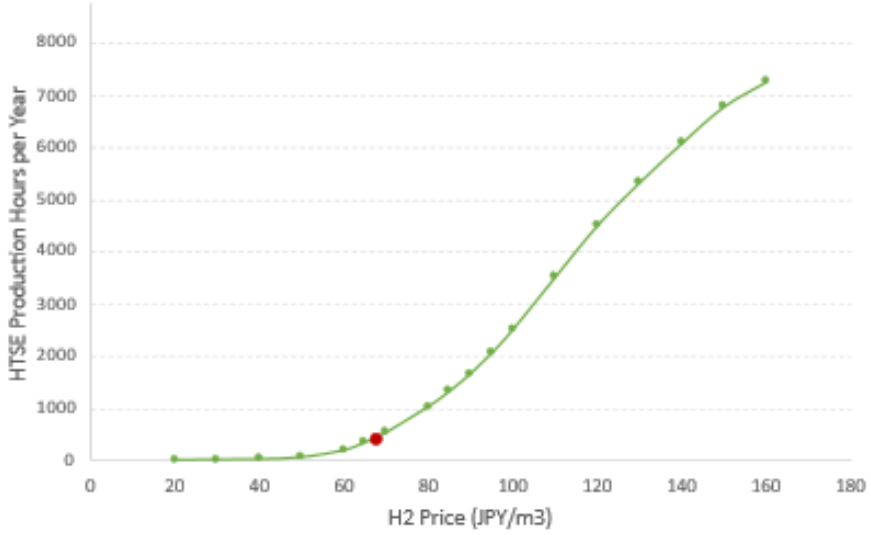

Figure 4.9: Utilization rate of the IS unit, plotted against the hydrogen price in the stochastic optimization scenario. The red dot represents the break even LCOH.

Table 4.3: Expected Dispatch Values for the System at a Levelized Hydrogen Cost of 67.5 JPY/m^3

Parameters	Expected Value (per Year)
Hydrogen Produced, m^3	127,020.4
Electricity Produced, MWh	5,126.6
Hours of Hydrogen Production	431.2

outputs the expected LCOH under a wide range of possible synthetic PDC. LCOH optimization using the historical data set gives an example of the LCOH found on a PDC that is slightly skewed to higher prices.

As with the stochastic case, Figure 4.10 shows that hydrogen is not dispatched at low hydrogen prices, and that there is a range in which a small amount of energy is dispatched for hydrogen production despite the inability to recover the IS capital cost. In this case, when hydrogen prices fall below approximately 80 JPY/m^3, the system does not dispatch hydrogen. At 80–98 JPY/m^3, a small amount of hydrogen is dispatched. At 98.1 JPY/m^3, the ΔNPV equals zero, thus representing the LCOH.

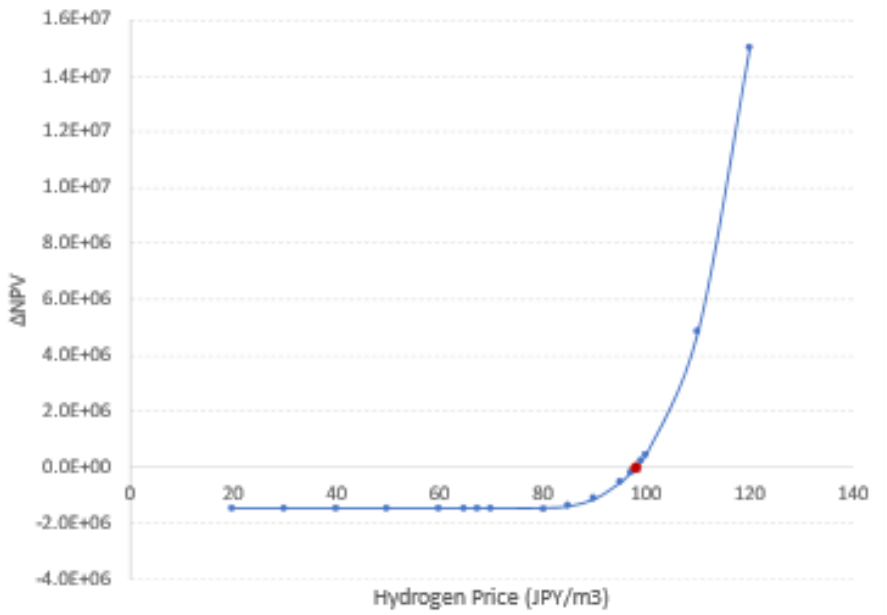

Figure 4.10: ΔNPV for various hydrogen prices, using the historical PDC as input. The red dot represents the breakeven LCOH.

Figure 4.11 shows the IS unit's utilization rate plotted against the hydrogen price. The utilization rate is zero hours when the hydrogen price is low. At an LCOH of 98.1 JPY/m^3, the IS unit produces hydrogen during 637 hours.

Table 4.4 summarizes the dispatch parameters found at an LCOH of 98.1 JPY/m^3.

Table 4.4: Dispatch Values for the System at a Levelized Hydrogen Cost of 98.1 JPY/m^3

Parameters	Expected Value (per Year)
Hydrogen Produced, m^3	18,791.5
Electricity Produced, MWh	5,064.9
Hours of Hydrogen Production	637.0

4.4 Discussion

The reported LCOH values should not be relied on as a basis for making investment decisions. Rather, they help us understand the implications of different inputs, so that when economic competitiveness is evaluated, the correct breadth of input data can be applied.

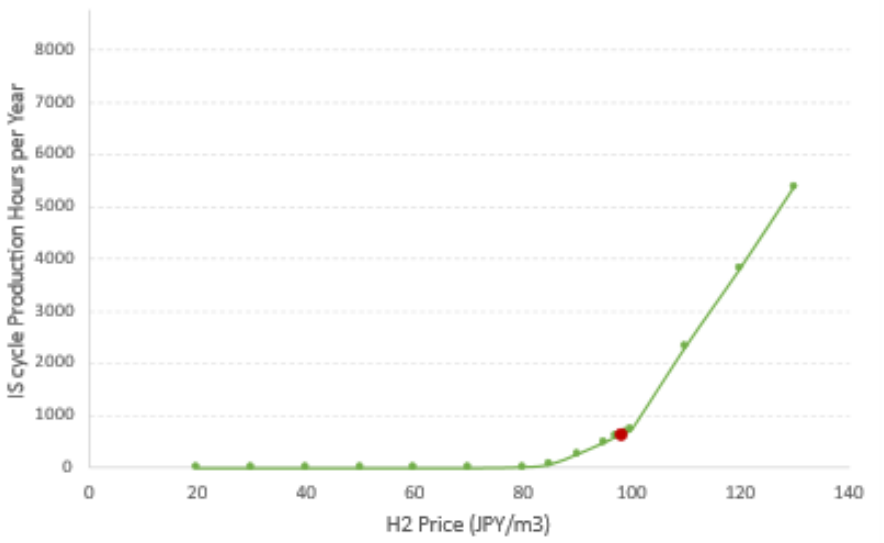

Figure 4.11: Utilization rate of the IS unit, plotted against the hydrogen price. As the hydrogen price rises, hydrogen deployment becomes increasingly more economically advantageous than electricity sale, so the number of hydrogen production hours increases. The red dot represents the breakeven LCOH.

The effects of price distribution can be viewed by comparing the stochastic optimization case to the historical PDC case. The hydrogen dispatch is driven by two factors: the hours having the lowest electricity prices and the price of hydrogen. By raising the price of hydrogen, selling hydrogen becomes more profitable during more hours. Lower electricity prices and more incidences of low electricity prices also make hydrogen more economically advantageous than electricity.

The lowest-priced hours of the electricity price distribution are what dictate system profitability, since the capacity is fixed and the hydrogen price varied. The stochastic optimization case uses synthetic price histories in an attempt to produce the expected LCOH. On average, the synthetic histories showed lower electricity prices at the tail than did the historical price distribution. This led to a lower LCOH than in the historical case.

This lowest-priced hour distribution phenomenon is illustrated in Table 4.5. The lowest 500 hours of electricity prices from the year are averaged and compared with the LCOHs for several different synthetic histories. The average electricity price over the year is also provided. The LCOH shares a stronger correlation with the bottom-hour average than with the total yearly price average.

Synthetic data produced using the ARMA method outputted cheaper bottom-500-hour price averages, as well as overall average prices that were lower than the historical averages. This meant that the distribution of PDCs was slightly more favorable to hydrogen dispatch than the historical PDC. As such, the LCOH was lower in the stochastic case than in the historical case.

This analysis demonstrates that careful consideration should be taken when applying PDCs to this type of economic dispatch problem. The breakeven price of hydrogen highly depends on the PDC input. Stochastic optimization helps reduce uncertainty, but care should still be taken to produce PDCs that are meaningful in in regard to the chosen timeframe of analysis. For example, using a 2020 PDC to predict the 2030 LCOH would be inappropriate. A projection of 2030 prices would be acceptable, but the best practice would be to use a host of projected possibilities to produce an expected LCOH. The results

Table 4.5: Impacts of Distribution on LCOH

Scenario	Avg Electricity Price, Cheapest 500h (JPY/kWh)	Avg Yearly Electricity Price (JPY/kWh)	LCOH (JPY/m^3)
Minimum	2.14	6.91	38.1
Minus 1 Standard Deviation	3.16	7.73	45.0
Mean	5.92	10.56	68.2
Historical	6.80	11.09	83.2
Plus 1 Standard Deviation	7.87	13.40	88.0
Maximum	8.43	14.84	94.0

from this study also show that lower overall electricity prices and more incidences of low prices would provide greater economic incentives for hydrogen production. This means that NPPs in locations with depressed electricity prices due to factors such as zero- or negative-bid renewable energies, mild climates, or low electricity demand could provide hydrogen at a lower price, yet still breakeven or potentially turn a profit.

Several other pathways exist for reducing the LCOH. Reducing capital expenditures would depress the LCOH. The effects and sizes of potential storage options could be explored in more detail. Additional cashflows generated by the NPP's ability to participate in other areas of the electricity market would lower the ΔNPV and thus the LCOH, as well. Before investment decisions are made, each of these sensitivities should be investigated to better understand their feedback.

4.5 Conclusion

This analysis explored the economics of dispatching a nuclear-IS co-generation unit. The results demonstrate the economic potential of such a system when compared to only selling electricity. These results highly depend on input assumptions, specifically the magnitude and distribution of electricity prices. The LCOH in this report should not be taken as a final value for the HTTR-GT/H_2's profitability, but as an exploration of the impacts of input assumptions on the final answer. Special care should be taken in this type of dispatch analysis to produce a host of meaningful electricity price time histories that represent possibilities for the evaluation years. In this regard, the FARMA approach shows great potential.

This study also serves as another indicator that dispatching hydrogen and electricity could be more economically advantageous than just selling electricity in the right conditions. Much of the nuclear hydrogen production and dispatch work focuses on light water reactors and U.S. electricity markets while focusing on electrolysis hydrogen production technology. This study performs the economic dispatch on a unique reactor, hydrogen production system, and electricity market and shows the break even price of hydrogen. Performing these analysis at different locations and with different technologies is important for understanding the economic competitiveness of producing hydrogen from nuclear.

Efforts to further this research could include running a larger stochastic optimization case aimed at optimizing the size of the IS unit on a commercial reactor, or at optimizing different sensitivities (e.g., capital cost).

4.6 Acknowledgements

This manuscript (the work encompassing Chapter 3 of this dissertation) has been authored by a contractor of the US Government for the U.S. Department of Energy, Office of Nuclear Energy (DOE-NE), under DOE-NE Idaho Operations Office contract DEAC0705ID14517.

Chapter 5: Development of Economic Dispatch Model for Evaluating Nuclear-Hydrogen Integrated Energy System Profitability

5.1 Introduction

Changes to electricity producing systems in the 21st century have created—and continue to create—new paradigms for electricity producers. For example, the steadily declining cost of renewables has hastened the deployment of intermittent generators, and the build-out of variable renewable energy (VRE) generally requires some type of flexible backup (e.g., natural gas). Coincidentally, the last 20 years have seen reduced natural gas prices as a result of technological developments (e.g., horizontal drilling and fracking). Both these factors have led to the massive build-out of flexible natural gas.

Cheap gas, concerns over carbon emissions, and the reduced cost of renewables have put economic pressure on larger, inflexible types of generators such as those for coal and nuclear. These inflexible generators are required to either turn down or curtail their energy production whenever excess VRE is generating. This phenomenon will occur more frequently as VRE continues to increase its share of electricity generation. This means that flexible power solutions such as natural gas, energy storage, or demand response will complement the VRE, while the other generators will lose more money if they cannot—or are not set up economically to—turn down their energy production in times of very high VRE generation [69].

This problem has created new challenges for currently operating nuclear power plants (NPPs). NPPs have a high fixed cost and low marginal costs [70]. The fixed cost is an operation and maintenance (O&M) cost that is required regardless of the plant's power output level. This could include employee salaries, required yearly capital maintenance investments, and taxes. The fuel in NPPs could even be thought of as a fixed cost, since it is loaded approximately once every 18–24 months and is acquired on a contractual basis. These fixed costs comprise the vast majority of an NPP's yearly expenses, so adjusting the plant power output up or down has little to no savings implications for the plant. Additionally, flexing the reactor core thermal output can increase water costs as well as the wear to components, thus shortening their lifetimes. This means that NPP stakeholders would prefer to run their plants at the highest possible level for the longest possible time. Running an NPP in this configuration conflicts with having to flex the plant when VRE generation is high.

As VRE adoption continues to increase and greater emphasis is placed on carbon reduction, much research is being conducted into developing "firm" carbon-free technologies. Such technologies are defined as being dispatchable (i.e., controllable as needed), in addition to carbon-free. Studies have shown that the inclusion of firm technologies (e.g., biomass-, battery-, or nuclear-related technologies) could reduce the cost of decarbonization [12, 71, 72].

Nuclear power is a large source of clean firm energy, but flexibility remains a concern. Several options are being explored to enable current light-water reactors to fulfill the promise of clean firm energy, despite economic challenges as well as some technical ones. One solution is to simply load follow the plant. For

the reasons discussed above, this is generally not ideal, but could be profitable if system flexibility is incentivized as VRE penetrations increase [73, 74]. Another option for improving the current fleet's synergy with intermittent resources would be to use the heat or energy provided by an NPP to produce a commodity other than electricity [75].

The ability to produce more than one commodity would enable NPPs to output a consistent amount of heat, thus keeping reactor conditions constant. That heat could then be used to produce some other commodity whenever electricity is not needed. This system, which includes an NPP capable of dispatching at least one commodity other than electricity, is known as an integrated energy system (IES). Running the NPP as an IES would mean that times of high VRE production (when the NPP would traditionally have to curtail or turn down its energy production) or low electricity prices could be taken advantage of in order to produce and sell another commodity.

Such commodities could include desalinated water, heat for industrial processes, or hydrogen. Allowing the NPP to alternate between dispatching electricity and some other commodity could add value to both the grid and the NPP itself.

An IES would be able to flexibly provide power to the grid, effectively acting as a demand response system. If electricity prices are high and the full output of the NPP is needed, the IES could divert power to the turbines and sell electricity. If electricity prices are low or VRE generation is very high, the IES could send power from the reactor to the secondary commodity production facility, then sell hydrogen, ammonia, water, etc.

Several commodities are producible from IES configurations. Heat from the NPP can be sold as-is for use in thermal storage or process heating applications. Nuclear heat or electricity can be diverted to desalinate water [76, 77]. Hydrogen can be produced via high-temperature steam electrolysis (HTSE) [21, 78], low-temperature electrolysis [79], the iodine-sulfur cycle [23], or the copper-chloride cycle [24].

Evaluating IES profitability is a complex endeavor requiring knowledge of electricity systems and market structures, nuclear systems, and secondary commodity markets. Epiney et al. used an economic framework to model an IES system in conjunction with a larger nuclear-renewable hybrid system. The study tests the limitations of the developed framework and concludes that temporal resolution has a large effect on the results, with the levelized cost of electricity for cases that used representative days differing from those that used entire years. This discrepancy affects the profitability of the system [51]. Sorgulu and Dincer studied the break-even price of hydrogen at two Turkish NPPs. The study incorporates costs resulting from the NPP, hydrogen production units, and transportation, but does not evaluate a hydrogen-vs.-electricity economic dispatch scenario [80]. Frick et al. evaluated adding a hydrogen production unit to an existing NPP. The analysis used the differential net present value (NPV) between hydrogen-vs.-electricity economic dispatch and a baseline of electricity production only. Frick et al. found that positive cash flows resulting from hydrogen-vs.-electricity economic dispatch are possible. But because of the complexity of the dispatch, only the hydrogen price and discount rate sensitivities were run [49]. Borowiec et al. developed an economic dispatch model for nuclear with thermal energy storage (TES). The study finds that a nuclear-TES IES can be profitable, but input assumptions such as renewable penetration, output flexibility, and storage unit size greatly impact the final NPV [81].

The reviewed studies each evaluate IES economics while discussing the limitations of the assumptions used in their own models. Such limitations could be due to the uncertainty in the inputs, the lack of temporal resolution, or simply because the solution space is a complex combination of so many different

factors.

The current study aimed to develop a model that could evaluate the profitability of adding a hydrogen production unit to an existing NPP. Because the solution space was so complex, a limit surface sampling method was used to explore the interactions among the following three varied parameters: amount of hydrogen delivered, capital expenditure (CAPEX), and a credit for producing hydrogen via carbon-free methods. A case study was run on two plants: the Monticello Nuclear Generating Plant and the Prairie Island (PI) Nuclear Generating Plant.

5.2 Model Formulation

A model was developed within this study in order to evaluate the profitability of an IES system according to several sensitivities (e.g., size and capacity).

The PI and Monticello NPPs were chosen for this analysis because they are owned and operated by Xcel Energy, which was awarded a funding opportunity by the U.S. Department of Energy (DOE) to investigate building a nuclear-hydrogen IES at one or both of their plants. PI is a two pressurized water reactors with a total 1,096 MW nameplate capacity. Monticello is a single boiling water reactor plant with a capacity of 671 MW. Both plants are located in Minnesota.

Hydrogen was chosen as the secondary commodity for this analysis, both due to the funding award for hydrogen research at these plants and because hydrogen produced without carbon emissions could be a important commodity in a decarbonized economy.

The dispatch and optimization model was developed using the Risk Analysis Virtual Environment (RAVEN) framework developed at Idaho National Laboratory [56]. RAVEN is a multipurpose code for regression analysis, optimization, uncertainty quantification, and data analysis. This dispatch model uses RAVEN's conjugate gradient optimization, sensitivity analysis, and multi-level run features. The model also leverages an economic plugin called the Tool for Economic Analysis (TEAL) to track financial parameters throughout the lifetime of an HTSE facility. TEAL extends RAVEN's economic capabilities by affording it the ability to track and discount cash flows, apply taxes or depreciation, and calculate economic parameters such as NPV or internal rate of return.

The model operates in a two-loop configuration. The outer loop varies the HTSE capital cost, HTSE demand, and clean hydrogen credits. This allows the user to explore the intersection of these three variables and their effect on profitability. The model's inner loop performs the electricity-vs.-hydrogen economic dispatch, optimizes hydrogen storage parameters, and calculates the NPV. A schematic of the model architecture is shown in Figure 5.1. The optimization model is explained in more detail in subsequent sections.

5.2.1 Model Formulation and Inputs

The optimization model inputs can be divided into two categories: physical and economic. The physical inputs come from a process model details the material and energy balance requirements and operating modes, including hot standby. The Process mode provides capital and operating cost curves. Other economic costs include storage costs, electricity prices, and hydrogen market prices.

HTSE was chosen as the hydrogen production method for this analysis. HTSE systems utilize a solid oxide electrolyzer cell stack to split hydrogen and oxygen via an electrolyzer. Inputs to the HTSE system include electricity as well as heat via steam from an auxiliary loop that draws from the nuclear reactor.

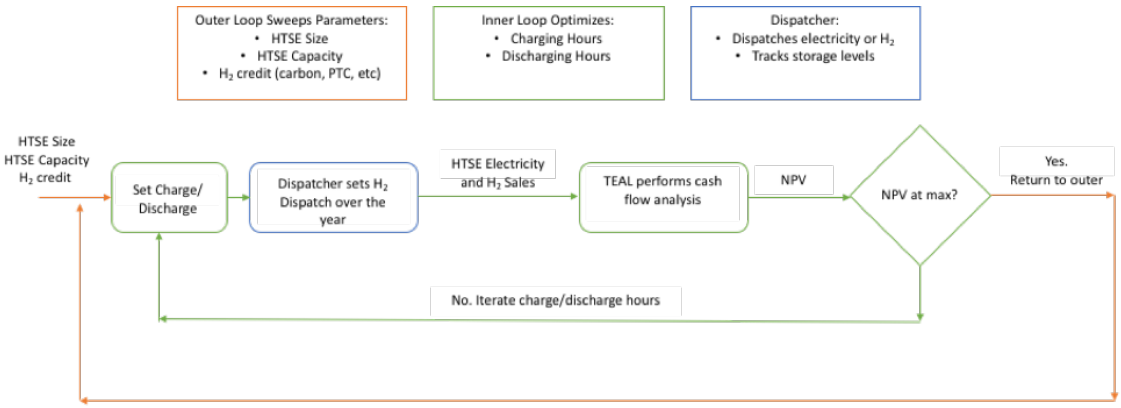

Figure 5.1: Economic dispatch and optimization model schematic.

An HTSE IES uses heat from the NPP to vaporize water, then employs recuperating heat exchangers and topping heaters to achieve higher steam temperatures.

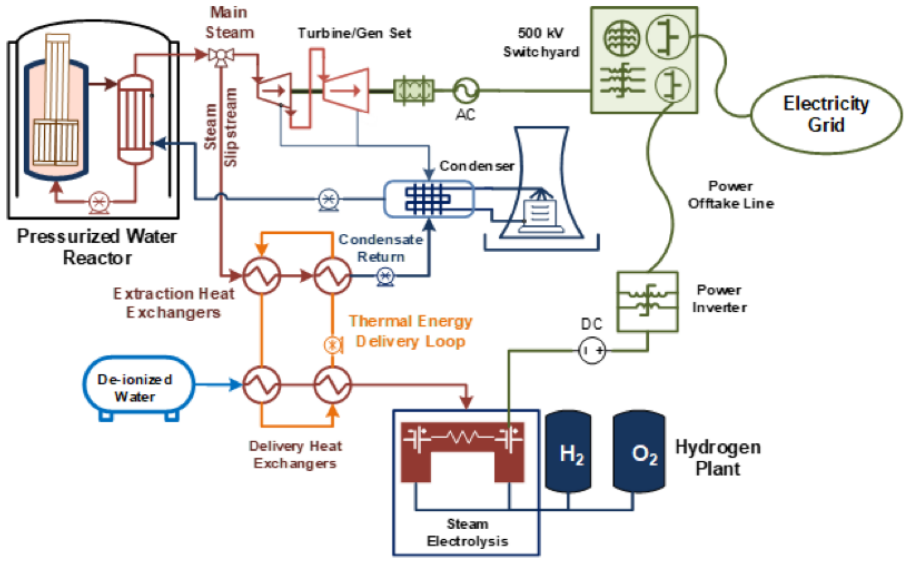

Figure 5.2: Example diagram of NPP-HTSE integration.

AspenTech Hysys [82] process modeling software was used to model the entire HTSE plant with nuclear heat and electricity input. This analysis uses as inputs the energy requirements and operating cost from the process modeling.

Table 5.1 details the physical inputs to the optimization model which were taken from the process modeling work. The HTSE O&M costs, also from the process modeling work, are given in Table 5.2.

Hydrogen storage costs were taken from the Pappadias and Ahluwalia [83]. Figure 5.3 shows the cost curves for various hydrogen storage technologies. Underground pipe storage is assumed. The correlation for the underground pipe storage is given in Equation 5.1, with the coefficients shown in Table 5.3.

$$CAPEX_{Storage} = exp(a * ln(m^2)^2 - b * ln(m) + c) \tag{5.1}$$

Table 5.1: Physical inputs to the dispatch and optimization model

Input Parameter	Value
Electricity Requirement	37.4 kWh-e/kg H_2
Thermal Requirement	6.4 kWh-t/kg H_2
Electrical Hot Standby	0.9% of HTSE MW_e
Thermal Hot Standby	3.2% of HTSE MW_{th}
Cell Degradation Factor	0.953/yr
NPP Thermal Efficiency	0.346
NPP Capacity (PI)	1,096 MW
NPP Capacity (Monticello)	671 MW

Table 5.2: HTSE O&M costs

Input Parameter	Value or Equation
Variable O&M Cost ($/MWh)	$5.20 * Cap_{HTSE}^{-0.004}$
Fixed O&M Cost ($/kW-yr)	$75.51 * Cap_{HTSE}^{-0.208}$

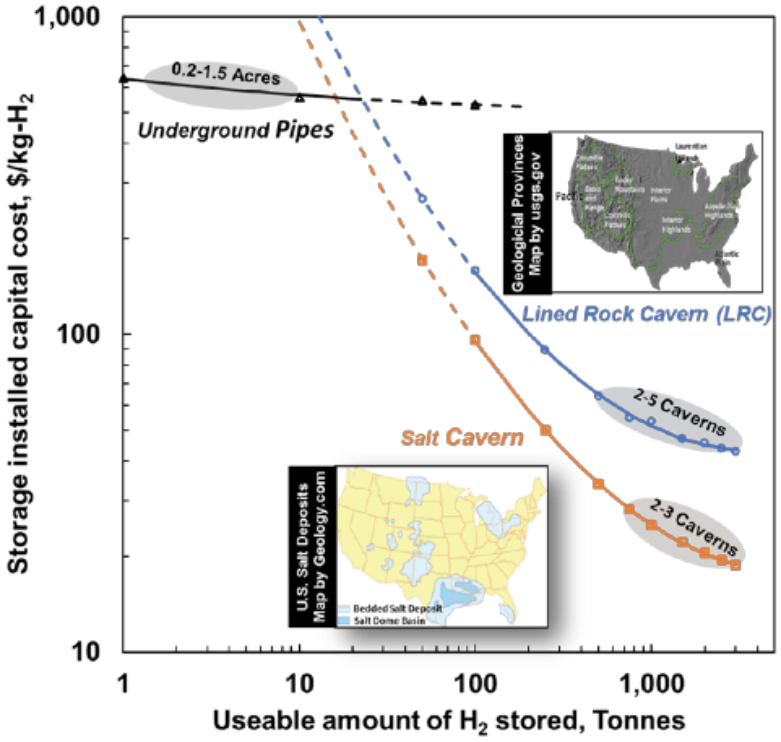

Figure 5.3: Hydrogen storage cost curves.

Table 5.3: Coefficients for storage capital cost

Storage	a	b	c
Underground Pipe Storage	0.0041617	0.060369	6.4581
Underground Lined Rock Caverns	0.095803	1.5868	10.332
Underground Salt Caverns	0.092548	1.6432	10.161

In addition to economic inputs, electricity prices must be provided in order to perform the electricity-vs.-hydrogen economic dispatch. The electricity locational marginal prices (LMPs) were output by several PLEXOS dispatch model runs that also served as the input to Frew et al. (forthcoming, [84]). PLEXOS is a commercial dispatch software capable of using an input set of electricity-generating units in a given region to find the LMP at various nodes in the optimization model, thus accounting for the clearing price for electricity generators and the transmission congestion effects [85].

The area of interest is the region surrounding the two plants in the Northern States Power region. The exact region is shown in [84]. A Regional Energy Deployment System (ReEDS) [86] capacity expansion run was performed to gauge the capacity of electricity generators in this region, as well as in the surrounding area [86]. The capacity was input into PLEXOS, and the LMP for the nodes in which Monticello and PI reside were output. The specific LMP profiles input into the optimization model represent three different model years—2026, 2030, and 2034—at an hourly resolution. The LMPs represent wholesale electricity prices. Different sets of LMP time histories exist for the two different plant locations.

5.2.1.1 Hydrogen Market Inputs

A supply curve is required for representing the hydrogen sale market. The curve can aid in quantifying the revenues from hydrogen sale and help the model understand appropriate HTSE output as it optimizes capacity.

An analysis that looked at hydrogen consumers forecasted future users in proximity to both the PI and Monticello plants. Each hydrogen consumer within a 100-mile radius was included, as shown in Figure 5.4, for the PI plant. Current consumers include refineries, while future consumers include natural-gas plants for blended electricity production, plants for direct iron reduction, syngas plants, and projected fuel cell electric vehicle manufacturers (by 2030). The distance to each consumer was accounted for, and the hydrogen transportation cost to the consumer was included in the hydrogen market sale price calculations.

At PI, the projected main hydrogen consumers are refineries, synfuel producers, and natural-gas plants. The PI plant is near two refineries that account for a 310 MT/day demand in hydrogen. It is assumed that five ethanol plants that produce high-purity CO_2 could buy hydrogen to produce synfuels. These plants would require 400 MT/day. Also, 38 natural-gas plants in close proximity to PI are assumed to blend 30% H_2 by volume with natural gas in order to reduce emissions. In total, the region has approximately 905 MT/day potential hydrogen demand by 2030.

The Monticello area's demand is assumed to stem mainly from the surrounding natural-gas plants, fuel cell electric vehicle manufacturers, and refineries. Figure 5.5 shows a map of projected H_2 consumers. Twenty-seven natural-gas plants located within 100 miles of Monticello could eventually utilize natural gas blended with hydrogen. There would be local potential for synfuels, though less so than at PI.

The two refineries that were accounted for in the PI demand analysis are also located within 100 miles of Monticello. For the purposes of this analysis, it is assumed that only one plant at a time is operating an IES hydrogen production facility. In reality, the size of the other IES would be impacted if one plant was to cover the hydrogen needs of both refineries.

Overall, the projected 2030 demand within 100 miles of Monticello is 650 MT/day. This is signifi-

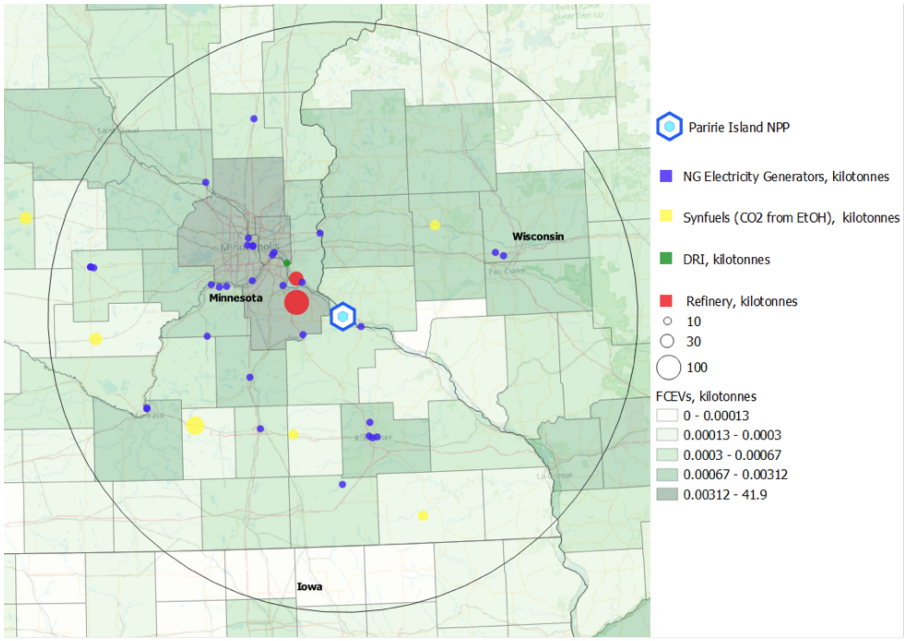

Figure 5.4: Future hydrogen demand in the region surrounding PI.

cantly less than PI because there is greater potential for H_2-NG blending and synfuel production around PI.

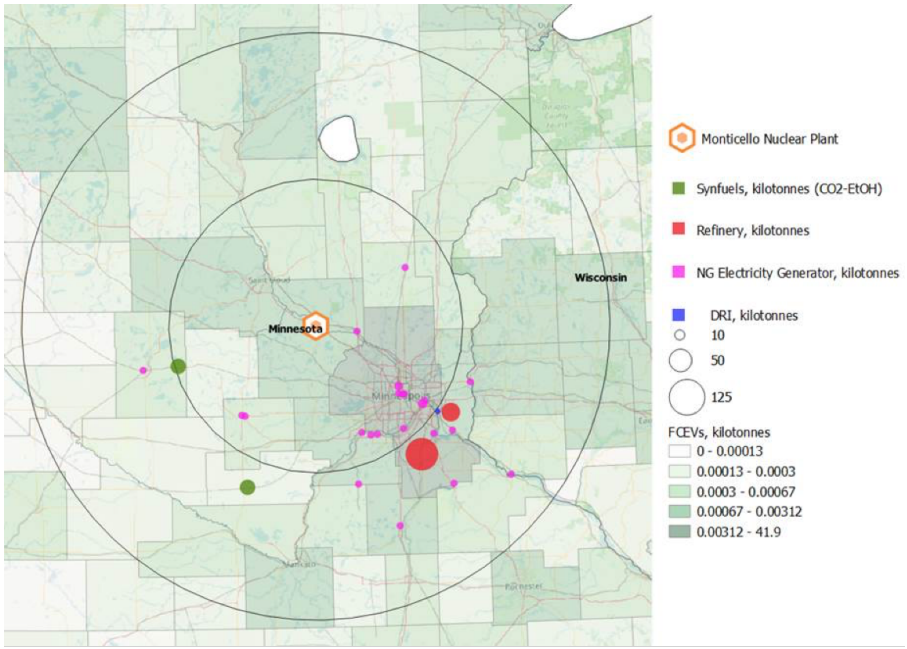

Figure 5.5: Future hydrogen demand in the region surrounding Monticello.

Future hydrogen demand curves were produced for each region by aggregating the demand from each consumer and comparing the break-even hydrogen cost for a specific market—plus any carbon costs and less the hydrogen transmission cost (see Equation 5.2).

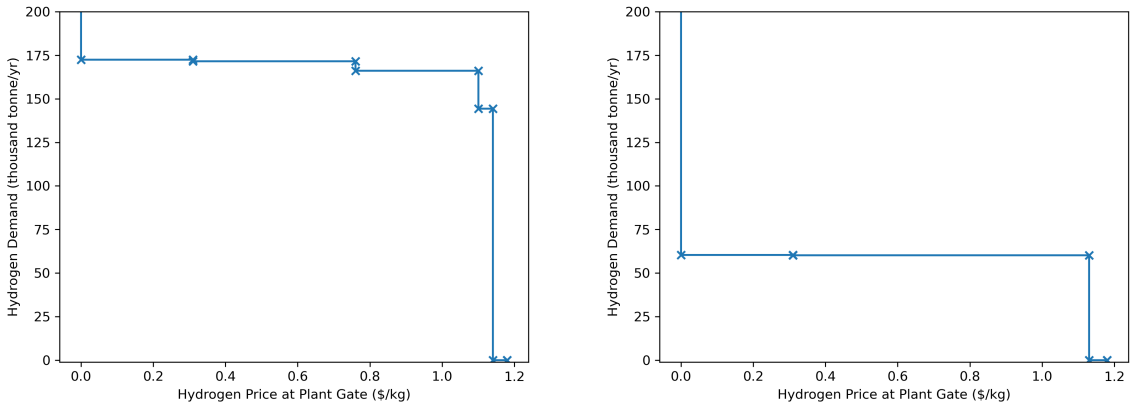

(a) (b)

Figure 5.6: Demand curves for (a) the region around PI and (b) the region around Monticello. These represent the projected price at which an IES could sell hydrogen in 2030.

$$P_{H_2} = C_{breakeven} - C_{H_2 Transmission} + C_{CarbonCredit} \tag{5.2}$$

The break-even hydrogen price is the price at which hydrogen can be sold by competitors. In this case, steam methane reforming is currently the cheapest hydrogen production method, and the hydrogen price will be benchmarked against it.

A carbon tax of $22.20 per short ton CO_2 is applied as an adder to price. If steam methane reforming is competing with an IES system, a carbon tax would make the IES more competitive as a result of the nuclear system not emitting CO_2. This adder was used because the Xcel Energy 2019 Integrated Resource Plan (IRP) projects a $22.20 per short ton CO_2 tax/penalty by 2030 [87].

The hydrogen transportation costs were taken into account and found for each point using the Hydrogen Delivery Scenario Analysis Model [88]. The addition of the hydrogen transportation cost and the hydrogen production cost produced the graphics shown in Figure 5.6. These curves provide the projected price that an IES could sell hydrogen at the consumer's specific location.

The hydrogen demand curves serve as input to the overall dispatch model. The model determines a sale price from Figure 5.6, based on the size of the HTSE that the sampler proposes. The model assumes a single sale price for a fixed HTSE size, rather than selling at different prices.

5.2.2 Dispatch Logic

Within the inner loop, the dispatch routine receives the hydrogen demand, HTSE capital costs (in $/MW), and clean hydrogen credits from the outer loop, as well as the physical and economic parameters from Tables 5.1 and 5.2. The inner loop also introduces the hydrogen storage charge/discharge hours optimized by RAVEN. Charge hours are the number of hours in which the HTSE expects to overproduce and send excess hydrogen to storage. Conversely, the discharge hours represent the expected amount of time in which the HTSE will reduce its load and use storage exclusively to meet the hydrogen demand. It is assumed that the hydrogen demand must be met in each hour of the year.

For the purposes of this study, charge is defined as the act of sending hydrogen to storage, and

discharge is defined as the act of withdrawing hydrogen from storage. When the system is discharging, it provides all or some of the hourly hydrogen demand from storage. When the system is charging, the HTSE meets the hourly hydrogen demand while sending the excess to storage.

The dispatcher in the model first sets the physical sizes for H_2 storage and the HTSE, in accordance with the inputs. The HTSE total capacity is the hydrogen demand plus any oversize used to fill hydrogen storage during grid electricity off-peak hours. The total HTSE capacity is constrained by the capacity of the NPP with which it is associated. The oversize excess capacity corresponds to the ratio of storage charge to discharge hours. The HTSE must produce the amount of hydrogen required to meet demand, while also filling the hydrogen storage. Additionally, the storage size is set by the discharge hours, with the system needing to have the storage capacity to meet demand in the all the discharge hours. An adder of 4 hours is used in the dispatch model to increase the storage margin in the event of multiple discharge events occurring in a row. Equations for each of these calculated physical parameters are given in Equation 5.3, where D_{H_2} is the H_2 demand passed into the dispatch by the outer loop.

$$\begin{aligned} Cap_{HTSE} &= D_{H_2}(MW) * (1 + \frac{t_{charge}}{t_{discharge}}) \\ Oversize &= D_{H_2}(MW) * \frac{t_{charge}}{t_{discharge}} \\ Cap_{storage} &= D_{H_2}(kg) + (t_{discharge} + t_{marginadder}) \end{aligned} \tag{5.3}$$

The dispatcher looks at the LMP in each hour and decides to dispatch via one of three modes. When the LMP is low, the dispatcher will choose charge mode and produce more hydrogen than is required to meet demand, prioritizing the production and storage of hydrogen over sending electricity to the grid. When the LMPs are high, the dispatcher will operate in discharge mode, using hydrogen from storage to meet demand and maximizing the amount of electricity sold to the grid. In the intermediate mode, the HTSE only produces the amount of hydrogen required to meet the hydrogen demand, selling any remaining electricity to the grid. This means that the HTSE system effectively acts as a demand response system that can shift its load to hours of low electricity prices and maximize electricity production in hours of high prices.

To decide when the charge and discharge events should occur, the dispatcher searches LMPs over a 24-hour period, looking for the minimum and maximum. The dispatcher sets a block of hours (equal to the number of discharge hours) surrounding the maximum LMP. The dispatcher then looks to set a block equal to the number of charge hours) surrounding the minimum LMP. The charge is allowed to happen over seperate blocks of time, but the discharge block must be contiguous. This means that, in a 4-hour discharge scenario, the dispatcher finds the hour of the highest LMP and backfills another three hours around it, for a total of four. For a charge scenario, the same process is used around the lowest LMP. If sufficient storage is unavailable to meet the hydrogen demand, the dispatcher prioritizes meeting this demand and reduces the amount of electricity sold to the grid.

Figure 5.7 shows this dispatch strategy over a 4-day period. Note that when the LMP is high, the storage flows are negative, meaning that hydrogen is leaving the storage tank in order to be sold. At that same time, hydrogen generation falls to zero, and the electricity sold to the grid is maximized. In the periods surrounding the times of low electricity prices, the HTSE overproduces hydrogen and sends

the excess to storage. The duration of these charge and discharge periods are optimized by the model and made consistent throughout the year.

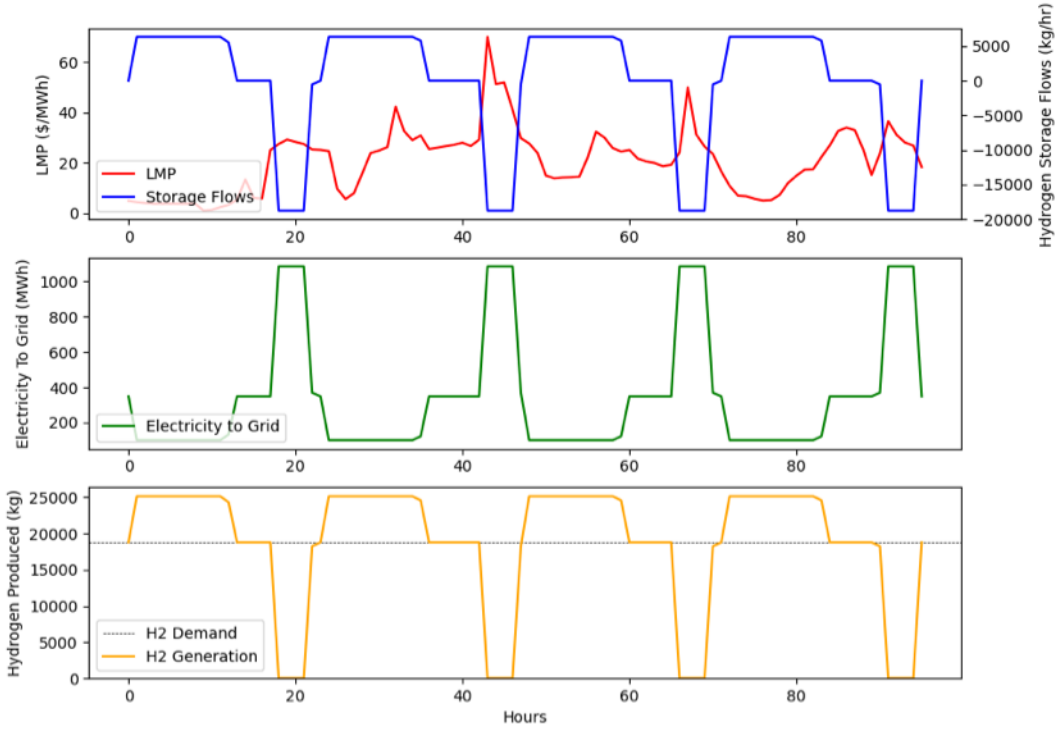

Figure 5.7: Demonstration of model dispatch logic over a 4-day period.

The model operates similarly to a traditional storage arbitrage approach. In high-price electricity hours, electricity to the grid is maximized, and storage is used to meet the hydrogen demand. In low-price electricity hours, when the NPP might traditionally lose money on electricity sales, it produces as much hydrogen as it can to store for later. The load shifting is also similar to demand response systems.

This approach also assumes the NPP-HTSE to be a price taker, meaning that the model does not change the price of electricity as the amount of the HTSE load changes. The LMPs were generated while the NPP was in a standard operating mode, without the HTSE. In reality, the load of the HTSE, and thus the reduced capacity available to the NPP to bid into the day-ahead electricity market, could alter the clearing price of electricity.

5.2.3 Economic Inputs

With the yearly dispatch completed for each of the three input years (i.e., 2026, 2030, and 2034), the equipment costs and hourly electricity-production profile are used to compare the NPP-HTSE NPV to the BAU nuclear NPV (see Equation 5.4). This comparison provides an ΔNPV value usable to assess profitability. A positive ΔNPV means that the NPP-HTSE system is profitable relative to running the plant in typical fashion. A negative ΔNPV means that the NPP-HTSE would make less money than running the NPP in standard operation. An ΔNPV equal to 0 reflects the exact point at which operation of the NPP-HTSE produces the same value as the BAU approach.

$$\Delta NPV = NPV_{NPP+HTSE} - NPV_{BAU} \tag{5.4}$$

The advantage of the ΔNPV approach is that the economics of the HTSE system can easily and quickly be compared to the BAU approach. Only those cash flows that are present in some cases but not in others need to be represented. NPP cash flows that remain consistent from case to case (e.g., nuclear fixed-O&M or capital expenditures) need not be quantified. This simplifies the simulation and reduces the uncertainty that would be present in a standard, absolute NPV analysis. It should be noted that this type of analysis only quantifies profitability relative to the BAU approach, and does not reflect the overall profitability of the NPP-HTSE.

The cash-flow parameters in Table 5.4 are fed to the RAVEN plugin TEAL to calculate the NPV. Hydrogen sales are calculated according to the amount delivered and the demand curve for the corresponding plant. The electricity sales are calculated by determining the amount of electricity sent to the grid during each hour, then multiplying that by the respective LMP.

Table 5.4: Cash flows for ΔNPV calculation

NPV w/ Nuclear-HTSE	NPV w/ Nuclear BAU
HTSE Capital Cost	Electricity Sales (2026, 2030, 2034)
HTSE Fixed Operating and Maintenance	
HTSE Variable Operating and Maintenance	
HTSE Variable Operating and Maintenance	
Cost of Capacity Replacement	
Hydrogen Storage CAPEX	
Electricity Sales (2026, 2030, 2034)	
Hydrogen Sales (2026, 2030, 2034)	

An extra-capacity cost is accounted for in the NPP-HTSE NPV. This cost is intended to quantify the replacement cost of the amount of capacity lost to consistent HTSE hot standby. Regardless of hydrogen-production level, any amount of hot standby will decrease the capacity of the NPP. This lost capacity will require a different generator in order to replace the capacity within Xcel Energy's IRP.

To quantify the lost-capacity value, Xcel ran several capacity-expansion cases to determine system costs for various scenarios. These scenarios varied the level of nuclear capacity lost, and let the resource-planning model replace capacity. Scenarios in which the nuclear capacity was replaced and Xcel's carbon goals were met were averaged to back out the approximate cost (per MW-yr) of capacity replacement. The replacement cost equates to $188,337/MW-yr. As an example, the range of HTSE capacities for PI generally requires less than 20 MW_e of hot standby.

A traditional metric for quantifying a capacity replacement cost is the cost of new entrant, which is usually equivalent to the cost of adding a combustion turbine gas generator. The replacement cost used in this analysis is higher than the cost of new entrant because it requires low- or zero-carbon replacements rather than a simple gas turbine replacement.

Xcel Energy's financial parameters (e.g., discount and tax rates) were used. The project life is 25 years, starting in 2026. The 2026 LMPs are applied for the first 4 years, the 2030 LMPs for the next 4 years, and the 2034 LMPs for all the years thereafter. A Modified Accelerated Cost Recovery System (MACRS) depreciation schedule was used for the first 15 years.

5.2.4 Model Assumptions and Limitations

This report deals with investigating the profitability solution space for several parameters. While it does generate insights into the unique conditions of the NPPs being studied, the impact of the input assumptions is so large that each must be well understood. If the assumptions below were altered, or different inputs used, the solution space for each plant would change as well. The value of this analysis arises from the ability to sample and display the solution space succinctly.

- **Storage arbitrage operation:** The hydrogen storage operates in a daily arbitrage fashion. The dispatcher finds the highest LMP for a given day and discharges according to the number of discharge hours. Conversely, the dispatcher finds the lowest LMP for a given day and charges for as many hours as needed to fill the storage. This effectively shifts the load from times of high electricity prices to time of low prices, so that electricity sale during high-price hours can be maximized.
- **Price-taker dispatch:** The dispatch model operates in a price-taker fashion, assuming that the change in electricity delivery due to HTSE load does not affect electricity prices. Work is ongoing to quantify the effect of this assumption and extend the model to make it more consonant with the price-maker approach.
- **NPP refueling:** NPP refueling assumes that each plant operates at 50% capacity during the refueling period (3 weeks in a shoulder season, with the exact time depending on the specific NPP). Since refueling occurs in the 2026, 2030, and 2034 profiles, there is some refueling in each year. During refueling, the HTSE uses as much energy from the NPP as it can, then buys the remaining electricity from the grid. Additional capital cost is associated with the extra resistance heaters needed to make this possible. The arbitrage is not performed during refueling, meaning that the HTSE meets hydrogen demand but does not produce excess for storage or shift load to storage. The storage amount in the refueling period is held static. Refueling is also accounted for in the BAU case.
- **Wholesale electricity prices:** The dispatch is performed with wholesale-electricity-price LMPs. Any buying or selling of electricity is based on these wholesale prices.
- **Dispatch prioritizes hydrogen:** The dispatcher prioritizes meeting the hydrogen demand over selling electricity. This means that if there is not enough hydrogen storage to cover all discharge hours, the system uses electricity to produce hydrogen and misses the high-priced electricity sales. This is done to simulate something akin to a hydrogen purchase agreement or a consumer who uses the hydrogen for chemical or industrial processes that require hydrogen at all times.
- **Hydrogen demand is a constant:** A constant hourly amount throughout optimization lifetime.
- **Hydrogen price is a single price, based on demand:** The hydrogen price is founded on the demand curves, based on the input hydrogen-demand parameter. The demand sets the price, which remains constant throughout the optimization lifetime.
- **Clean hydrogen credit:** A clean hydrogen credit is applied as a sensitivity parameter. In the model, it functions as an adder to the sale price. In reality, this would have the same effect as a production tax credit (PTC), or a carbon tax on competitor hydrogen that raises hydrogen prices in the market.

- **Degradation as a capital cost adder:** The year-over-year electrolysis cell degradation was found to effectively reduce the capacity of the hydrogen production facility to 95.3% of its starting value at the beginning of the year. The O&M costs account for the stack addition/replacement to restore the design point hydrogen production at the beginning of each year. This degradation was accounted for in the optimization model by scaling the capacity up by 4.9% (HTSE capacity/0.953) in the cost and O&M calculations. The capacity available for producing hydrogen is fixed at the degraded value rather than quantifying the complexity of degradation effects from hour to hour. This generates a more conservative estimate, since the capacity in the beginning of the year would actually be able to produce slightly more than what is accounted for in this model.
- **Capacity payment and/or replacement covers only the changes from HTSE hot standby:** This assumes that the rated capacity of the NPP is only decremented by the constant hot-standby amount. The plant operates in a mode different from the baseline BAU case, but the capacity (minus the HTSE hot standby) is still available, especially in high-price hours when it draws on the storage. This is semi-idealized, because there may be instances in which this storage is insufficient and hydrogen is prioritized, causing the NPP to miss electricity sale during high-price, high-demand events. Further work should be done to provide insights on this issue.
- **No downtime for HTSE cells:** Downtime for HTSE cell replacement or other maintenance is not included in the hourly dispatch.

5.3 Results

The optimization model facilitated the exploration of several parameters in order to understand their effects on profitability when comparing the NPP-HTSE with the BAU case. The storage-dispatch hours were optimized in the inner loop to maximize the ΔNPV. The hydrogen demand, hydrogen CAPEX, and carbon-free hydrogen credits were varied in the outer loop to determine the range in which the system is profitable (otherwise known as the "envelope of profitability").

The outer loop used an advanced sampling technique called the limit surface search which is available in RAVEN [89]. This technique zeros in on areas in which the ΔNPV changes from negative to positive. As it does, the model bounds the actual points at which the transition from unprofitable to profitable occurs. This means that a projection of the profitable region of this surface can quickly show what combination of the three variables—HTSE CAPEX, hydrogen demand (HTSE capacity), and clean hydrogen credits—will yield a profitable system. This envelope of profitability will illustrate the trade-offs among these three variables in a profitable system. This is valuable for aiding decision-makers in studying these charts and analyzing hypothetical scenarios in which these variables will change, thus enabling them to infer the rough ΔNPV under such scenarios.

5.3.1 Prairie Island

5.3.1.1 Storage Dynamics and Size

First, it is important to understand the underlying optimization that occurs under each combination of capacity, CAPEX, and carbon-free hydrogen credits. In each run, the hydrogen storage charge/discharge hours are optimized by RAVEN. The hydrogen discharge hours effectively set the storage size. The discharge-to-charge ratio sets the HTSE oversize that, along with hydrogen demand, determines

the overall HTSE capacity. The plots in Figure 5.8 show the effect of HTSE capital cost on both the charge and discharge hours. The ΔNPV was maximized at 4 discharge hours in the lower HTSE CAPEX case, and at 2 hours in the high. The system trades higher HTSE capacity and storage capital costs for selling more electricity at high-price hours. The high CAPEX plot shows that the system prefers to miss times of high electricity prices and instead minimize the HTSE size when the HTSE capital cost is high. A lower capital cost creates more value in storage arbitrage; thus, building a slightly larger HTSE to facilitate a larger storage capacity is advantageous. This holds true up until the ΔNPV peaks and starts to drop (e.g., in the 5th and 6th discharge hours in the lower-CAPEX case). The value of arbitrage diminishes with each additional discharge hour, because each subsequent hour will have a lower LMP than the one previously captured. This means that selling electricity at that time is not worth the increase in HTSE and storage size. While the charge hours do have a peak, the optimization shows that it is advantageous to maximize the number of discharge hours. In Figure 5.8, each line corresponds to a different number of charge hours. In both capital-cost cases, the ΔNPV is maximized with the largest number of charge hours. This dynamic is observed because charge hours are inversely proportional to HTSE capacity oversize. If there are more hours during which to overproduce and store hydrogen, the requirement for discharge can be met with less capacity. Minimizing HTSE capacity was advantageous to the system economics, because it is such a large driver of cost.

The plots in Figure 5.8 were run with two different HTSE capital costs, but with a fixed carbon-free hydrogen credit ($1/kg) and a fixed hydrogen demand requirement (746 MWe). The carbon-free hydrogen credit does not affect storage size, because the hydrogen sale is dictated by hydrogen demand, not arbitrage. Since the dispatch prioritizes hydrogen, the same amount is sold no matter the size of the carbon-free hydrogen credit, regardless of arbitrage. Similarly, different hydrogen demands do not affect the storage, because hydrogen is prioritized and sold at the same rate, regardless of arbitrage. This effect of capital cost on storage charge and discharge lengths could create a trade off when there are so few discharge hours that the nuclear capacity requires more replacement capacity. That effect is not quantified in this analysis, but should be considered when deciding on HTSE operational modes. In some cases, there may be enough margin to build larger storage systems and flex the HTSE in a non-optimal configuration in order to avoid necessitating extra replacement capacity. Ultimately, this will depend on the operational mode, the HTSE CAPEX provided by the manufacturers, and how much extra capacity might need to be built elsewhere in the system.

The storage optimization is done on the inner loop. Each individual point that the outer loop samples as part of the subsequent results reflected an optimal storage amount determined by the model.

5.3.1.2 Demand, CAPEX, Carbon-Free Credit Sensitivities

Understanding the relationships among HTSE CAPEX, hydrogen demand, and clean hydrogen credits is important for understanding when the PI NPP-HTSE system is more profitable than the BAU approach. Figure 5.9 shows four different static cases for a hypothetical HTSE plant installed at PI. These four cases help illustrate several important effects. Note that, for each combination of the three variables, the storage charge/discharge hours are optimized in the inner loop.

Adding an HTSE to PI yields a profitable system for a small amount of configurations at very low HTSE capital cost. This region is where the hydrogen demand is maximized without the market being

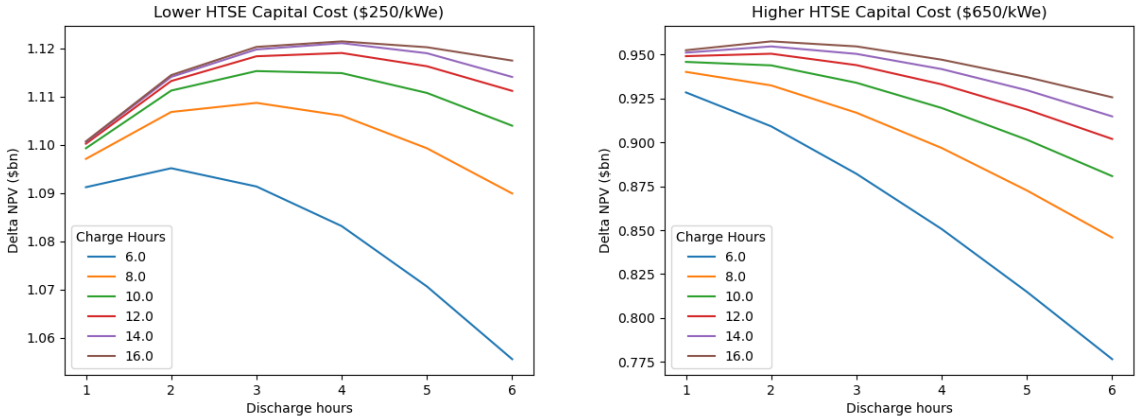

(a) (b)

Figure 5.8: Effect of HTSE capital cost on storage charge/discharge hours on ΔNPV for the project's 25-year lifetime at Prairie Island. All cases include a fixed carbon-free hydrogen credit ($1/kg) and a fixed hydrogen demand requirement (746 MWe).

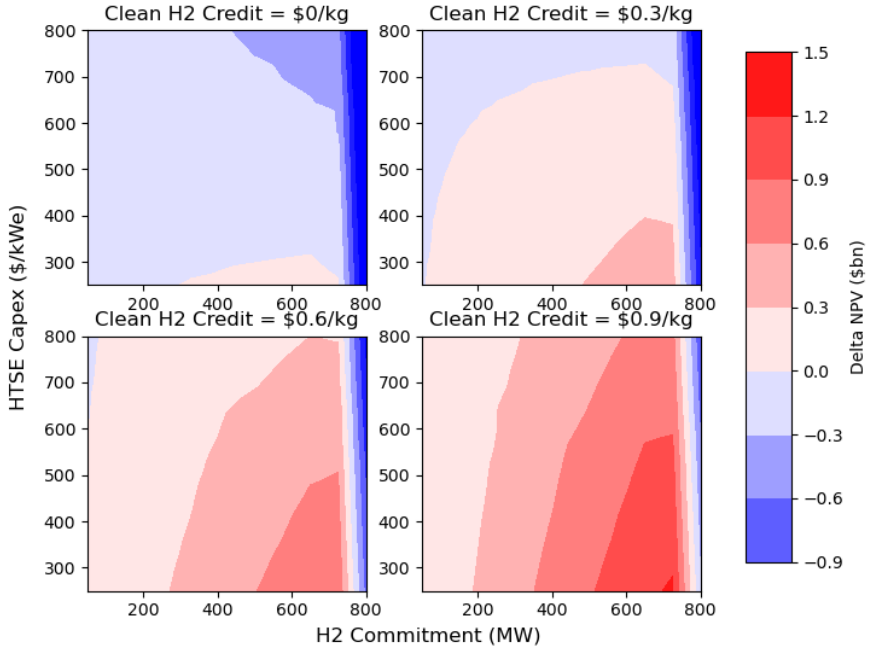

Figure 5.9: HTSE CAPEX (total capital investment), hydrogen demand, carbon-free hydrogen credits, and their effect on the ΔNPV for the NPP-HTSE plant vs. the BAU approach at Prairie Island. For reference, using the full output from the two reactors at PI could produce up to 29,290 kg/hr (703 ton/day) of hydrogen, while a single 545-MW reactor could produce up to 14,570 kg/hr (350 ton/day) of hydrogen.

saturated. In the hydrogen-demand curve for the region surrounding PI, a drop off occurs when the hydrogen supply saturates the demand market as the demand market shifts to the next lowest price tier, pushing the price of hydrogen from $1.14 to $1.10/kg. At $1.10/kg, the profit from hydrogen sales is insufficient to justify larger HTSE facilities. At even higher hydrogen demands, the hydrogen is sold for even less, driving the ΔNPV even lower at higher demand values. The lower sale price prevents the system from recovering the capital cost and other costs, making it less profitable than the BAU approach. This effect can still be seen in cases that include carbon-free hydrogen credits.

By adding a carbon-free hydrogen credit, the system becomes more profitable at higher CAPEX values, as shown in Figure 5.9. With a credit of $0.70/kg, the system is more profitable than the BAU approach in regard to every tested CAPEX prior to the market becoming saturated. The optimal ΔNPVs are still found in the region where the hydrogen demand maximizes the amount sold at the $1.32/kg base hydrogen price. It is conceivable that a small hydrogen credit of less than $0.50/kg would flip a large portion of potential HTSE facilities at PI from unprofitable to profitable (relative to the BAU approach).

Figure 5.9 also demonstrates that the HTSE at PI will be limited by market size rather than NPP capacity. The shallow hydrogen market causes a significant drop off in profitability before the HTSE is large enough to receive all the energy that PI can provide (recall that this is up to 29,290 kg/hr of hydrogen), but as has already been mentioned, the price of hydrogen drops significantly after the supply exceeds 17,600 kg/hr. This means there is still enough capacity at PI to provide electricity to the grid 100% of the time. At a hydrogen production rate of 17,600 kg/hr, PI still has approximately 340 MW to consistently send to the grid, depending on storage capacity and the extra HTSE capacity used for flexing. These results apply to the projected H_2 supply as presented in the assumptions in Figure 5.6 of this article. If higher levels of carbon-free H_2 market demand materialize, the assumptions regarding the H_2 market—and thus of this analysis—would change.

5.3.1.3 Envelope of Profitability

The previous section gives an example of the economic implications of the three varied parameters, but the coarseness of the sampling does not quantify the exact combinations would make the system profitable. To remedy this coarseness in sampling, RAVEN's limit surface search capability was used. The limit surface search creates boundaries around the actual points at which the ΔNPV changes from negative to positive. The search is shown in Figure 5.10. The plot is a 3-D figure in which the varied parameters each exist on their own axis. The red surface represents a negative ΔNPV, and the green surface represents a positive one. The limit surface sampling strategy explored the solution space and honed in on the transition spots at which the sign of the ΔNPV changes. This sign change means that the system went from unprofitable (negative) to profitable (positive)—as compared to the BAU approach.

While the 3-D visualization is useful for illustrating the shape of the profitability transition region, it is difficult to understand the detailed interactions among the three degrees of freedom. To visualize this, the green surface can be projected onto a 2-D plane, as shown in Figure 5.11. This surface represents the boundary of profitable configurations. Representing the limit surface in this manner enables visualization of the relationship among the sampled variables.

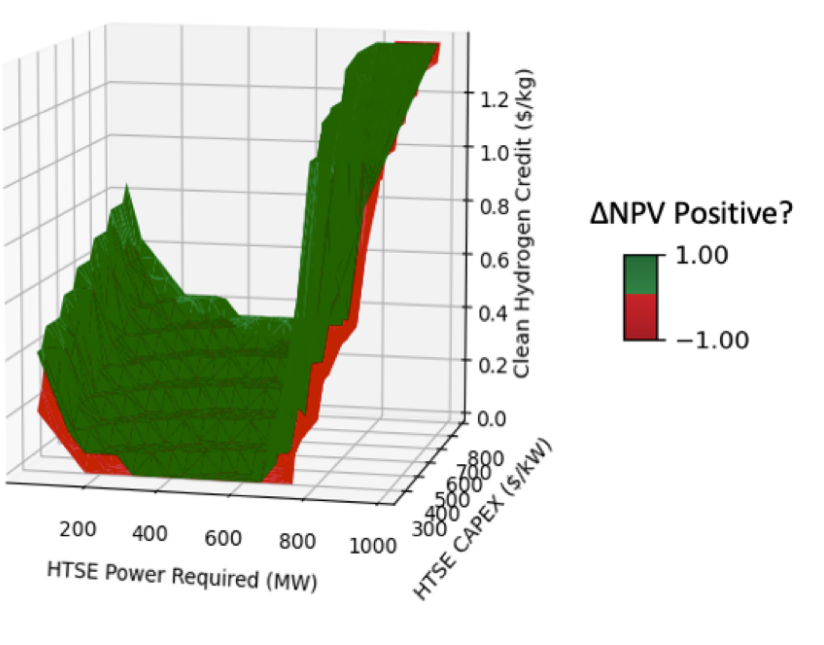

Figure 5.10: Limit surface search exploring the hydrogen delivered, HTSE CAPEX (total capital investment), and clean hydrogen credits at Prairie Island. The green surface represents a positive ΔNPV relative to BAU, and the red surface represents a negative ΔNPV relative to BAU.

Observing one or two parameters in Figure 5.10 indicates what the remaining degrees of freedom should be. For example, if a manufacturer can build the HTSE system at $500/kW total capital investment, and the hydrogen demand that PI expects to meet is 600 MW, then a modest production tax or some other carbon-free hydrogen credit of $0.20/kg is required in order to exceed the profitability of the BAU approach. Because Figure 5.11 is the projection of a profitable limit surface, every combination of points on this plot is a break-even point. Any improvement on these degrees of freedom (e.g., lower-than-expected capital cost at the fixed demand and credit price) will improve the overall ΔNPV.

These results show that an HTSE at PI could exceed the profitability of the BAU approach, even without any hydrogen credits at lower total HTSE capital cost values. The dynamic in which demand is maximized without saturating the market is shown in Figure 5.11, and is similar to what was discussed in the previous section. Once the HTSE provides more than 17,600 kg/hr (422 ton/day, a 740 MW capacity), the hydrogen is saturated and the price of hydrogen drops. Hydrogen credits are then required to make the system to profitable. This result suggests that new hydrogen demand must be created in order to use PI's full capacity to produce hydrogen. Note also that this analysis assumes that PI can meet all existing demand on its own, when in reality this demand will likely be spread across various energy providers. Hydrogen credits are also required to make the system profitable at total HTSE system capital costs of over $500/kW at the largest hydrogen delivery before saturation. To compete with BAU at lower hydrogen delivery rates and without any hydrogen credits, very low capital costs are required. Carbon-free hydrogen credits of as much as $1/kg are required in each configuration (prior to market saturation) in order to generate higher profits than the BAU approach. Larger carbon-free hydrogen credits are needed if the hydrogen demand requires over 740 MW and the hydrogen price decreases.

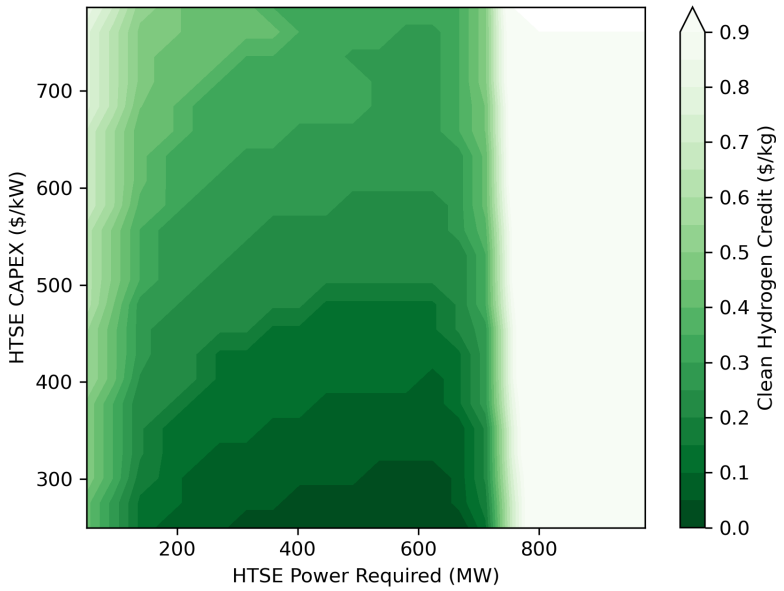

Figure 5.11: Profitable limit surface of HTSE CAPEX (total capital investment), hydrogen demand, and carbon-free hydrogen credits at Prairie Island. For reference, the maximum energy that PI could provide (1096 MW) to an HTSE could produce up to 29,290 kg/hr (703 ton/day). A single 545 MW reactor could produce up to 14,570 kg/hr (350 ton/day).

5.3.2 Monticello

5.3.2.1 Storage Dynamics and Size

Monticello features storage size dynamics similar to those of PI. Figure 5.12 shows that lower HTSE capital costs facilitate more discharge hours. Lower capital costs would lead to greater hydrogen storage capacity and a larger HTSE in order to overproduce and store hydrogen. The amount of hydrogen production and size of the carbon-free hydrogen credits were fixed for both these plots. Much like PI, lower capital costs lead to hydrogen storage tank sizes capable of meeting demand for 4 hours, while higher capital cost cases point to hydrogen storage capacity in the range of 2–3 hours of demand as being more desirable.

5.3.2.2 Demand, CAPEX, and Carbon-Free Credit Sensitivity

Similar to PI, the hydrogen delivery, CAPEX, and carbon-free hydrogen credits were varied for the Monticello NPP. These three parameters and their effect on the ΔNPV is shown in Figure 5.13. Monticello has a much smaller potential hydrogen market, meaning that profitability is only possible in much smaller HTSE sizes.

No combination of CAPEX and hydrogen production amount made the Monticello plant more profitable than BAU unless a PTC or carbon-free hydrogen credit was included. The system started to see profitability at low CAPEX and optimal demand, along with a carbon-free hydrogen credit of $0.30/kg. This differed from PI, where a small range of CAPEX and demands were enough to demonstrate ample

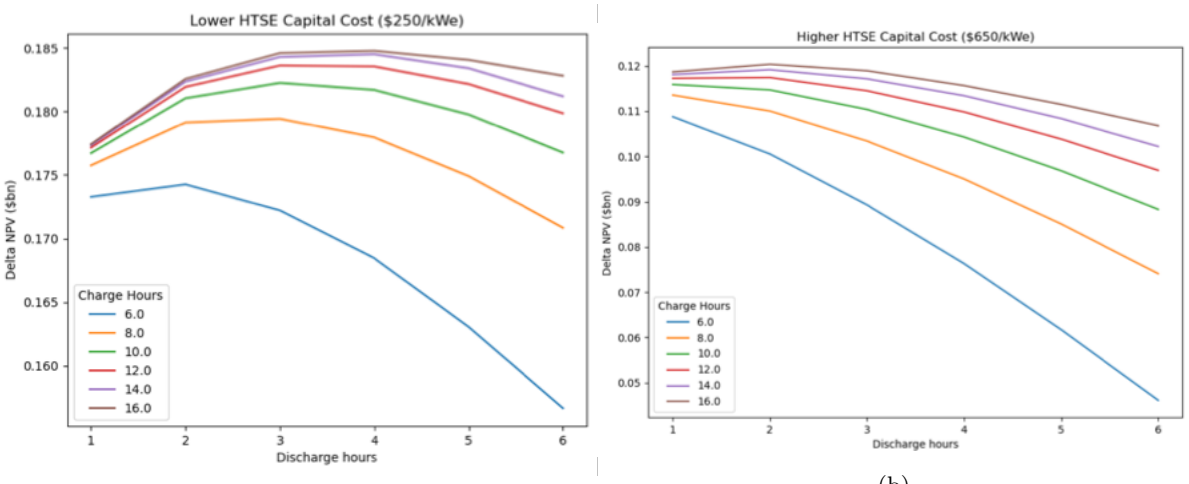

(a) (b)

Figure 5.12: Effect of HTSE capital cost on storage charge/discharge hours on the ΔNPV over the project's 25-year lifetime at Monticello. All cases have a fixed carbon-free hydrogen credit ($1/kg) and a fixed hydrogen demand requirement (746 MWe).

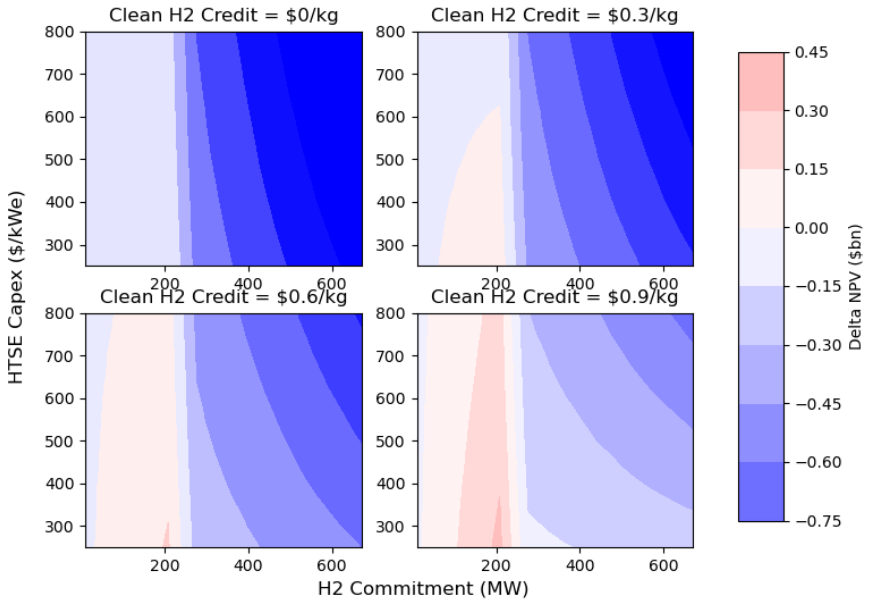

Figure 5.13: HTSE CAPEX (total capital investment), H_2 demand, carbon-free hydrogen credits, and their effect on the ΔNPV vs. BAU at Monticello. For reference, the maximum energy that Monticello could provide to an HTSE could produce up to 17,930 kg/hr (430 ton/day).

profitability, even without any PTC. The difference is due to the higher demand surrounding PI, thus facilitating large HTSEs before the market is saturated and the price drops.

5.3.2.3 Envelope of Profitability

The envelope of profitability for the Monticello NPP was calculated via the same limit surface search approach used in the PI analysis. Figure 5.14 shows the limit surface for the Monticello NPP, produced by varying the amount of hydrogen delivered, the HTSE CAPEX (total capital investment), and the clean hydrogen credits. Compared to PI, adding an HTSE at Monticello creates a smaller band of profitability vs. BAU. The analysis shows that some type of PTC or carbon-free hydrogen credit is required to make Monticello profitable at every demand level and CAPEX point investigated, due to the smaller hydrogen market and slightly lower hydrogen sale price.

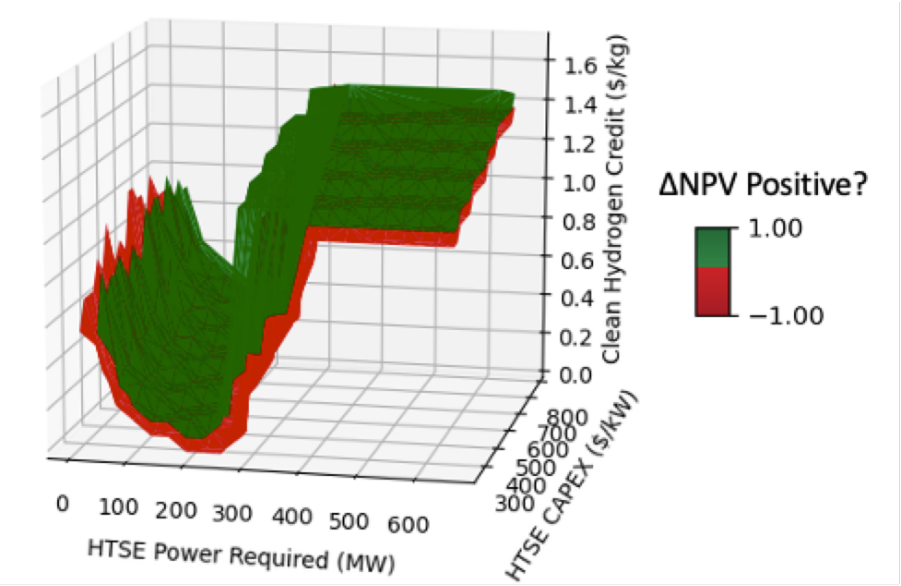

Figure 5.14: Limit surface search exploring the H_2 delivered, HTSE CAPEX (total capital investment), and carbon-free hydrogen credits at Monticello. The green surface represents a positive ΔNPV relative to the BAU approach, and the red surface represents a negative ΔNPV relative to the BAU approach.

As was done for PI, the profitable surface was extracted from Figure 5.14 and plotted on Figure 5.15, which shows the combinations of clean hydrogen credits, total HTSE system CAPEX, and hydrogen delivery amount necessary for the system to break even relative to the BAU approach. The white space means that there were no break-even configurations for the combination of parameters investigated. This plot shows that even at hydrogen delivery amounts prior to market saturation, a PTC of $0.05–$0.50/kg is required.

5.4 Discussion

The results of the economic and dispatch optimization modeling show that a hybrid nuclear-HTSE approach can be profitable at both the PI and Monticello NPPs. In each instance, the trade-offs among the amount of hydrogen delivered, the HTSE CAPEX, and any clean hydrogen credits is important for understanding the sizes and economic parameters needed to achieve profitability over the BAU approach.

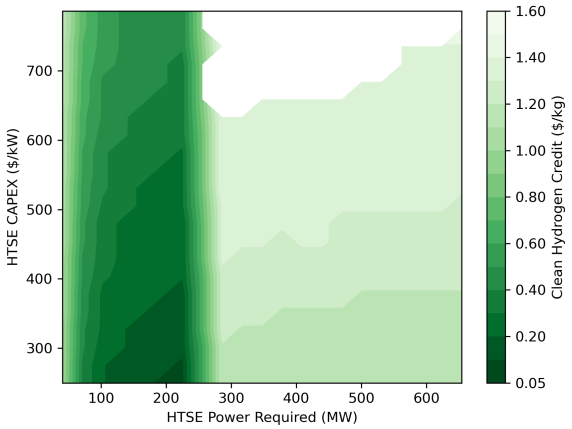

Figure 5.15: Profitable limit surface vs. BAU with HTSE CAPEX (total capital investment), hydrogen demand, and carbon-free hydrogen credit sensitivities at Monticello. For reference, the maximum energy that Monticello could provide to an HTSE could produce up to 17,930 kg/hr (430 ton/day).

HTSE profitability highly depends on the local hydrogen market. The optimal hydrogen delivery was to commit as much hydrogen as possible per hour, without saturating the market and reducing the sale price of hydrogen. The hydrogen market surrounding PI was larger than that around Monticello, so hydrogen delivery amounts—and thus HTSE sizes—could be larger at PI than at Monticello. Monticello's optimal hydrogen delivery amounts on a kg/hr basis were nearly three times less than those of PI. This hydrogen market result could be further investigated by looking at hydrogen market sensitivities or understanding the various hydrogen sale contracts into which the hybrid nuclear-hydrogen system might enter. This simulation could later be extended to include more hydrogen-market and demand projections throughout the 25-year life of the project, rather than using a static hydrogen curve. This would allow the model to capture hydrogen demand increases stemming from new users who may come online in the 2030s.

In addition to dependence on the hydrogen market, system profitability is driven by the overall sale price of hydrogen. The plants generally required some type of adder to what hydrogen could be sold for in the market. This adder could come in the form of a PTC, a carbon tax on competitors, or simply an end user willing to pay more for carbon-free hydrogen. Adder amounts ranged from \$0–\$0.9/kg at PI, and \$0.07–\$1.6/kg at Monticello. For context, the Wyden energy tax credit bill that cleared the Senate Finance Committee seeks to implement up to \$3/kg in PTCs or a 30% tax break on capital costs as an investment tax credit [90]. Either option would make both PI and Monticello profitable using this set of inputs.

HTSE capital costs had a large effect on profitability, and the limit surface search captured a large range of possibilities. The DOE Hydrogen and Fuel Cell Technologies Office Record suggests a capital cost of around \$700/kW [91]. Regardless of the configuration of either plant, this would require some type of carbon-free hydrogen credit. Several electrolyzer manufacturers maintain that their capital costs would be less than \$500/kW, meaning that PI could run profitably without a PTC or a carbon-free hydrogen credit. Such was not the case for Monticello, where a credit of \$0.60/kg would still be needed. The amount of credits needed by the NPP-HTSE system would highly depend on HTSE capital costs,

but credits of more than $1.00 and $1.50/kg at PI and Monticello, respectively, would make the hybrid system competitive in regard to all CAPEX values under $800/kW prior to saturation of their respective hydrogen markets.

Discussions on the profitability of Monticello will differ from those on the profitability of PI, mainly due to their respective hydrogen markets and sizes. The capital cost (on a $/kW basis) is reduced as the plant grows larger. If the hydrogen market can handle the delivery from the bigger plant, it will be advantageous to maximize the plant size.

5.5 Conclusions

This report demonstrated the ability to model and assess the profitability of an IES system in regard to various combinations of sizes, capital costs, and credits for carbon-free hydrogen production. The results show that, under specific inputs and assumptions, adding an HTSE system to PI and Monticello could generate higher profits than generated via the BAU approach. The limit surface search revealed the optimal HTSE size to be as large as possible without saturating the market and reducing the H_2 price. For this model to be used in making investment decisions, each location should be tested using more inputs. This model could be run for any location or plant, so long as the economic data, electricity prices, and hydrogen demand are known.

Future work should include strategic improvement to each assumption. This model operates as a price taker, but understanding how the fluctuations in HTSE load affect electricity prices would be important. Additional sensitivities pertaining to hydrogen consumers would also help in better understanding the required HTSE size for a specific region.

5.6 Acknowledgements

The author's would like to acknowledge and thank Bethany Frew, Daniel Levie, and Mark Ruth from the National Renewable Energy Laboratory for providing PLEXOS model outputs that were used in this research.

This manuscript (the work encompassing Chapter 4 of this dissertation) has been authored by a contractor of the US Government for the U.S. Department of Energy, Office of Nuclear Energy (DOE-NE), under DOE-NE Idaho Operations Office contract DEAC0705ID14517.

Chapter 6: Microreactor Techno-Economic Analysis

Each of the three previous studies focused on integrated energy system applications of existing reactors and quantified the effects of temporal resolution on profitability and economics. This study delves into the spatial component of integrated energy systems and their techno-economic analysis. It also uses a microreactor as the nuclear power source, providing insight into a greenfield, "new build" system.

6.1 Introduction

Microreactors are small nuclear reactors that are less than 20 MW_e capacity. These reactors are being developed for replacement of diesel generators, remote energy needs, standard electricity production, or process heat applications. Their small size gives them an advantage over traditional reactors in that they can be deployed quickly and to a variety of locations. Time between refueling is typically longer than LWRs, simplifying the supply chain. Some microreactors can also be developed for mobile uses, such as military energy or shipping and transportation applications.

Unlike traditional, large light water reactors, the microreactor technologies under development use a variety of coolants, fuel configurations, and power conversion systems. Several vendors are developing high temperature gas reactor variants that use TRISO fuel. Ultra Safe Nuclear Corp (USNC) is also developing a TRISO fueled, high temperature reactor; the Micro Modular Reactor (MMR) [30]. The MMR is a 5 MW_e reactor that uses Fully Ceramic Microencapsulated (FCM) fuel. The FCM fuel encapsulates TRISO fuel kernels in a silicon carbide matrix using additive manufacturing techniques. Oklo Inc is developing a fast spectrum microreactor, Aurora, that uses heat pipes rather than flowing coolant to transfer heat from the core into the power conversion systems [92]. Aurora is planned to be only 1.5 MW_e and use recycled fuel from legacy reactors. The x-energy xe-100 is an 80 MW_e, which shares similarities with microreactors, but may not fit the strict, under 20 MWe definition. The xe-100 reactor does use TRISO fuel in embedded in fuel pebbles, can reach temperatures of 750°C, and uses helium as a coolant. Modular manufacturing will be employed to build xe-100 reactor units [93]. MicroNuclear LLC is developing the Molten Salt Nuclear Battery (MsNB) which is a molten salt reactor that uses natural circulation phenomena and heat pipes to extract heat for electricity production or process heat uses [94].

While the design of microreactors can vary, there are several features shared between designs, such as modularity. Fabricating all or part of the reactor in a factory helps these reactors avoid the long construction projects that have led to cost overruns in the U.S. and European reactor projects in the 21st century. That modularity could also contribute to cost improvements from one reactor to the next as the reactor fabrication processes and facilities mature.

The small size of these reactors can be an asset from a planning perspective as well. With less nuclear material, licensing could be easier with smaller exclusion zones and smaller onsite waste storage footprints. Other cost reductions, such as shared employees between multiple reactors or autonomous control, could also bring microreactor costs down relative to their larger counterparts.

While there are distinct advantages to microreactors, there are also disadvantages that need to be understood. First, while the economy of numbers can reduce the capital costs, the microreactors lose out on the economy of scale compared to traditional LWRs. On a per kW basis, microreactors are projected to be more expensive than traditional light water reactors and small modular reactors. To add more capacity, a microreactor would have to add more units in parallel, necessitating more material use and more cost per kW. That could limit microreactor applications to niche cases that a large reactor would not be suitable for, such as remote installations. A microreactor would need to offset its small size and relatively expensive cost of energy with the advantages of factory fabrication and its ability to enter markets that traditional light water reactors could not enter.

For Microreactors, competing against variable renewable electricity (VRE) is difficult because the levelized cost of electricity (LCOE) from a microreactor is expensive when compared to VRE. The selling point of a microreactor would be its consistent power output. If consistency and reliability are valued, the microreactor could be attractive to power producers or consumers. This would be especially useful in remote locations, such as the arctic, whose harsh conditions make production of renewable electricity difficult and resiliency of the utmost importance.

When compared to other energy production methods, microreactors could offer carbon free heat, which would compete with natural gas with carbon capture, biomass burning, or concentrating solar power. Each of these technologies is either expensive or low-greenhouse gas emissions instead of zero emissions. The likeliest low-carbon heat competitor, natural gas with carbon capture, still uses natural gas and emits some CO_2 at the plant. There are few truly carbon free heat sources, meaning microreactors that could produce high enough heat for cheap enough could take advantage of the market gap.

The carbon free heat from a microreactor could be used for a host of applications including, but not limited to, water desalination, steel production, chemical production, or hydrogen production. Producing a commodity like chemicals or hydrogen that require continuous operation could improve microreactor economics relative to competitors.

The location and application of a microreactor is important for the overall profitability of a project. The purpose of this study is to evaluate a microreactor with hydrogen IES and the economic potential of co-locating microreactors versus building a centralized plant and distribution network. The microreactor utilizes an HTSE to produce hydrogen and the profitability is evaluated. A low capital cost cast case, representative of a small modular reactor (SMR), is also run for comparison to larger capacity reactors.

6.2 Microreactor IES Methodology

This study employs the Molten Salt Nuclear Battery (MSnB) as the microreactor technology. A schematic of the MsNB is given Figure 6.1. The MSnB is a 10 MW_{th} microreactor that uses fluorine, lithium, beryllium (FLIBE) salt and a 20% enriched uranium mixture. The fuel and coolant eutectic circulates in the reactor via natural convection. At the upper end of the reactor vessel, heat pipes move heat from the primary circulating coolant to a helium secondary loop. This creates a density gradient such that the hotter, less dense salt mixture from the inside of the reactor vessel flows upwards and the cooler, more dense salt after heat is removed flows downward.

The secondary loop extracts heat by passing helium over the opposite side of the heat pipe bundles.

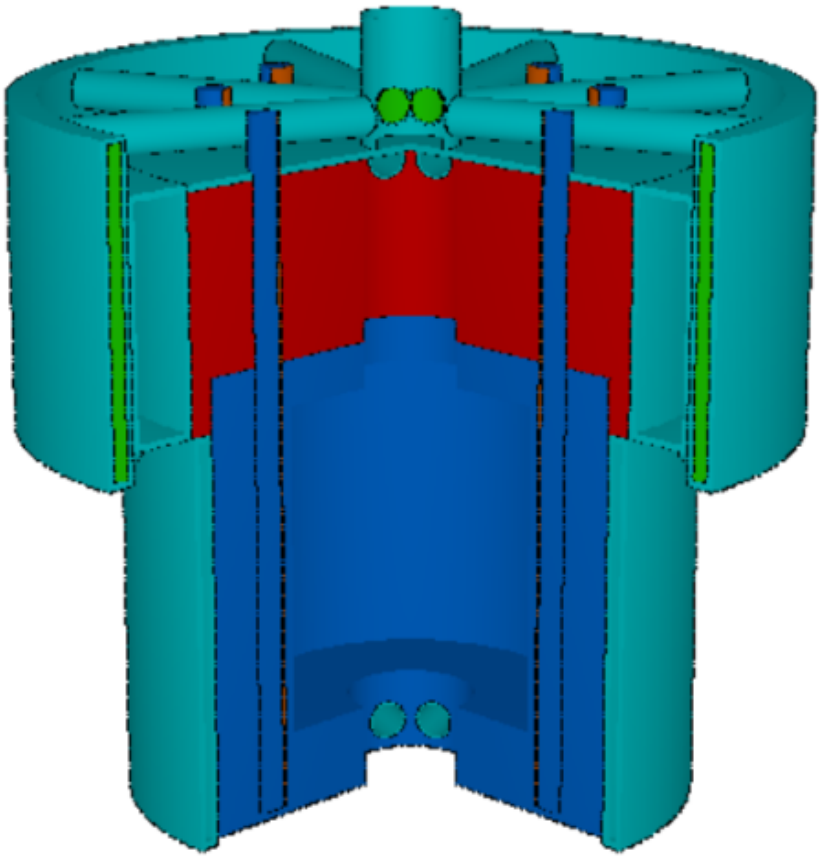

Figure 6.1: Cross section of molten salt nuclear battery.

The helium is used in a recuperated brayton cycle power conversion unit. The MsNB is projected to operate with a 37% thermal efficiency and produce 3.7 MW_e. It is possible to build multiple MsNBs at a single site to meet larger energy demands.

The MsNB hybrid system produces hydrogen via HTSE. The capital and O&M costs for the HTSE were taken from the curve fits in Section 5.2.1. An energy to hydrogen conversion efficiency of 37.4 kWh_e/kg H_2 with an additional 6.4 kWh_{th}/kg H_2 is assumed, taken from Table 5.1.

6.2.1 Regional Cases

In order to demonstrate effects of location on the MsNB with hydrogen economics, two regional cases were developed for this model; Texas and Alaska. The Texas case is meant to represent a standard U.S. market and the Alaska case is a rural location where competing energy is more expensive, demand is smaller, and transportation distances are greater.

Because hydrogen demand is scarce and projections are difficult, the hydrogen demand was based on refinery needs. Oil refineries currently represent the largest hydrogen consumers in the United States. Refining in the US consumes, on average, 200-300 SCF of hydrogen per barrel of oil refined [95]. This equates to 0.3 to 0.75 kg of hydrogen per barrel refined. Around 30% of hydrogen is produced on site as a byproduct of the refining process, with the other 70% procured from steam methane reforming or hydrogen produced as a byproduct of other chemical processes [96]. This analysis assumes that the MsNB hydrogen production plant provides 1/3 of the total hydrogen consumed by the refinery.

6.2.1.1 Texas Hydrogen Demand and Transmission

The Houston area was chosen as a target zone for the Texas case. The reasoning was that East Texas has a large refining capacity, and thus a large hydrogen demand, in a small radius. The large demand in a relatively small area would also be the opposite of the rural case that has a smaller demand in a larger geographical area. An MsNB site was chosen approximately in the middle of the demand centers.

Figure 6.2 shows a map of the Texas area refineries targeted and the proposed location of the central MsNB hydrogen production hub. Two refineries reside in Houston, two in Texas City, with the MsNB hub located south of Houston. Note that nuclear siting is a complex process that involves environmental and geological review, community comments, and licensing activities. This study does not propose exact locations for nuclear activities. Rather, it uses these sites as examples of how distances would affect hydrogen cost.

Table 6.1 shows the specific distances and needs for hydrogen production. Hydrogen consumption is assumed at a rate of 0.53 kg H_2 per barrel of oil (bby). At a hydrogen conversion rate of approximately 40 kWh_e/kg H_2, the refineries listed require 58,000 to 138,000 kg/day of hydrogen. Under the assumption that the MsNB plant produces 1/3 of the hydrogen demand, the plant needs to produce 19,000 to 46,000 kg/day, requiring anywhere from 9 to 21 MsNBs.

This energy demand, requiring approximately 69 MsNBs and 250 MW_{th} for all the hydrogen production, is quite a large demand to be met exclusively with microreactors. A small modular reactor (SMR) case was added as a comparison to the centralized production scenario. The SMR scenario assumes a lower capital cost on a per kW basis and acts as another benchmark.

The compression costs are calculated by using outlet pressure of the HTSE stack and sizing a com-

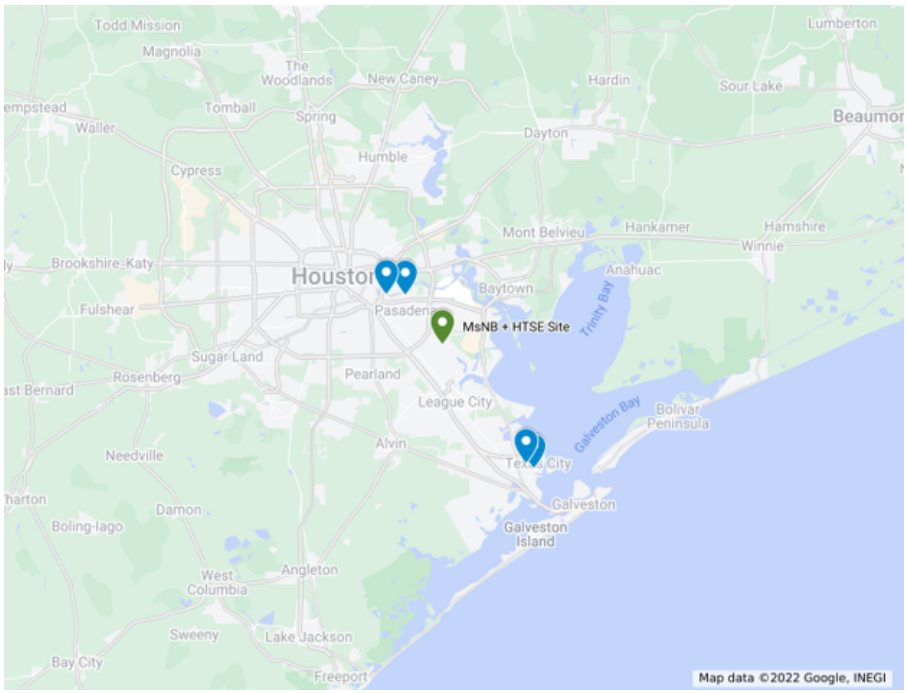

Figure 6.2: East Texas refineries and MsNB location for this analysis.

Table 6.1: Texas Scenario Refineries and Hydrogen Demand

Refinery	Distance to Central Hub	Oil Produced (bby/yr)	Hydrogen Demand (kg/day)	Electric Capacity Requirement (MW)	No. MsNB Units
Valero Texas City	21.4 mi	260,000	45,933	76	21
Marathon Texas City	20.0 mi	220,00	39,750	66	18
Chevron Pasadena	8.5 mi	110,00	19,433	32	9
Valero Houston	10.3 mi	255,00	45,50	75	21

pressor to provide the pipeline inlet pressure that delivers the correct pipeline outlet pressure when pressure drop is accounted for. Pressure drop was calculated according to Darcy-Weisbach equation, given in Equation 6.1.

$$\Delta P = f_D * L * \frac{\rho}{2} * \frac{v^2}{D} \tag{6.1}$$

Where:

- ΔP, pressure drop in pipe
- f_D, darcy friction factor
- L, pipeline length
- ρ, hydrogen density
- v, average velocity of fluid, found by using the required flow rate and cross sectional area of the pipe
- D, pipe diameter

In Texas, there were two main hydrogen supply lines and two lower flow rate lines. Two refineries are north and two refineries are south of the central site. All pipes use a 0.6096m (24in) diameter pipe. The pipe is assumed to be welded steel with a roughness of 1.5e-05 m. Hydrogen density at pipeline conditions, 25°C and 24,821 kPa (3600 psi), is 17.32 kg/m^3. Viscosity is 9.5e-06 Pa-s.

Table 6.2 shows the parameters for each line in the Texas pipe network. Main lines run to the closest refineries in the north and south direction to the central location. The spur lines are sent on to the outer refineries and thus have lower overall flow rates.

Table 6.2: Pressure Drop Calculation and Inputs, Texas Case

Parameter	Main Line, South	Spur Line, South	Main Line, North	Spur Line, North
Length (m)	32187	2253	16576	2253
Flow rate (kg/s)	0.99	0.46	0.75	0.52
Velocity (m/s)	0.2	0.09	0.15	0.10
Reynolds Number	215,759	100,095	162,376	113,441
f_D	0.010	0.010	0.011	0.0112
Pressure Drop (Pa)	170.39	2.66	54.17	3.92
Total Pressure Drop (Pa)	231.14			

The pressure drop within this pipeline is relatively small when compared to natural gas or other gas transmission. Hydrogen is less dense and less viscous than natural gas and therefore is does not lose pressure as quickly as natural gas. These transmission distances are also relatively short and have a larger diameter pipe.

Pipeline pressure drops of under 2,068 kPA (300 psi) are considered acceptable, meaning this system is easily within desired pipeline specifications.

The majority of compression power in the hydrogen line comes from raising HTSE stack outlet to pipeline transmission pressure. The required compressor power can be calculated according to Equation 6.2.

$$P_{comp} = \frac{kZRT_1}{k-1} * [(\frac{P_2}{P_1})^{(k-1)/k} - 1] * Q_m \tag{6.2}$$

Where:

- P_{comp}, Compressor power
- k, Heat capacity ratio or adiabatic index
- Z, Compressibility factor
- R, Ideal gas constant
- T_1, Compressor inlet temperature
- P_1, P_2, Compressor power in and out, respectively
- Q_m, Molar flow rate of hydrogen

The inputs and output of Equation 6.2 are given in Table 6.3. The number of an 18.06 MW compressor is required. The pump would consume 158,224 MWh of energy during a full year's operation. This assumes one compressor at the central MSnB and HTSE location that compresses hydrogen at the head of the distribution pipeline.

Table 6.3: Compressor Power Calculation and Inputs, Texas Case

Parameter	Value
k	1.405
Z	1.162
R	8.31 J/mol-K
T_1	298 K
P_1	500,000 Pa
P_2	24,821,000 Pa
Q_m	869 mol/s
P_{comp}	18.06 MW

6.2.1.2 Alaska Hydrogen Demand and Transmission

A map of the Alaska refineries and central hydrogen production location are shown in Figure 6.3. Distance between production hub and refinery is larger in Alaska is larger and the demand is smaller. There are only two refineries in Alaska, Kenai and Valdez, and both are relatively small when compared to their Texas counterparts. The central case places a hydrogen production hub in the Anchorage area and pipeline distribution from Kenai and Valdez refineries. The details of the two refineries considered are shown in Table 6.4. An SMR centralized case is also considered in the Alaska scenarios.

Table 6.4: Alaska Scenario Refineries and Hydrogen Demand

Refinery	Distance to Central Hub	Oil Produced (bby/yr)	Hydrogen Demand (kg/day)	Electric Capacity Requirement (MW)	No. MsNB Units
Kenai	70.0 mi	68,000	12,013	20	6
Valdez	117 mi	60,000	10,600	18	5

The same method was used to find pressure drop and compressor power in the Alaska case. Table 6.5 shows the calculation of pressure drop in the Alaska pipeline network. A 0.3048 m (12 in) diameter pipe was used because of the Alaska case's lower hydrogen demand and flow rates. The Alaska hydrogen

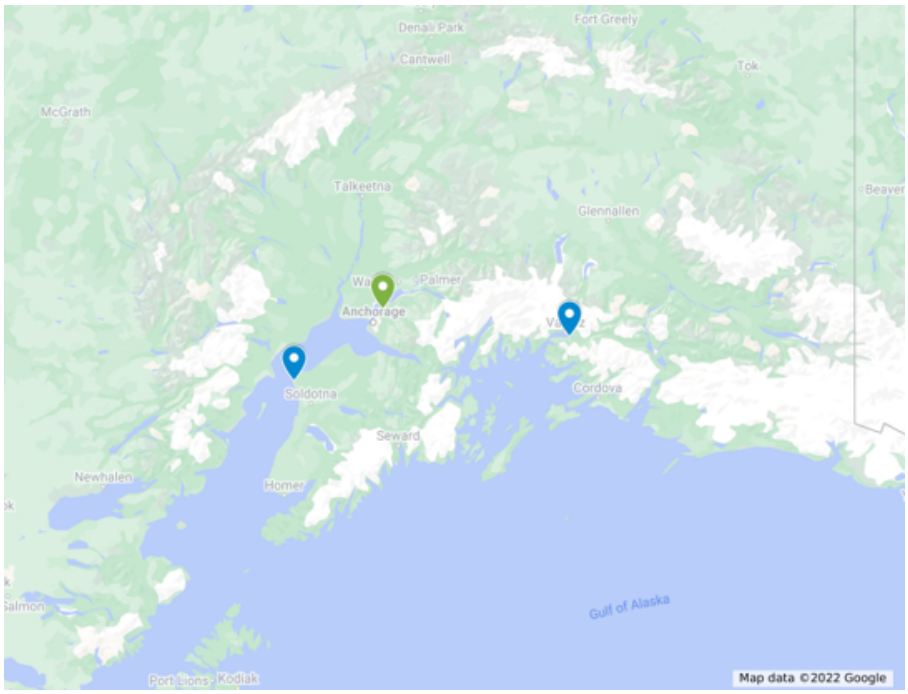

Figure 6.3: Alaska refineries and MsNB location for this analysis.

pipeline network only has two main pipelines, north and south. The pipeline distances are also much greater than the Texas network. Much like the Texas case, the pressure drop is quite small compared to the operating pressure.

Table 6.5: Pressure Drop Calculation and Inputs, Texas Case

Parameter	Main Line, South	Main Line, North
Length (m)	112,653	188,292
Flow rate (kg/s)	0.14	0.12
Velocity (m/s)	0.11	0.10
Reynolds Number	60,502	53,384
f_D	0.0097	0.0100
Pressure Drop (Pa)	375	505
Total Pressure Drop (Pa)	880	

Compressor power was also calculated for Alaska. Table 6.6 shows the calculation parameters and compressor power. To run over the course of the year, the compressor consumes 23,826 MWh of energy.

6.2.2 MSnB and HTSE Cash Flows

Three main costs reactor cost categories were used to quantify MsNB cost; capital cost, operating and maintenance cost (O&M), and refueling cost. Capital cost and O&M costs were derived from three sources. The lowest cost projections came from the MsNB developer, Micronuclear LLC. Micronuclear estimated the capital cost and O&M to be \$6500/kW_e and \$100 kW_e-yr, respectively. These costs were cross referenced with literature and industry projections. Abou Jaoude et al. produced cost estimates for a microreactor that employs heat pipe cooling at approximately \$10,000/kW_e [97]. This value was

Table 6.6: Compressor Power Calculation and Inputs, Texas Case

Parameter	Value
k	1.405
Z	1.162
R	8.31 J/mol-K
T_1	298 K
P_1	500,000 Pa
P_2	24,821,000 Pa
Q_m	131 mol/s
P_comp	2.72 MW

used for the mid case and a value of \$13,000/kW_e was used as an upper bound. Mid and upper scenarios also used O&M values of \$173 kW_e-yr and \$250 kW_e-yr.

The refueling cost was calculated based on the cost of high assay, low enriched uranium (HALEU) fuel and FLiBe salt. From previous MsNB analysis, one core load contains 13.7 tons of FLiBe and fuel mixture and 361 kg HALEU. The separative work unit (SWU) cost of HALEU is approximately \$9,500 as of quarter 2, 2022, meaning that the HALEU cost is \$3,400,000. FLiBe consists of 52% LiF and 48% BeF_2 by mass. With a total FLiBe load of 13,339 kg, LiF and BeF_2 will cost \$1,040,000 and \$615,000, respectively. With a cost total of \$5,055,000 in fuel salt costs, the balance of refueling costs account for salt preparation and processing, transportation, new cask, etc. These extra costs are relatively unknown for new designs, so a multiplier of 2 was applied to the calculated fuel salt cost resulting in a base refueling cost of \$10,000,000. The MsNB is designed to operate like a battery, where the core can be replaced in it's entirety. If the heat pipes and other thermal infrastructure is removed and replaced after every refueling period, it is conceivable that the refuel cost could be dominated by fuel salt and new core fabrication costs. There are many uncertainties with this estimation that would be reduced as the MsNB design becomes more mature. For the purposes of this study, a rough estimate and sensitivity should suffice. The low, mid, and high refueling costs are set at \$8,000,000, \$10,000,000, and \$12,000,000, respectively.

With the refueling, capital, and O&M cost, the MsNB costs can be quantified in the model. Table 6.7 shows the values for each cost sensitivity run through the MsNB IES model.

Table 6.7: MsNB Costs by Sensitivity

Parameter	Low	Mid	High
Capital Cost (\$/kW)	\$6,500	\$10,000	\$13,250
Operation & Maintenance Cost (\$/kW-yr)	\$100	\$172	\$243
Refuel Cost	\$8,000,000	\$10,000,000	\$12,000,000

HTSE capital cost are set at \$650/kW_e. Variable and fixed O&M costs come from Sections 5.2.1.

This analysis assumes hydrogen pipeline transportation. Costs can be broken into two categories; pipeline capital cost and pipeline O&M costs. The base pipeline capital cost were set at \$1,000,000/mile, as found in [49]. This cost encompasses pipeline and compressor capital costs. Pipeline O&M costs were derived from the compressor electricity cost required to move hydrogen to its final location.

The electricity price differs between Texas and Alaska scenarios. Texas electricity was assumed to

be $30/MWh and Alaska electricity was assumed to be $75/MWh. Total electricity cost is found by multiplying the energy consumption found in Section 6.2. The variable O&M pipeline cost is assumed to only include electricity cost.

With HTSE, transport, and MsNB costs quantified, the model produces a levelized cost of hydrogen (LCOH) for each case and each scenario. LCOH in this analysis is defined in Equation 6.2.2. The LCOH is the sale price of hydrogen that makes the whole system NPV equal to zero. LCOH is explained further in Section 4.2.4.

$$0 = \sum_{t=0}^{t=lifetime} \frac{LCOH * m_{sold} * (1 - tr)}{(1 + r)^t} - (DCF_{MsNB} + DCF_{HTSE} + DCF_{pipeline})$$

Where,

- $LCOH$, levelized cost of electricity in $\$/kgH_2$
- m_{sold}, total hydrogen sold in kg
- tr, tax rate
- r, discount rate
- t, time period, in years
- DCF_{MsNB}, discounted MSnB cashflow including capital cost, capital depreciation, fixed O&M
- DCF_{HTSE}, discounted HTSE cashflow including capital cost, capital depreciation, variable and fixed O&M
- $DCF_{pipeline}$, discounted pipeline cashflow including capital cost, capital depreciation, variable O&M

The financial parameters used in the LCOH model are listed in Table 6.8.

Table 6.8: Financial Parameters

Parameter	Value
Discount Rate (Real)	7%
Depreciation	MACRS 15-year
Project Lifetime	40 years
Tax Rate	25%
Inflation Rate	3%

6.3 Results

6.3.1 Texas Case

In the low, medium, and high cases, the LCOH was nearly identical between the central and co-located scenarios. LCOH for the mid case showed a difference of only $0.02, as shown in Figure 6.4. The SMR case was substantially cheaper, showing a savings of at least $1.30 over the MsNB mid cases.

Figure 6.5 shows the LCOH breakdown between MsNB mid cases and SMR. Nuclear capital costs and MsNB refueling costs are the largest contributors to LCOH.

The central case requires one less MsNB because reactors can be shared amongst all the refineries rather than requiring an extra, partially used reactor on site. While this saving is useful, on a levelized

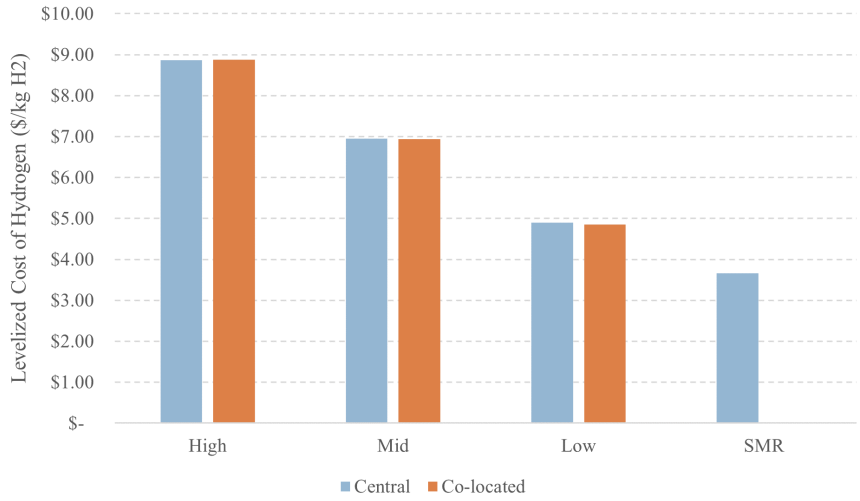

Figure 6.4: LCOH for each Texas scenario run.

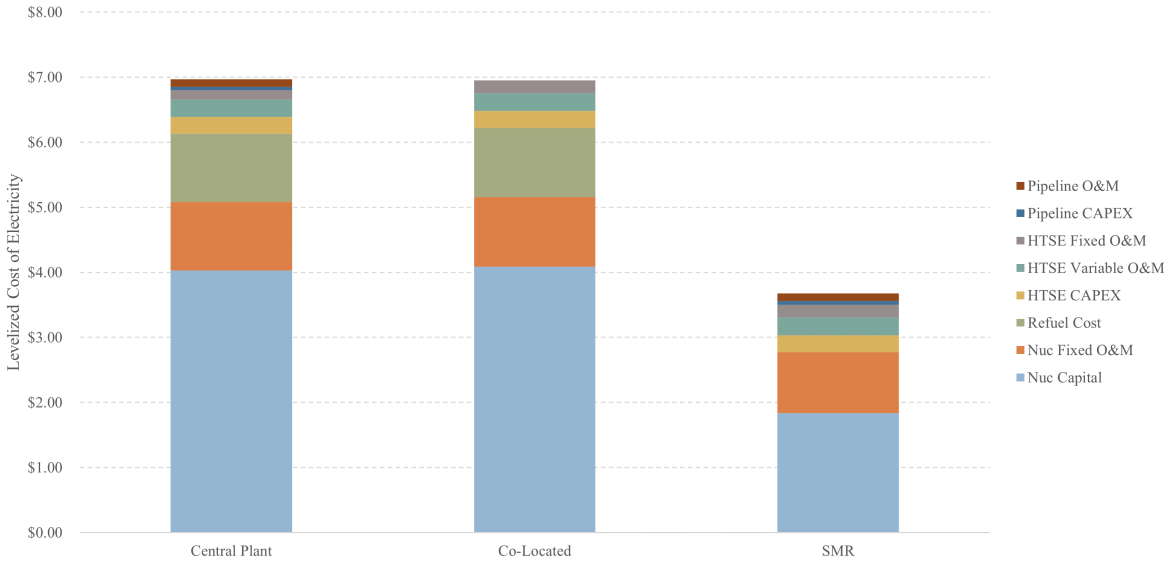

Figure 6.5: Texas mid co-located, mid central, and SMR plot showing the contribution of each cash flow to LCOH.

basis it is minor for the Texas case. There are 68 microreactors in total at the centralized site, so avoiding one extra reactor only represents less than 2% savings in nuclear capital cost.

The pipeline cost (or avoided cost for the co-located case) is also relatively small. The small transmission distance means that the pipeline capital cost only contributes \$0.12/kg H_2 to the overall LCOH. By eliminating pipeline costs in the co-located case, but adding the extra MSNB, the LCOH between cases is nearly identical.

The SMR easily has the lowest LCOH of any of the Texas scenarios. The high hydrogen demand and low transmission costs mean that the cheaper capital of a larger reactor is advantageous.

This Texas scenario shows that in high hydrogen demand areas, MsNBs would likely be a poor investment for producing hydrogen. Shorter transmission distances would be feasible in higher demand areas, decreasing the pipeline's effect on LCOH. Without expensive transmission cost, the incentive to co-locate microreactors on site would not overcome the high CAPEX. Lower capex options, such as SMR or existing LWRs, would be a more attractive option. Texas specifically also benefits from relatively low electricity cost for pipeline compressors, which further depresses pipeline cost impact.

6.3.2 Alaska Case

The Alaska case is essentially the opposite of the Texas case; low hydrogen demand, large transmission distances, high electricity prices.

The low, mid, and high MsNB cases, as well as an SMR case is shown in Figure 6.6. The co-located case is significantly cheaper for all cases when compared to the central counterpart. The low MsNB case LCOH is also lower than the SMR case.

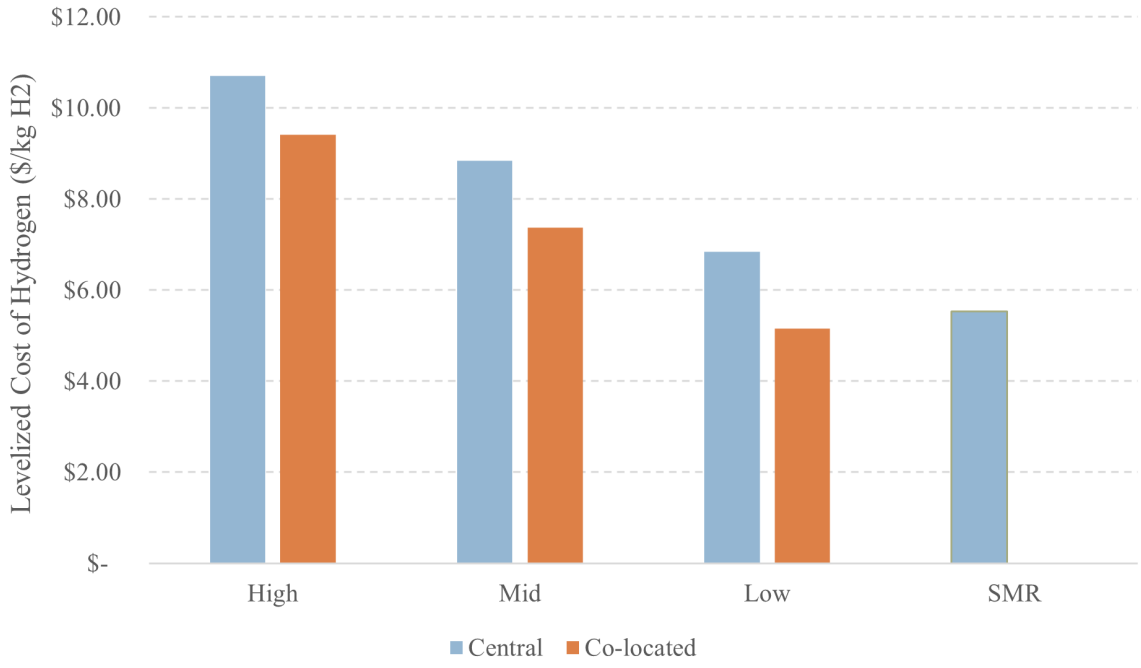

Figure 6.6: LCOH for each Alaska scenario run.

Figure 6.7 breakdown the LCOH for Alaska mid and SMR cases by cost categories. The pipeline

CAPEX and energy costs contribute significantly to the LCOH in the SMR and central cases, adding $1.86 and $0.29 to pipeline CAPEX and O&M, respectively. Collectively, transmission accounts for 24% of the LCOH for the mid case.

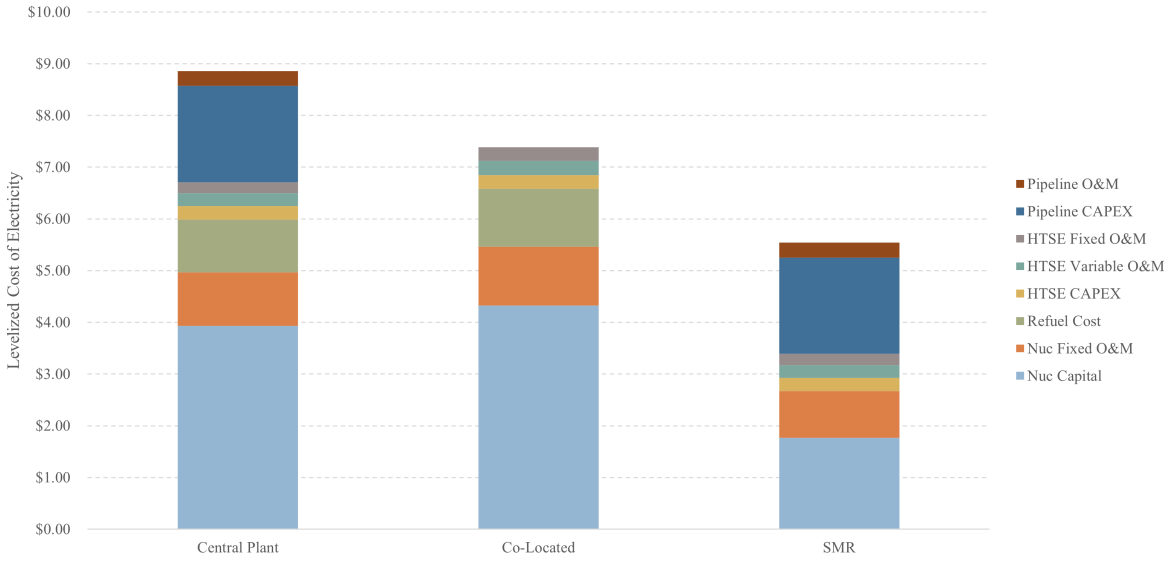

Figure 6.7: Alaska mid co-located, mid central, and SMR plot showing the contribution of each cash flow to LCOH.

The demand in Alaska is lower, so using an extra MsNB for the co-located scenario is more pronounced than in the Texas cases. The Alaskan demand would require 10 MSnBs when co-located at their respective refineries. Thus, an extra MsNB in a central location increases capital costs by 9%. When comparing co-located and central, increase in costs from the extra costs is less than the hydrogen transmission costs. Thus, in Alaska, co-locating the hydrogen production and microreactor with hydrogen load would make sense.

The Alaskan case shows that the economics favor co-location in areas with longer transmission distances and higher electricity cost.

This model uses relatively favorable assumptions for hydrogen transmission. The pipeline cost inputs for Alaska were equivalent to Texas, which may not be the case. Traditional pipeline construction in Alaska is more expensive per mile due to harsher conditions, permafrost, and more remote regions of pipeline. Any extra cost in hydrogen transmission would further justify co-location.

6.3.3 MsNB LCOH Versus Other Production Methods

Hydrogen from the MsNB is expensive relative to its other production methods. Steam methane reforming, splitting hydrogen off of methane via chemical reaction, is the cheapest at around $1/kg. Blue hydrogen, or steam methane reforming with carbon capture, is the cheapest low carbon option. Green hydrogen, or electrolysis coupled with renewable energy, is the most expensive and least carbon emitting technology that is currently available.

Figure 6.8 shows the range of costs for producing hydrogen from various sources.

In certain scenarios, the MsNB would be competitive with hydrogen generated by electrolysis and

renewables. The upper end of renewables, at over \$7.50 / kg H_2 occurs would be equivalent to the mid, co-located Alaska scenario and more expensive than the mid Texas scenarios. This demonstrates that there is a possibility for MsNB competition if nuclear low nuclear capital and O&M costs can be realized. The MsNB could also be competitive in locations that require consistent output and have little renewable energy resource. Reformation of natural gas, both with and without carbon capture, is cheaper than the MsNB. Drastic capital costs or drastic increases in fossil prices would be required to bring MsNB and natural gas hydrogen to parity. A subsidy, such as the clean hydrogen subsidy and clean electricity ITC in the Inflation Reduction Act, could help bridge the gap.

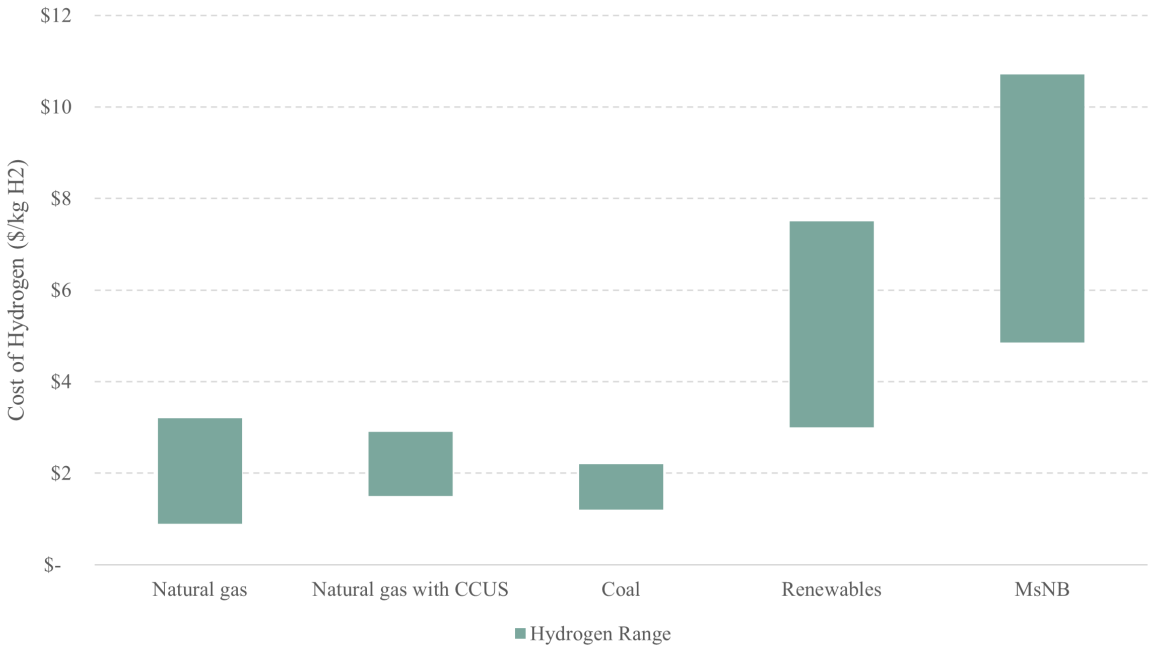

Figure 6.8: Comparison of hydrogen production costs across technologies.

6.4 Conclusions

The analysis from this chapter shows that cost of hydrogen from MsNB and HTSE varies greatly depending on configuration and location. In areas of high hydrogen demand and short transmission distances, siting the MsNB in a central location or co-locating with the hydrogen consumer did not make a large difference. In areas of sparse, low hydrogen demand, co-locating the MsNB makes more economic sense. The high demand areas would also benefit greatly from an SMR or existing nuclear reactor with lower capital costs. The advantage of the MsNB comes when hydrogen users are spread far and are meeting demands where a larger reactor might not make sense.

When compared to other hydrogen production methods, the MsNB is only viable when compared to renewable hydrogen production in certain cases. The locations where the MsNB would excel relative to other sources (low demand, sparse regions) would also be difficult for renewables. The MsNB might also be competitive against renewable hydrogen if constant, round the clock hydrogen is required.

This analysis is based on limited publicly available data for the Texas and Alaska refineries. It is not

meant to propose sites for microreactors. Rather is is meant to demonstrate the effects that different areas can have on the overall economics of an MsNb with hydrogen project and the effects of co-location versus central plants.

This work could be furthered by interrogating some of the sensitivities explored here. For example, the exact pipeline characteristics and demand where the co-located and central cases could be found via an optimization algorithm.

Additional work on specific MsNB characteristics would also improve estimations. This study took MsNB estimations as the low end cost and sought to understand a wider range of possibilities. The design of the reactor should be used to produce more substantial cost estimates. If the low \$6500/kW CAPEX can be realized, the MsNB would be much more competitive than other options, as seen in the Alaska case where the co-located LCOH was cheaper than a central SMR.

Chapter 7: Summary and Conclusions

This dissertation investigated several IES configuration and put forth methods for quantifying their value within the bounds of technical feasibility. Project finance principles, such as net present value and discounted cash flow analysis, were applied to technical models of IES. The following section summarizes the conclusions and contributions related to modeling, the conclusions based on the physical systems, and suggestions for future work in this space.

7.1 Modeling Conclusions

Several modeling techniques were leveraged in unique ways to improve the accuracy of results. In the study of adding hydrogen to Prairie Island and Monticello, a highly resolved temporal model was layered underneath a limit surface search to optimize and understand multiple sensitivities. The iterative two loop approach has been used in IES models recently, such as in models that use the HERON plugin for RAVEN, but leveraging the limit surface search broadens this method's usefulness.

Observing the boundaries of the limit surface gave a wider range of feasibly combinations than a simple optimization might. Providing more combinations is advantageous to businesses and decision makers. It allows them to understand the margins that they might have and how to negotiate with suppliers or builders.

The limit surface also allowed for high temporal resolution while still obtaining an optimal system. Because the storage size and duration was optimized within each inner loop iteration, the model did not need to make an assumption on sizing. This is one of the first truly optimized hydrogen systems for economics that also includes storage and hourly time resolution.

The APS water system model was one of the first movements into coupling water chemistry with the economics of desalination. The physical transfer functions for multiple water treatment systems, such as the RO and WRF, were incorporated. Using fitted surrogate models meant the model could rapidly run sensitivities. This method is useful over traditional costing methods because the constraints are automatically account for and the user does not need to filter data to come to conclusions about the system's cost.

The HTTR hydrogen work demonstrated how stochasticity could impact decision making and improve uncertainty understanding. Using a singular time history as an input could lead to biased results. By running the model in a stochastic manner, a band of possibilities were developed.

The HTTR model also uses the ARMA to synthetically produce input time histories. Temporal input data can be difficult to find in the quantities required to run stochastic models. The HTTR model shows that the ARMA can create time series with good agreement, avoiding over-fitting data.

The MsNB model demonstrates a rapid spatial model for decision making. Most IES models do not include spatial components, so this model moved forward spatial coupling methods, which will only become more important as microreactor economics are evaluated.

7.2 Technical and Economic Conclusions

Each of these studies provides important conclusions about IES economics and several general conclusions can be drawn from all of the modeling efforts.

First, utilizing existing equipment and infrastructure will give advantages to IES projects. PVGS has an extensive water treatment network, cooling towers, and evaporation ponds. By taking advantage of the tertiary water loop, an RO could be built without redundant extra infrastructure.

Second, it can be better for the nuclear plant to mostly sell the secondary commodity and only sell electricity on a periodic basis. The Prairie Island and Monticello optimization found that smaller hydrogen storage facilities were ideal. The cheaper the hydrogen was to produce, the smaller the storage facility. This was because there were potential profits on the hydrogen and the electric prices were low. It would benefit some nuclear plant owners and operators to find a commodity to sell and view electricity as the secondary commodity.

Additionally, hydrogen can be competitive, relative to simply selling electricity. In both the HTTR-PM/G_2 and the existing light water optimizations, options existed for selling hydrogen for higher profit than selling electricity alone. Prairie Island and Monticello optimization showed that the value proposition of hydrogen could be improved with reduced HTSE capital cost or a modest PTC of around \$1/kg H_2. Recently, the United States introduced a tax credit as part of the Inflation Reduction Act that includes a PTC of up to \$3/kg H_2.

Producing hydrogen from smaller reactors is a difficult value proposition unless they are co-located. The MSnB IES model showed that high hydrogen demand areas are not a good fit for microreactor produced hydrogen. Large transmission distances also affect the profitability.

While the transmission distances in the MSnB case had a profound impact on the cost of hydrogen, the energy (and water) transmission did not have a large effect on the cost of water in the PVGS cases. This is because hydrogen is expensive to move and the water infrastructure already existed to move waste to PVGS. For desalination, co-locating the energy supply, the product production, and the end consumer is less important than hydrogen.

Transmission distance effects were also seen as a secondary effect within the local Prarie Island and Monticello markets. The demand curve for both was a step function that saw significant price reduction because of both greater supply, but also greater distances to consumers. The economics were move favorable in the region local to the plants. Understanding the local hydrogen market will be key to evaluating hydrogen IES projects.

7.3 Future Work

Future work could include the combination of temporal and spatial models to optimize greenfield locations. The combination of spatial and temporal fidelity would reduce the uncertainty associated with these profitability calculations. Achieving this would require optimization of codes and different techniques to avoid large computational burdens. Many energy system models sacrifice temporal resolution for spatial, or vice versa. A model that could adequately capture both would be of great value to researchers and companies making investment decisions.

Using the PVGS desalination IES as a guide would help understand applicability if integrating water system with ROs at other plants. The Turkey Point Nuclear Plant in Florida City, Florida has proposed a similar water treatment facility to PVGS. Bakarah Nuclear Plant in the United Arab Emirates may also be a candidate because of its cooling system, proximity to a source, and the demand for potable water in the area.

Another future work in the IES technoecomic space could focus on opening capacity expansion models to co-products. Capacity expansion models, used for electricity and energy asset and environmental forecasting, often do not build nuclear under current economic assumptions. Allowing the model to choose to produce and sell a secondary commodity would show the potential for co-production over a large area (such as the U.S.) and over many years. A capacity expansion model would also show the effect that IES might have on overall grid and capacity construction. For example, if hydrogen storage is available and a nuclear plant switches between the two products, it could improve the capacity value, and thus deployment, of renewable energy technologies.

Future IES TEA could also focus on greenfield sites. Much of the current IES work is tied to existing reactors. Understanding more of the different economic values of different sizes and types of reactors would help expand the work do done in this dissertation.

Bibliography

[1] Aaron S Epiney, James D Richards, Jason K Hansen, Paul W Talbot, Pralhad Hanumant Burli, Cristian Rabiti, and Shannon M Bragg-Sitton. Case study: Integrate nuclear water desalination–regional potable water in arizona, 9 2019.

[2] L Todd Knighton, Daniel Wendt, James Richards, Cristian Rabiti, Abdalla Abou-Jaoude, Tyler Westover, Kurt Vedros, Samuel Bates, Richard Boardman, Amgad Elgowainy, Adarsh Bafana, Krishna Reddi, Guiyan Zang, Mark Ruth, Bethany Frew, Daniel Levie, Paige Jadun, Jal Desai, Sherry Bernhoft, Brittany Westlake, David Mccollum, Daniel Ludwig, Molly Strasser, and Bryan Ramler. Technoeconomic analysis of product diversification options for sustainability of the monticello and prairie island nuclear power plants in collaboration with. 2021.

[3] Mark Morey. U.s. nuclear electricity generation continues to decline as more reactors retire, 4 2022.

[4] R James, S Hessler, and J Bistline. Program on technology innovation: Fossil fleet transition with fuel changes and large scale variable renewable integration. Technical report, 2015.

[5] Doe announces $20 million to produce clean hydrogen from nuclear power — department of energy.

[6] Private-public partnership will use nuclear energy for clean hydrogen production - inl.

[7] Electricity explained, 3 2021.

[8] California iso - reliability requirements.

[9] Hourly load data archives, 2019.

[10] Tianrun Yang, Wen Liu, Gert Jan Kramer, and Qie Sun. Seasonal thermal energy storage: A techno-economic literature review. *Renewable and Sustainable Energy Reviews*, 139:110732, 2021.

[11] Nestor A. Sepulveda, Jesse D. Jenkins, Fernando J. de Sisternes, and Richard K. Lester. The role of firm low-carbon electricity resources in deep decarbonization of power generation. *Joule*, 2:2403–2420, 11 2018.

[12] Wesley J. Cole, Danny Greer, Paul Denholm, A. Will Frazier, Scott Machen, Trieu Mai, Nina Vincent, and Samuel F. Baldwin. Quantifying the challenge of reaching a 100% renewable energy power system for the united states. *Joule*, 6 2021.

[13] Executive summary pacific northwest zero-emitting resources study. Technical report, E3 Consulting, 2020.

[14] Energy Information Administration. Annual energy outlook 2021 narrative. Technical report, Energy Information Administration, 2021.

[15] Wesley Cole, J Vincent, Carag Contributing, Maxwell Brown, Patrick Brown, Stuart Cohen, Kelly Eurek, Will Frazier, Pieter Gagnon, Nick Grue, Jonathan Ho, Anthony Lopez, Trieu Mai, Matthew Mowers, Caitlin Murphy, Brian Sergi, Dan Steinberg, and Travis Williams. 2021 standard scenarios report: A u.s. electricity sector outlook. Technical report, 2021.

[16] James Richards and Wesley J. Cole. Assessing the impact of nuclear retirements on the u.s. power sector. *Electricity Journal*, 30:14–21, 11 2017.

[17] Energy Information Agency. California wholesale electricity prices are higher at the beginning and end of the day, 7 2017.

[18] Bethany Frew, Wesley Cole, Yinong Sun, James Richards, and Trieu Mai. 8760-based method for representing variable generation capacity value in capacity expansion models: Preprint. Technical report.

[19] Market prices, 2022.

[20] J E O'brien, M G Mckellar, E A Harvego, and C M Stoots. High-temperature electrolysis for large-scale hydrogen and syngas production from nuclear energy - summary of system simulation and economic analyses. *International Journal of Hydrogen Energy*, 35:4808–4819, 2009.

[21] Jong Suk Kim, Richard D. Boardman, and Shannon M. Bragg-Sitton. Dynamic performance analysis of a high-temperature steam electrolysis plant integrated within nuclear-renewable hybrid energy systems. *Applied Energy*, 228:2090–2110, 10 2018.

[22] Jessica Hübner, Benjamin Paul, Aleksandra Wawrzyniak, and Peter Strasser. Polymer electrolyte membrane (pem) electrolysis of h2o2 from o2 and h2o with continuous on-line spectrophotometric product detection: Load flexibility studies. *Journal of Electroanalytical Chemistry*, 896:115465, 9 2021.

[23] Seiji Kasahara, Yoshiyuki Imai, Koichi Suzuki, Jin Iwatsuki, Atsuhiko Terada, and Xing L. Yan. Conceptual design of the iodine–sulfur process flowsheet with more than 50 *Nuclear Engineering and Design*, 329:213–222, 2018.

[24] G. F. Naterer, S. Suppiah, L. Stolberg, M. Lewis, Z. Wang, V. Daggupati, K. Gabriel, I. Dincer, M. A. Rosen, P. Spekkens, S. N. Lvov, M. Fowler, P. Tremaine, J. Mostaghimi, E. B. Easton, L. Trevani, G. Rizvi, B. M. Ikeda, M. H. Kaye, L. Lu, I. Pioro, W. R. Smith, E. Secnik, J. Jiang, and J. Avsec. Canada's program on nuclear hydrogen production and the thermochemical Cu-Cl cycle. *International Journal of Hydrogen Energy*, 35(20):10905–10926, oct 2010.

[25] M. H. Khoshgoftar Manesh, M. Amidpour, and M. H. Hamedi. Optimization of the coupling of pressurized water nuclear reactors and multistage flash desalination plant by evolutionary algorithms and thermoeconomic method. *International Journal of Energy Research*, 33:77–99, 2009.

[26] Xing Yan, Hiroki Noguchi, Hiroyuki Sato, Yukio Tachibana, Kazuhiko Kunitomi, and Ryutaro Hino. Study of an incrementally loaded multistage flash desalination system for optimum use of sensible waste heat from nuclear power plant. *International Journal of Energy Research*, 37:1811–1820, 11 2013.

[27] Nuclear desalination - world nuclear association, 2020.

[28] Martin Leurent, Frédéric Jasserand, Giorgio Locatelli, Jenny Palm, Miika Rämä, and Andrea Trianni. Driving forces and obstacles to nuclear cogeneration in europe: Lessons learnt from finland. *Energy Policy*, 107:138–150, 2017.

[29] Ville Olkkonen, Jussi Ekström, Aira Hast, and Sanna Syri. Utilising demand response in the future finnish energy system with increased shares of baseload nuclear power and variable renewable energy. *Energy*, 164:204–217, 12 2018.

[30] Ultra safe nuclear corporation.

[31] Demonstrating the natrium™ reactor and integrated energy system, 2022.

[32] Daniel C Stack and Charles Forsberg. Improving nuclear system economics using firebrick resistance-heated energy storage (fires) 2015 ans annual meeting. 2015.

[33] Humberto E. Garcia, Jun Chen, Jong S. Kim, Michael G. McKellar, Wesley R. Deason, Richard B. Vilim, Shannon M. Bragg-Sitton, and Richard D. Boardman. Nuclear hybrid energy systems - regional studies. west texas and northeastern arizona. Technical report, Idaho National Laboratory, 4 2015.

[34] Xing L. Yan, Hiroyuki Sato, Junya Sumita, Yasunobu Nomoto, Shoichi Horii, Yoshiyuki Imai, Seiji Kasahara, Koichi Suzuki, Jin Iwatsuki, Atsuhiko Terada, Yukio Tachibana, M. Oono, S. Yamada, and Kazumasa Suyama. Design of httr-gt/h2 test plant. *Nuclear Engineering and Design*, 329:223–233, 2018.

[35] Jin Iwatsuki, Seiji Kasahara, Shinji Kubo, Yoshiyuki Inagaki, Kasuhiko Kunitomi, and Masuro Ogawa. Economic evaluation of htgr is process hydrogen production system. Technical report, Japan Atomic Energy Agency, 2014.

[36] Lázaro García, Daniel González, Carlos García, Laura García, and Carlos Brayner. Efficiency of the sulfur-iodine thermochemical water splitting process for hydrogen production based on ads (accelerator driven system). *Energy*, 57:469–477, 8 2013.

[37] L. C. Juárez-Martínez, G. Espinosa-Paredes, A. Vázquez-Rodríguez, and H. Romero-Paredes. Energy optimization of a sulfur–iodine thermochemical nuclear hydrogen production cycle. *Nuclear Engineering and Technology*, 53:2066–2073, 6 2021.

[38] Zhang Ping, Wang Laijun, Chen Songzhe, and Xu Jingming. Progress of nuclear hydrogen production through the iodine–sulfur process in china. *Renewable and Sustainable Energy Reviews*, 81:1802–1812, 1 2018.

[39] Young Soo Kim, Hee Cheon No, Ho Joon Yoon, and Jeong Ik Lee. An intermediate heat exchanging-depressurizing loop for nuclear hydrogen production. volume 240, pages 2957–2962, 10 2010.

[40] Piyush Sabharwall. *Engineering design elements of a two-phase thermosyphon to transfer nuclear thermal energy to a hydrogen plant.* PhD thesis, 2009. Copyright - Database copyright ProQuest LLC; ProQuest does not claim copyright in the individual underlying works; Last updated - 2021-05-18.

[41] Wenqiang Zhang, Bo Yu, and Jingming Xu. Efficiency evaluation of high-temperature steam electrolytic systems coupled with different nuclear reactors. *International Journal of Hydrogen Energy*, 37:12060–12068, 9 2012.

[42] Farrukh Khalid, Ibrahim Dincer, and Marc A. Rosen. Comparative assessment of candu 6 and sodium-cooled fast reactors for nuclear desalination. *Desalination*, 379:182–192, 2 2016.

[43] Stephen Hills, Seth Dana, and Hailei Wang. Dynamic modeling and simulation of nuclear hybrid energy systems using freeze desalination and reverse osmosis for clean water production. *Energy Conversion and Management*, 247, 11 2021.

[44] Jong Suk Kim, Jun Chen, and Humberto E. Garcia. Modeling, control, and dynamic performance analysis of a reverse osmosis desalination plant integrated within hybrid energy systems. *Energy*, 112:52–66, 10 2016.

[45] L. M. Germeshuizen and P. W.E. Blom. A techno-economic evaluation of the use of hydrogen in a steel production process, utilizing nuclear process heat. *International Journal of Hydrogen Energy*, 38:10671–10682, 8 2013.

[46] Salah Ud Din Khan. Using next generation nuclear power reactors for development of a techno-economic model for hydrogen production. *International Journal of Energy Research*, 43:6827–6839, 10 2019.

[47] Giorgio Locatelli, Sara Boarin, Andrea Fiordaliso, and Marco E. Ricotti. Load following of small modular reactors (smr) by cogeneration of hydrogen: A techno-economic analysis. *Energy*, 148:494–505, 4 2018. Did a flexing case, but found hours per yr via a hydrogen price and didn't do sequential dispatch. Assumed a hydrogen price.

[48] Konor Frick, Daniel Wendt, Paul Talbot, Cristian Rabiti, and Richard Boardman. Technoeconomic assessment of hydrogen cogeneration via high temperature steam electrolysis with a light-water reactor. 2021.

[49] Konor Frick, Paul Talbot, Daniel Wendt, Richard Boardman, Cristian Rabiti, Shannon Bragg-Sitton, Daniel Levie, Bethany Frew, Mark Ruth, Amgad Elgowainy, and Troy Hawkins. Evaluation of hydrogen production feasibility for a light water reactor in the midwest. 2019.

[50] Tian Zhang. Techno-economic analysis of a nuclear-wind hybrid system with hydrogen storage. *Journal of Energy Storage*, 46, 2 2022.

[51] A. Epiney, C. Rabiti, P. Talbot, and A. Alfonsi. Economic analysis of a nuclear hybrid energy system in a stochastic environment including wind turbines in an electricity grid. *Applied Energy*, 260, 2 2020.

[52] Charles W. Forsberg, Daniel C. Stack, Daniel Curtis, Geoffrey Haratyk, and Nestor Andres Sepulveda. Converting excess low-price electricity into high-temperature stored heat for industry and high-value electricity production. *The Electricity Journal*, 30:42–52, 7 2017.

[53] Mark Ruth, Paul Spitsen, and Richard Boardman. Opportunities and challenges for nuclear-renewable hybrid energy systems: Preprint. Technical report, 2019.

[54] Rudy Kahsar. The potential for brackish water use in thermoelectric power generation in the American southwest. *Energy Policy*, 2019.

[55] Aaron Epiney, Cristian Rabiti, Paul Talbot, Jong Suk Kim, James Richards, and Shannon Bragg-Sitton. Case study: Nuclear-renewable-water integration in arizona, 2018.

[56] Andrea Alfonsi, Cristian Rabiti, Diego Mandelli, Joshua Cogliati, Congjian Wang, Paul W. Talbot, and Daniel P. Maljovec. RAVEN User Guide. Technical report, Idaho National Laboratory, Idaho Falls, ID (United States), jun 2018.

[57] Shannon M. Bragg-Sitton, Richard Boardman, Cristian Rabiti, and James O'Brien. Reimagining future energy systems: Overview of the us program to maximize energy utilization via integrated nuclear-renewable energy systems. *International Journal of Energy Research*, 44:8156–8169, 8 2020.

[58] L. C. Juárez-Martínez, G. Espinosa-Paredes, A. Vázquez-Rodríguez, and H. Romero-Paredes. Energy optimization of a sulfur–iodine thermochemical nuclear hydrogen production cycle. *Nuclear Engineering and Technology*, 12 2020.

[59] Andhika Yudha Prawira, Phil Seo Kim, and Man-Sung Yim. Techno-economic analysis of hydrogen production using nuclear power plant electricity generation in korea. Technical report.

[60] Ronaldo Szilard, Phil Sharpe, Edward Kee, Edward Davis, and Gene Grecheck. Economic and market challenges facing the u.s. nuclear commercial fleet - cost and revenue study. Technical report, Idaho National Laboratory, 2017.

[61] JEPIC. The electric power industry in japan. Technical report, Japan Electric Power Information Center, INC, 2019.

[62] Hydrogen and Fuel Cell Strategy Council. The strategic road map for hydrogen and fuel cells - industry-academia-government action plan to realize a " hydrogen society " - hydrogen and fuel cell strategy council. Technical report, Ministry of Economy, Transportation, and Industry (METI), 2019.

[63] Xing L. Yan. Status of httr and technology developments for near term deployment of nuclear process heat applications in japan. 9 2017.

[64] KR SCHULTZ, LC BROWN, GE BESENBRUCH, and CJ HAMILTON. Large-scale production of hydrogen by nuclear energy for the hydrogen economy. Technical report, Oakland Operations Office, 2 2003.

[65] H. Noguchi, H. Takegami, Y. Kamiji, N. Tanaka, J. Iwatsuki, S. Kasahara, and S. Kubo. R&d status of hydrogen production test using is process test facility made of industrial structural material in jaea. *International Journal of Hydrogen Energy*, 44:12583–12592, 5 2019.

[66] Xavier Vitart, Philippe Carles, and Pascal Anzieu. A general survey of the potential and the main issues associated with the sulfur–iodine thermochemical cycle for hydrogen production using nuclear heat. *Progress in Nuclear Energy*, 50:402–410, 3 2008.

[67] Paul W Talbot, Abhinav Gairola, Prerna Prateek, Andrea Alfonsi, Cristian Rabiti, and Richard D Boardman. HERON as a Tool for LWR Market Interaction in a Deregulated Market. Technical report, 2020.

[68] Paul W Talbot, Abhinav Gairola, Prerna Prateek, Andrea Alfonsi, Cristian Rabiti, and Richard D Boardman. HERON as a Tool for LWR Market Interaction in a Deregulated Market. Technical report, Idaho National Laboratory, Idaho Falls, ID (United States), jan 2020.

[69] S. Clemmer, J. Richardson, S. Sattler, and D. Lochbaum. The Nuclear Power Dilemma Declining Profits, Plant Closures, and the Threat of Rising Carbon Emissions. Technical report, Union of Concerned Scientists, 2018.

[70] 2021 Annual Technology Baseline, 2021.

[71] J. D. Jenkins, Z. Zhou, R. Ponciroli, R. B. Vilim, F. Ganda, F. de Sisternes, and A. Botterud. The benefits of nuclear flexibility in power system operations with renewable energy. *Applied Energy*, 222:872–884, jul 2018.

[72] Executive Summary Pacific Northwest Zero-Emitting Resources Study. 2020.

[73] Paul W Talbot, Pralhad Burli, James D Richards, Aaron S Epiney, Mohammad G Abdo, Cristian Rabiti, and Richard D Boardman. Analysis of Differential Financial Impacts of LWR Load-Following Operations. Technical report, Idaho National Laboratory, 2019.

[74] J. D. Jenkins, Z. Zhou, R. Ponciroli, R. B. Vilim, F. Ganda, F. de Sisternes, and A. Botterud. The benefits of nuclear flexibility in power system operations with renewable energy. *Applied Energy*, 222:872–884, jul 2018.

[75] Mark F. Ruth, Owen R. Zinaman, Mark Antkowiak, Richard D. Boardman, Robert S. Cherry, and Morgan D. Bazilian. Nuclear-renewable hybrid energy systems: Opportunities, interconnections, and needs. *Energy Conversion and Management*, 78:684–694, feb 2014.

[76] Amani Al-Othman, Noora N. Darwish, Muhammad Qasim, Mohammad Tawalbeh, Naif A. Darwish, and Nidal Hilal. Nuclear desalination: A state-of-the-art review. *Desalination*, 457:39–61, may 2019.

[77] Humberto E. Garcia, Jun Chen, Jong S. Kim, Richard B. Vilim, William R. Binder, Shannon M. Bragg Sitton, Richard D. Boardman, Michael G. McKellar, and Christiaan J.J. Paredis. Dynamic performance analysis of two regional Nuclear Hybrid Energy Systems. *Energy*, 107:234–258, jul 2016.

[78] Seiji Fujiwara, Shigeo Kasai, Hiroyuki Yamauchi, Kazuya Yamada, Shinichi Makino, Kentaro Matsunaga, Masato Yoshino, Tsuneji Kameda, Takashi Ogawa, Shigeki Momma, and Eiji Hoashi. Hydrogen production by high temperature electrolysis with nuclear reactor. *Progress in Nuclear Energy*, 50(2-6):422–426, mar 2008.

[79] J. E. O'Brien, M. G. McKellar, E. A. Harvego, and C. M. Stoots. High-temperature electrolysis for large-scale hydrogen and syngas production from nuclear energy – summary of system simulation and economic analyses. *International Journal of Hydrogen Energy*, 35(10):4808–4819, may 2010.

[80] F. Sorgulu and I. Dincer. Cost evaluation of two potential nuclear power plants for hydrogen production. *International Journal of Hydrogen Energy*, 43(23):10522–10529, jun 2018.

[81] Katarzyna Borowiec, Aaron Wysocki, Samuel Shaner, Michael S Greenwood, and Matthew Ellis. Increasing Revenue of Nuclear Power Plants With Thermal Storage. *Journal of Energy Resources Technology, Transactions of the ASME*, 2019.

[82] Aspen HYSYS — Process Simulation Software — AspenTech, 2021.

[83] D.D. Papadias and R.K. Ahluwalia. Bulk Storage of Hydrogen. *International Journal of Hydrogen Energy*, (In Press), 2021.

[84] B Frew, D Levie, J Richards, J Desai, and M Ruth. Modeling Multi-Output Hybrid Energy Systems as Price-Maker Resources. *Applied Energy, submitted*, 2021.

[85] PLEXOS Market Simulation Software - Energy Exemplar, 2021.

[86] Maxwell Brown, Wesley Cole, Kelly Eurek, Jon Becker, David Bielen, Ilya Chernyakhovskiy, Stuart Cohen, Will Frazier, Pieter Gagnon, Nathaniel Gates, Daniel Greer, Sai Sameera Gudladona, Jonathan Ho, Paige Jadun, Katherine Lamb, Trieu Mai, Matthew Mowers, Caitlin Murphy, Amy Rose, Anna Schleifer, Daniel Steinberg, Yinong Sun, Nina Vincent, Ella Zhou, and Matthew Zwerling. Regional Energy Deployment System (ReEDS) Model Documentation: Version 2019. 2020.

[87] UPPER MIDWEST INTEGRATED RESOURCE PLAN. 2020.

[88] Argonne National Laboratory. Hydrogen Delivery Scenario Analysis Model, 2006.

[89] Andrea Alfonsi, Cristian Rabiti, Diego Mandelli, Joshua Joseph Cogliati, Ramazan Sonat Sen, and Curtis Lee Smith. Improving Limit Surface Search Algorithms in RAVEN Using Acceleration Schemes: Level II Milestone. Technical report, Idaho National Laboratory, Idaho Falls, ID (United States), jul 2015.

[90] Hydrogen tax credits — Norton Rose Fulbright - June, 2021, 2021.

[91] Katie Randolph, Ned Stetson, Sunita Satyapal, and Low Value. DOE Hydrogen and Fuel Cells Program Record 20006: Hydrogen Production Cost from High Temperature Electrolysis. Technical report, Department of Energy, 2000.

[92] Aurora nuclear plant — a tiny nuclear plant is coming to idaho.

[93] X-energy — htgr — advanced nuclear reactors (smr) & triso fuel.

[94] Introducing the molten salt nuclear battery – ans / nuclear newswire.

[95] Amgad Elgowainy, Marianne Mintz, Jeongwoo Han, Uisung Lee, Thomas Stephens, Pingping Sun, Anant Vyas, Yan Zhou, Leah Talaber, Stephen Folga, and Michael Mclamor. Hydrogen Demand Analysis for H2@Scale. pages 1–4, 2019.

[96] Susan Hicks and Peter Gross. Hydrogen for refineries is increasingly provided by industrial suppliers, 2016.

[97] Abdalla Abou Jaoude, Andrew Wilkin Foss, Yasir Arafat, and Brent W Dixon. An economics-by-design approach applied to a heat pipe microreactor concept. 7 2021.

Appendix A: RAVEN Workflows For TEA

This appendix includes the code from Chapter 6. It serves as an illustration as to what the code in an IES RAVEN model looks like and how it operates. The RAVEN script is run, which sends a set of values specified in the "grid" sampling block to the external model. The python external model prepares the costs for pipeline transmission, HTSE, and MsNB based on the inputs. The Python model outputs the costs and hydrogen production amounts to the TEAL plugin. The TEAL script defines the financial parameters, such as discount rate and lifetime, so that the TEAL plugin can perform an NPV search for the hydrogen price where the NPV is equal to zero. Once the levelized cost is found, the output is collected by raven and a new point from the "grid" block is sampled.

A.0.1 MSnB Raven Code

```
<?xml version="1.0" encoding="UTF-8"?>
<Simulation verbosity="debug">
  <RunInfo>
    <WorkingDir>.</WorkingDir>
    <Sequence>MCrun,printTOfile</Sequence>
  </RunInfo>

  <VariableGroups>
    <Group name="GRO_py_model_in">Multiplier, htse_capex, num_reactors1,num_reactors2,
        ↪ num_reactors3,num_reactors4,hydrogen_ref,refuel_cost_ref, msnbCap,
        ↪ msnb_capex, msnb_fixed_cost_ref, distance, compressor_power, e_prices,
        ↪ transpo_cost,mode</Group>
    <Group name="GRO_py_model_out">msnb_total_nuc_capex, total_h2_produced,hydrogen,
        ↪ pipeline_OM, msnb_fixed_cost, refuel_cost, htse_fixed_cost,
        ↪ htse_variable_cost, transpo_capex</Group> <!--total_fixed_cost-->
    <!-- <Group name="GRO_CashFlow_in">msnb_total_nuc_capex, total_h2_produced,
        ↪ pipeline_OM,transpo_capex,msnb_fixed_cost,refuel_cost,htse_fixed_cost,
        ↪ htse_variable_cost,transpo_capex</Group> -->
    <Group name="GRO_CashFlow_out">NPV_mult</Group>
  </VariableGroups>

  <Models>
    <ExternalModel name="Cash_Flow" subType="TEAL.CashFlow">
      <variables> GRO_py_model_in, GRO_py_model_out, GRO_CashFlow_out</variables>
      <ExternalXML node="Economics" xmlToLoad="lcoh_teal_transpo.xml"/>
    </ExternalModel>
    <ExternalModel ModuleToLoad="py_microreactor.py" name="cashflow_prep" subType="">
      <inputs>GRO_py_model_in</inputs>
      <outputs>GRO_py_model_out</outputs>
```

```
    <SolutionExport class="DataObjects" type="PointSet">SET_model_out</
        ↪ SolutionExport>
  </ExternalModel>
  <EnsembleModel name="microreactor_spatial" subType="">
    <Model class="Models" type="ExternalModel">
      cashflow_prep
      <Input class="DataObjects" type="PointSet">SET_model_in</Input>
      <TargetEvaluation class="DataObjects" type="PointSet">SET_model_out</
          ↪ TargetEvaluation>
    </Model>
    <Model class="Models" type="ExternalModel">
        Cash_Flow
      <Input class="DataObjects" type="PointSet">SET_CashFlow_in</Input>
      <TargetEvaluation class="DataObjects" type="PointSet">SET_CashFlow_out</
          ↪ TargetEvaluation>
    </Model>
  </EnsembleModel>
</Models>

<Distributions>
  <Uniform name="money">
    <lowerBound>0.0</lowerBound>
    <upperBound>5e10</upperBound>
  </Uniform>
</Distributions>

<Samplers>
  <Grid name="grid">
    <constant name="msnbCap">3.7</constant>
    <variable name="msnb_capex">
      <distribution>money</distribution>
      <grid type='value' construction='custom'>4500</grid> <!--6500 10000 13000-->
    </variable>

    <variable name="msnb_fixed_cost_ref">
      <distribution>money</distribution>
      <grid type='value' construction='custom'>150</grid> <!--100 172 253 -->
    </variable>

    <variable name="refuel_cost_ref">
      <distribution>money</distribution>
```

```
      <grid type='value' construction='custom'>0</grid> <!--8e6 10e6 12e6 -->
    </variable>

    <!--HTSE cost-->
    <variable name="htse_capex">
      <distribution>money</distribution>
      <grid type='value' construction='custom'>650</grid>
    </variable>

    <constant name="hydrogen_ref"> 8253867</constant> <!--amt h2 produced per year,
        ↪ total in kg h2/yr: 54810833, 8253867-->

    <!--transportation cost-->
    <variable name="transpo_cost">
      <distribution>money</distribution>
      <grid type='value' construction='custom'>1000000</grid> <!-->0.5e6 0.6e6 0.7e6
          ↪  0.8e6 0.9e6 1e6 1.1e6 1.2e6 1.3e6 1.4e6 1.5e6 -->
    </variable>
    <variable name="distance">
      <distribution>money</distribution>
      <grid type='value' construction='custom'>187</grid> <!--31.7 187-->
    </variable>

    <!-- number of reactors required for a given refinery demand -->
    <constant name="num_reactors1"> 6 </constant>
    <constant name="num_reactors2"> 5 </constant>
    <constant name="num_reactors3"> 0 </constant>
    <constant name="num_reactors4"> 0 </constant>

    <!-- <constant name="num_reactors1"> 21 </constant>
    <constant name="num_reactors2"> 18 </constant>
    <constant name="num_reactors3"> 9 </constant>
    <constant name="num_reactors4"> 21 </constant> -->
    <constant name="compressor_power"> 23826.9</constant> <!-- 158223.7 23826.9 MWh
        ↪ -->
    <constant name="e_prices">75</constant> <!--30 75 \$/MWh-->
    <constant name="mode">0</constant> <!-- 0 for centralized, 1 for colocated -->
    <constant name="Multiplier">1.0</constant>
  </Grid>
</Samplers>
```

```
  <DataObjects>
    <PointSet name="SET_CashFlow_in">
      <Input>GRO_py_model_out</Input>
      <Output>OutputPlaceHolder</Output>
    </PointSet>
    <PointSet name="SET_model_in">
      <Input>GRO_py_model_in</Input>
      <Output>OutputPlaceHolder</Output>
    </PointSet>
    <PointSet name="SET_model_out">
      <Input>GRO_py_model_in</Input>
      <Output>GRO_py_model_out</Output>
    </PointSet>
    <PointSet name="SET_CashFlow_out">
      <Input>GRO_py_model_in, GRO_py_model_out</Input>
      <Output>GRO_CashFlow_out</Output>
    </PointSet>
  </DataObjects>

  <Steps>
    <MultiRun name="MCrun" pauseAtEnd="True">
      <Input class="DataObjects" type="PointSet">SET_model_in</Input>
      <Model class="Models" type="EnsembleModel">microreactor_spatial</Model>
      <Sampler class="Samplers" type="Grid">grid</Sampler>
      <Output class="DataObjects" type="PointSet">SET_CashFlow_out</Output>
    </MultiRun>
    <IOStep name="printTOfile">
     <Input class="DataObjects" type="PointSet">SET_CashFlow_out</Input>
     <Output class="OutStreams" type="Print">dumpNPVsearch</Output>
    </IOStep>
  </Steps>
  <OutStreams>
    <Print name="dumpNPVsearch">
      <type>csv</type>
      <source>SET_CashFlow_out</source>
      <what>input,output</what>
    </Print>
  </OutStreams>
</Simulation>
```

A.0.2 MSnB Python External Model

```
import numpy as np
import pandas as pd

def cost_scaling(base_capex, total_num_units, scaling_factor = 0.6, base_cap = 3.7):
    scaled_capex = base_capex * total_num_units * base_cap * 1000
    return scaled_capex

def HTSE_OM_func(Cap, total_num_units, cf):
    #$/MWh * MWh
    vom = 5.20 * Cap**-0.004 * total_num_units* 3.7 * 8760 * cf
    #$/kW-yr * kW
    fom = 75.51 * Cap**-0.208 * total_num_units * 3.7 * 1000
    print('vom', 5.20 * Cap**-0.004)
    print('fom', 75.51 * Cap**-0.208)
    #returns total costs per yr
    return fom, vom


def initialize(self,runInfoDict,inputFiles):
    x=1
    return

def run(self,Input):
     location1 = self.num_reactors1[0]
     location2 = self.num_reactors2[0]
     location3 = self.num_reactors3[0]
     location4 = self.num_reactors4[0]
     total_num_units = location1 + location2 + location3 + location4
     msnb_cap = self.msnbCap[0]
     base_h2_produced = self.hydrogen_ref[0]

     distance = self.distance[0]
     compressor_power = self.compressor_power[0] #in MWh
     e_prices = self.e_prices[0]
     transpo_cost = self.transpo_cost[0] #$/kg/mi

     #total_h2_porduced
     total_h2_produced = base_h2_produced
     e_conversion = 37.4 #kwh_e/kg h2
```

```
th_conversion = 6.4 #kwh_th/kg_h2


#difference in transpo vs no transpo case --> Deeper cost reductions in the SMR
    ↪ vs centralized location
#SMR VS MsNB is the main analysis
#0 is centralized, 1 is co-located
base_capex = self.msnb_capex[0]
if int(self.mode[0]) == 0:
   #texas (and ak) uses 1 less reactors (rounding on site vs in totatl)
   total_num_units -= 1
   scaled_capex = cost_scaling(base_capex, total_num_units)
   print(scaled_capex)
   pipeline_OM = compressor_power*e_prices
   transpo_capex = distance*transpo_cost
   self.transpo_capex = transpo_capex
   self.pipeline_OM = pipeline_OM
   CF = 0.92
   htse_fom, htse_vom = HTSE_OM_func(msnb_cap*total_num_units, total_num_units,
       ↪ CF)


else:
   cf1 = 0.982
   location1_capex = cost_scaling(base_capex, location1)
   location1_fom, location1_vom = HTSE_OM_func(msnb_cap*location1, location1, cf1
       ↪ )
   cf2 = 0.992
   location2_capex = cost_scaling(base_capex, location2)
   location2_fom, location2_vom = HTSE_OM_func(msnb_cap*location2, location2, cf2
       ↪ )
   cf3 = 0.970
   location3_capex = cost_scaling(base_capex, location3)
   location3_fom, location3_vom = HTSE_OM_func(msnb_cap*location3, location3, cf3
       ↪ )
   cf4 = 0.963
   location4_capex = cost_scaling(base_capex, location4)
   location4_fom, location4_vom = HTSE_OM_func(msnb_cap*location4, location4, cf4
       ↪ )

   foms = [location1_fom, location2_fom, location3_fom, location4_fom]
```

```
        voms = [location1_vom, location2_vom, location3_vom, location4_vom]
        capexes = [location1_capex, location2_capex, location3_capex, location4_capex]
        print("capexes: ", capexes)
        scaled_capex = sum(capexes)
        htse_fom = sum(foms)
        htse_vom = sum(voms)
        print("fom: ", htse_fom)
        print("vom: ", htse_vom)

        self.transpo_capex = 0.0
        self.pipeline_OM = 0.0
        #send back to raven
        #msnb total capexes
        #total_H2 produced

    total_fixed_cost = self.msnb_fixed_cost_ref[0] * total_num_units * msnb_cap *
        ↪ 1000
   #do the FOM scaling here?
    self.msnb_fixed_cost = total_fixed_cost
    self.msnb_total_nuc_capex = scaled_capex
    self.total_h2_produced = total_h2_produced
    self.htse_fixed_cost = htse_fom
    self.htse_variable_cost = htse_vom
    self.refuel_cost = self.refuel_cost_ref[0] * total_num_units
    msnb_cap_th = msnb_cap / 0.37 #thermal efficinecy = 0.37
    total_conversion = e_conversion + th_conversion * 0.37
    self.hydrogen = total_h2_produced
```

A.0.3 MSnB TEAL Code

```
<Economics verbosity="0"> <!-- "0" all debug output, "1" some output, "100" only
    ↪ errors -->
  <Global>
    <DiscountRate>0.07</DiscountRate> <!-- %/100 -->
    <tax>0.253</tax> <!-- %/100 -->
    <inflation>0.03</inflation> <!-- %/100 -->
    <Indicator name='NPV_search' target='0'>
      msnb|capital
      msnb|fom
      msnb|refuel
      htse|fom
      htse|vom
```

```
    htse|capital
    htse|h2_sales
    pipeline|capex
    pipeline|om
  </Indicator>
</Global>
<Component name="msnb">
  <Life_time>40</Life_time> <!-- years -->
  <CashFlows>
    <!-- Capital Cost -->
    <!-- alpha in $ for the <reference> MW plant -->
    <Capex name="capital" tax="false" inflation="none" mult_target="false" multiply
        ↪ ="Multiplier">
      <driver>msnb_total_nuc_capex</driver>
      <alpha>-1</alpha>
      <reference>1</reference>
      <X>1</X>
      <depreciation scheme='MACRS'>15</depreciation>
    </Capex>
    <!-- Electric Revenue -->
    <!-- alpha is 1.0 -->
    <Recurring name="fom" tax="false" inflation="none" mult_target="false">
      <driver>msnb_fixed_cost</driver>
      <alpha>-1.0</alpha>
    </Recurring>
    <Recurring name="refuel" tax="false" inflation="none" mult_target="false">
      <driver>refuel_cost</driver>
      <alpha>0.0 0.0 0.0 0.0 0.0 0.0 0.0 0.0 0.0 0.0 0.0 -1.0 0.0 0.0 0.0 0.0 0.0
          ↪ 0.0 0.0 0.0 0.0 -1.0 0.0 0.0 0.0 0.0 0.0 0.0 0.0 0.0 0.0 -1.0 0.0 0.0
          ↪ 0.0 0.0 0.0 0.0 0.0 0.0 0.0</alpha>
    </Recurring>
  </CashFlows>
</Component>
<Component name="htse">
  <Life_time>40</Life_time>
  <CashFlows>
    <!-- Capital Cost -->
    <!-- alpha is power capacity of htse in MW, driver is $/MW capex-->
    <Capex name="capital" tax="false" inflation="none" mult_target="false" multiply
        ↪ ="Multiplier">
      <driver>htse_capex</driver>
```

```
      <alpha> -37574 </alpha>
      <!--TX: -249521 -->
      <!--AK: -37574-->
      <reference>1</reference>
      <X>1</X>
      <depreciation scheme='MACRS'>15</depreciation>
    </Capex>
    <!-- Electric Revenue -->
    <!-- alpha is 1.0 -->
    <Recurring name="fom" tax="false" inflation="none" mult_target="false">
      <driver>htse_fixed_cost</driver>
      <alpha>-1.0</alpha>
    </Recurring>
    <Recurring name="vom" tax="false" inflation="none" mult_target="false">
      <driver>htse_variable_cost</driver>
      <alpha>-1.0</alpha>
    </Recurring>
    <Recurring name="h2_sales" tax="true" inflation="none" mult_target="true">
      <driver>hydrogen</driver>
      <alpha>1</alpha>
    </Recurring>
  </CashFlows>
</Component>
  <Component name="pipeline">
    <Life_time>40</Life_time>
    <CashFlows>
      <!-- Capital Cost -->
      <!-- alpha in $ for the <reference> MW plant -->
      <Capex name="capex" tax="false" inflation="none" mult_target="false" multiply
          ↪ ="Multiplier">
        <driver>transpo_capex</driver>
        <alpha>-1.0</alpha>
        <reference>1</reference>
        <X>1</X>
        <depreciation scheme='MACRS'>7</depreciation>
      </Capex>
      <Recurring name="om" tax="false" inflation="none" mult_target="false">
        <driver>pipeline_OM</driver>
        <alpha>-1.0</alpha>
      </Recurring>
  </CashFlows>
```

```
  </Component>
</Economics>
```